RICE UNIVERSITY

Fermentative utilization of glycerol and lignocellulosic sugars and production of ethanol by *Paenibacillus macerans*

by

Ashutosh Gupta

A THESIS SUBMITTED
IN PARTIAL FULFILLMENT OF THE
REQUIREMENTS FOR THE DEGREE

Doctor of Philosophy

Approved, Thesis Committee:

Dr. Ramon Gonzalez, Chair
William Akers Assistant Professor in
Chemical and Biomolecular Engineering
and Assistant Professor in Bioengineering

Dr. Ka Yiu San
E. D. Butcher Professor in Bioengineering
and Professor in Chemical and
Biomolecular Engineering

Dr. Kyriacos Zygourakis
A.J. Hartsook Professor in Chemical and
Biomolecular Engineering and Professor in
Bioengineering

Houston, Texas
January, 2010

ABSTRACT

Fermentative utilization of glycerol and lignocellulosic sugars

and production of ethanol by *Paenibacillus macerans*

by

Ashutosh Gupta

With the recent volatility in crude oil prices and widespread concern regarding global warming, there is increased need for finding sustainable alternatives to petrochemical based fuels. One way to achieve this objective is through the production of biofuels such as ethanol by microbial fermentation. In this context, this study focuses on the anaerobic fermentation of renewable substrates; glycerol and lignocellulosic sugar mixtures for the production of ethanol by *P. macerans*. Further, metabolic flux analysis (MFA) was used as a systemwide tool to understand the role of various metabolic pathways in the fermentative utilization of these substrates.

Glycerol is a byproduct of biodiesel and bioethanol production, which is an abundant, inexpensive and renewable substrate. In this study, we have shown that *P. macerans* can anaerobically ferment glycerol in the absence of external electron acceptors. Nuclear magnetic resonance (NMR) analysis of the fermentation samples identified the production of ethanol, formate, acetate, succinate, and 1,2-propanediol (1,2-PDO) from glycerol. Use of U-^{13}C glycerol as substrate demonstrated the incorporation of glycerol in the cell biomass. Glycerol fermentation was stimulated in a medium

formulation with low concentrations of potassium and phosphate, cultivation at acidic pH, and the use of a CO_2-enriched atmosphere. Since the consumption of reducing equivalents in the production of 1,2-PDO balances the reducing equivalents generated in the production of cell biomass, the synthesis of ethanol and 1,2-PDO are proposed to be a metabolic determinant of glycerol fermentation in *P. macerans*.

Hexose and pentose sugars make the largest portion of lignocellulosic biomass, which is the ideal substrate for the production of biofuels. Most microorganisms can not utilize hexose and pentose sugars simultaneously. In this study, we have shown that *P. macerans* N234A can ferment hexose (glucose) and pentose (xylose and arabinose) sugars individually in the absence of external electron acceptors. Additionally, we have shown that *P. macerans* N234A can simultaneously utilize the three sugars of lignocellulosic biomass. We have also identified the factors pH and temperature, which improve the simultaneous sugar utilization by this microorganism.

Metabolic flux analysis was used as an *in vivo* tool for systemwide study of glycerol and sugar mixture fermentations to elucidate the role of various pathways. In the case of glycerol fermentation, MFA analysis identified the role of 1,2-PDO production in achieving the redox balance by consuming the redox equivalents being generated in the production of biomass. Flux analysis also showed the role of PFL in pyruvate dissimilation in the glycerol fermentation. Similarly, in the case of sugar mixture, MFA analysis showed the role of PFL and PDH enzymes in the utilization of sugar mixtures by *P. macerans*.

Acknowledgments

First of all I would like to thank God for providing me this learning opportunity and without his mercy, I wouldn't have learned so much during this work.

Next I would like to thank several people, who have helped, inspired and motivated me during this work. First and foremost, I thank my advisor Dr. Ramon Gonzalez, for all his advice, all kinds of support, guidance and encouragement during this research. He has been extremely patient and always approachable throughout this work. Next, I would like to thank Dr. Ka Yiu San and Dr. Kyriacos Zygourakis for agreeing to participate on my thesis committee and providing me with their valuable feedback and advice. I would also like to thank Dr. Sean Moran at Rice University for his help and guidance in learning the NMR spectroscopy technique and in obtaining good quality NMR spectra. I would also thank Dr. C. Glatz and his lab group at Iowa State University for their help in learning the proteomics techniques in their lab.

I would also like to thank Dr. J.V. Shanks and Dr. S. Mallapragada from Iowa State University for their advice and guidance during this work. I would also like to thank Dr. S. Sarkar and A. Kumar from IIT Kanpur for supporting and encouraging me to pursue higher studies. Not the least, I thank Dr. S. Palanki at University of South Alabama for his support in early part of my PhD.

I would also like to acknowledge the microorganisms, tiny creatures, which were the subject of this study, about whom I didn't knew anything before this work, but they became true companion all these years and from whom I learned so much about life.

Among friends, I would like to thank Dr. Pradeep Rai, whom I met in my first year at Rice and has been a close friend since then. I would also like to thank Dr. P. Jaiswal, N. Rohilla and A. Srivastava for making my stay at Rice memorable. I would like to thank B. Mishra for providing valuable advice and guidance during my stay in Houston. I would like to thank M.K. Choudhury and V. Binyala for making my stay at Iowa State an enjoyable experience. I would also like to acknowledge the ISCKON Houston and their weekly programs, which were very helpful in giving me the spiritual strength during this work. I would like to thank S. Mazumdar and J. Park for the interesting discussions in the lab. I would like to thank my research group members: Y. Dharmadi, S.Y. Yazdani, Y. Moon, G.W. Durnin, C. Dellomonaco, J. Clomburg, R. Sun, M. Rodriguez-Moya, A. Cintolesi, V. Rigou and M. Blankschien for their help and assistance during this work. I would specially like to thank S. Mazumdar for his help in proof-reading my thesis.

Lastly, I would like to thank my wife Sumati for her love and support that made this work possible. I dedicate this thesis to my parents for their love, support, and blessings during this work.

Contents

Figures

Tables

Nomenclature

Enzymes	
Abbreviation	Description
ACK	Acetate kinase
CcpA	Catabolite control protein A
FHL	Formate hydrogen lyase
G3PDH	Glycerol-3-phosphate dehydrogenase
GK	Glycerol kinase
HprK/P	HPr kinase/phosphatase
HPr	Histidine containing protein
PFL	Pyruvate formate lyase
PTA	Phosphotransacetylase

Pathways	
Abbreviation	Description
EMP Pathway	Embden–Meyerhof–Parnas pathway
PPP	Pentose phosphate pathway
PTS	phosphotransferase system
TCA	Tricarboxylic acid cycle

Metabolites	
Abbreviation	Description
13P2DG	1,3-Diphosphateglycerate
3PG	3-Phospho-D-Glycerate
3PDGL	3-phospho-D-glycerate
6PG	6-phospho-D-gluconate
AcCoA	Acetyl coenzyme A
AcP	Acetyl phosphate
ACAL	Acetaldehyde
ADP	Adenosine diphosphate
AMP	Adenosine monophosphate
ATP	Adenosine triphosphate
BDO	2,3-butanediol
CO_2	Carbon dioxide
CoA	Coenzyme A

DHA	Dihydroxyacetone
DHAP	Dihydroxyacetone phosphate
E4P	Erythrose-4-phosphate
F6P	Fructose-6-phosphate
FBP	Fructose-1,6-bisphosphate
FOR	Formate
FUM	Fumarate
G-1,5L6-P	D-glucono-1,5-lactone-6-phosphate
G3P	Glycerol-3-phosphate
G6P	Glucose-6-phosphate
Gly3P	Glyceraldehyde-3-phosphate
H_2	Hydrogen
HA	Hydroxyacetone
KG	α-ketoglutarate
MAL	Malate
MG	Methylglyoxal
NAD	Nicotinamide adenine dinucleotide
NADH	Nicotinamide adenine dinucleotide reduced
NADP	Nicotinamide adenine dinucleotide phosphate
NADPH	Nicotinamide adenine dinucleotide phosphate reduced
OAA	Oxaloacetate
Pi	Phosphate
PEP	Phosphoenolpyruvate
PYR	Pyruvate
R5P	Ribose-5-phosphate
RIBL	Ribulose
RL5P	Ribulose-5-phosphate
S7P	Sedoheptulose-7-phosphate
TCA	Tricarboxylic acid
XYL5P	Xylulose-5-phosphate
XYLU	Xylulose

Chapter 1

Introduction

1.1 Motivation

With the recent volatility in the crude oil prices, there is a significant concern worldwide on our reliance on the fossil fuels in everyday life. As can be seen in Figure 1.1 (A), oil price first increased upto $140 per barrel and then decreased to $30 per barrel in just six months. This volatility in crude oil prices has impacted everyone directly or indirectly.

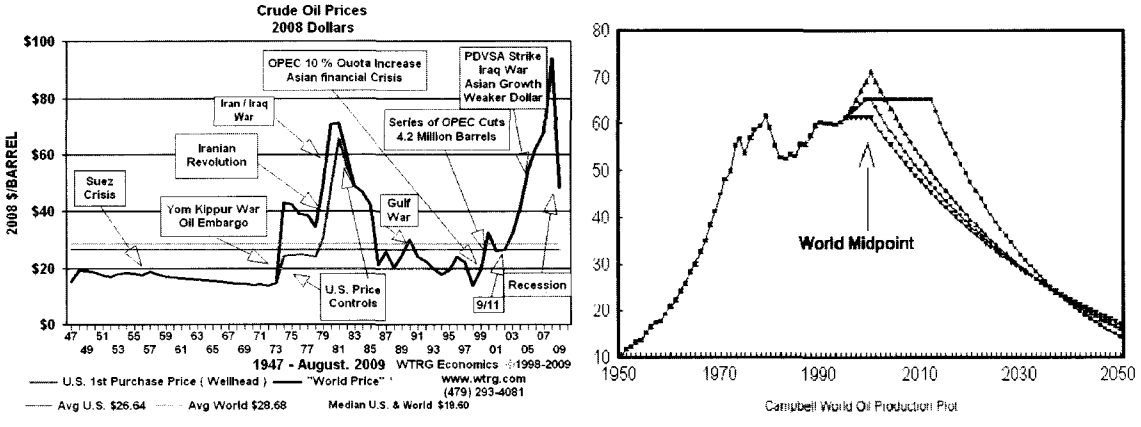

Figure 1.1: Crude Oil (A) prices (http://www.wtrg.com/oil_graphs/oilprice1947.gif) (B) and production over years. (http://www.oilcrisis.com/curves.htm)

One incentive to reduce our reliance on petrochemical based products is the ever increasing demand of these resources and their limited reserves. There is consensus building up worldwide that we have already reached the peak oil production and it is only going to decline in next fifty years (Figure 1.1 (B)) [1]. Hence, it is very important as well as urgent to find the alternatives to petrochemicals. One more reason to do so is the net production of carbon dioxide, when we use fuels and products derived from crude oil.

Emission of more and more carbon dioxide in the environment has been linked to global warming, as a result of which several nations could up under ocean because of increased sea levels [2].

Use of crude oil in our everyday lives can be categorized in two main groups: transportation fuels and petrochemicals. One of the best ways to reduce our use of fossil fuels in both of these categories is to use fuels and chemicals derived from biomass. This will lead to an economic transformation from being a petroleum based economy to a biobased economy (Figure 1.2). This is a viable and sustainable solution, which can avoid the many problems described in previous paragraphs with the use of

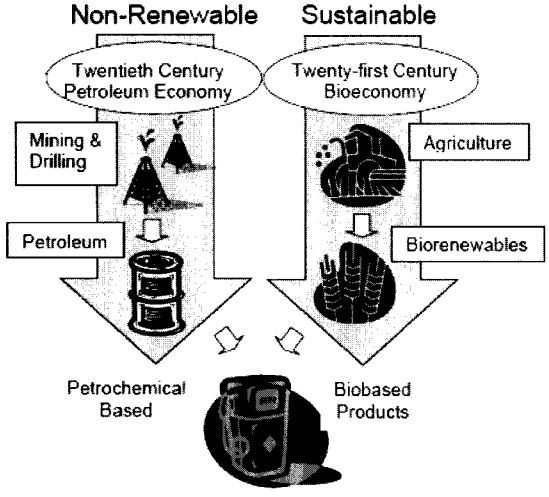

Figure 1.2: Bio-based economy as an important alternative to petroleum economy. reproduced from (http://www.biorenew.iastate.edu/aboutus/bioeconomy-brochure.pdf)

fossil fuels. With the increased realization of these factors, there is greater than ever focus on finding economically viable routes for the production of biofuels and biochemicals [2]. Currently there are two main routes for the production fuels and chemicals from biomass: thermochemical and biochemical routes. In the thermochemical route, biomass is transformed into fuels through the use of high pressure and temperature conditions,

while in the biochemical route it is transformed through the use of microorganisms as biocatalysts.

There are many different types of microorganisms that have been used for the industrial production of biofuels and biochemicals for a long time, including both prokaryotic and eukaryotic species. *Escherichia coli* and *Saccharomyces cerevisiae* are two of those microorganisms, which have been extensively used in the biotechnology industry. Ethanol is one such biofuel that is produced through biocatalysts industrially. Since it can be used as a transportation fuel, its production has increased significantly in recent years.

1.2 Production of biofuels

The increased focus on production of biofuels has lead to exponential increase in the production of biodiesel, which is a type of biofuels, and is produced through the transesterification of vegetable oils or animal fats. For every 10 lbs of biodiesel produced by this method, 1 lb of glycerol is also generated as byproduct [3]. With the increased production of biodiesel, there is surplus of glycerol in the market. Other than this oversupply, glycerol is also produced in the production of bioethanol. As a result, the prices of crude glycerol have decreased tremendously in last few years. Hence, glycerol is currently an inexpensive and abundant feedstock, which can be utilized for the production of fuels and chemicals.

Although glycerol is an inexpensive and non-food substrate available for biocatalysis, not many microorganisms can utilize glycerol in the absence of external electron acceptors. Only few microorganisms from species such as *Citrobacter* and

Klebsiella can ferment glycerol and they do it in a 1,3-propanediol (1,3-PDO) dependent manner, i.e if they have a pathway for the production of 1,3 PDO they can utilize glycerol in a fermentative manner [4]. But recently, it has been reported that the workhorse of modern biotechnology *E. coli*, can also ferment glycerol, but in a 1,2-propanediol (1,2-PDO) dependent manner [5]. One of the problems associated with glycerol utilization by *E. coli* is that this process is very slow. Hence, it is very important to find biocatalysts, which can utilize glycerol at high rates and yields. This study analyzes the fermentative utilization of glycerol by one such biocatalyst, *Paenibacillus macerans* and elucidates the pathways and factors responsible for its utilization.

Ethanol is another biofuel that has been produced for a long time, but has seen significant increase in its production in last decade. Ethanol is produced in industry by fermentation of starch from corn using yeast *Saccharomyces cerevisiae*. But, use of corn for the production of bioethanol is not a sustainable option, as corn is also used as food source. This has also led to the debate on the topic of farm vs fuel. A more long term and sustainable approach is the use of lignocellulosic biomass from plants. Lignocellulose contains 15-25% lignin and carbohydrates (cellulose and hemicellulose) make up the remaining 75-85% (Figure 1.3) [6]. Hexose and pentose sugars are major fractions of hemicellulose portion of biomass [7]. The fraction of these sugars in biomass can change depending on the source of biomass, going from 40% in corn stover to 22.2% in cotton gin trash for hexose sugars, while going from 21.6% in wheat straw to 6.9% in cotton gin trash for pentose sugars [8, 9]. Glucose, galactose and mannose are the hexose sugars, while xylose and arabinose are the pentose sugars of the carbohydrate portion. A major problem with the viability of bioethanol production is that yeast *Saccharomyces*

cerevisiae can not ferment pentose sugars. This makes the yield of bioethanol from plant carbohydrates relatively low. Another problem with most microorganisms that can ferment pentose sugars is that they are not able to ferment pentose sugars in the presence of glucose. The workhorse of modern biotechnology, *E. coli* is an example of such a microorganism. Although, it can ferment pentose sugars efficiently under anaerobic conditions, utilization of pentose sugars is completely blocked in the presence of glucose in the sugar mixture. Hence, there is a need for biocatalysts, which can utilize five and six carbon sugars simultaneously and can make the production of bioethanol from lignocellulosic biomass cost effective [10, 11].

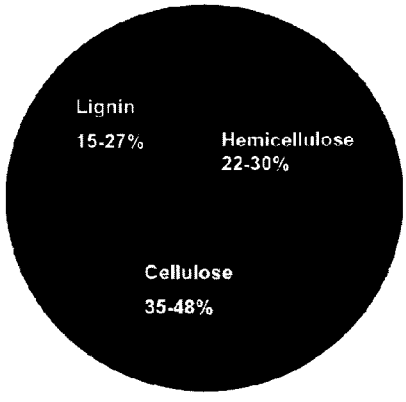

Figure 1.3: Typical composition of lignocellulosic biomass (http://www.farmdoc.illinois.edu/policy/research_reports/ethanol_report/ethanol%20report%20-%20ch%207.pdf)

Aforementioned phenomenon, where the presence of certain carbon sources inhibits the utilization of other carbon sources has been studied for a long time and is called carbon catabolite repression (CCR). Although, it has been known and characterized since 1970s, because of its complexity and levels of regulations involved, our understanding of this process is still very limited [12-14]. Hence, a systemic study involving phenotypic characterization of *Paenibacillus macerans* growing on a mixture

of carbon sources along with the quantification of extracellular levels of substrates as well as the metabolic products is very important for the understanding of sugar mixture utilization by this microorganism.

Although, we have biocatalysts such as *Saccharomyces cerevisiae*, which can produce ethanol from glucose in a robust manner in industrial settings, these biocatalysts are not always the best option. In nature, most microorganisms utilize a given carbon source to produce mixed acid fermentation products, which include formate, lactate, acetate, ethanol and succinate. The ability of microorganisms to fermentatively utilize a given substrate through mixed acid fermentation depends on many factors, most important of which are the substrate and growth environment. To grow in a given condition, microorganism has to maintain the redox balance and generate energy in the process. Since microorganisms are not naturally evolved to produce a specific product, the yield of the desired product is often less than the theoretical maximum possible. Hence, system level studies of these microorganisms are very important for understanding the complex architecture of cellular function and behavior. Information from these studies will give us the required knowledge for modifying their genetic network, so that they can be tailored to produce the desired fuel or chemical at high yields and productivities with no byproducts [15].

One of the most important factors, which affect the cellular phenotype, is its growth environment. Parameters, which define the growth conditions, may include the pH and temperature of the culture, composition of culture media, addition of rich supplementation and requirement of oxygen for growth. All of these factors play a very important role in cellular behavior and production of desired products. Since the ultimate

aim in any new biocatalyst development is that it should be cost competitive in industrial setting, all of above parameters are optimized to reduce the process cost. One such factor is the requirement of oxygen for the production of desired fuel or chemical. Although oxygen supports the faster cell growth by serving as external electron acceptor, it usage in industrial biotechnology processes is avoided because of two reasons: on commercial level, use of oxygen in the process increases the cost of the operation in the form of oxygen mixing requirements; on the fundamental level, oxygen use in the process reduces the maximum yields of the products such as ethanol from reduced substrates that can be achieved through fermentative process. In this context, this study intends to analyze the fermentative utilization of reduced substrate (glycerol) and neutral substrate (sugars), optimizing the use of substrate and operating conditions.

In this context, systemwide analysis tools become very important as they provide a holistic view of the role of different pathways in the production of desired chemicals. Use of such tools provides the knowledge required for development and improvement of bioprocesses. One such analysis, which has been used extensively for better understanding of cellular metabolism, is metabolic flux analysis (MFA) [16-19]. Although there are other types of flux analysis techniques available; including flux balance analysis and ^{13}C labeling based metabolic flux analysis, at its core all these techniques are balances based on the chemical structures of the metabolites. The metabolic flux analysis approach is based on mass balances for each intracellular metabolite based on the reaction stoichiometry and metabolic pathway information. MFA is an *in vivo* analysis, as it uses the extracellular metabolites concentration data for solving the metabolic flux model. Since this analysis provides knowledge about the

relative role of each of the pathway in the utilization of a given substrate, it is very important in developing strategies for the improved production of desired chemical with increased yields, which has also been described in several reviews [20-22]. Given its importance, this study uses the MFA technique to elucidate the role of various pathways in the fermentative utilization for the glycerol as well as sugar mixture fermentations. It will also provide information which can be used for further metabolic engineering studies.

1.3 Objective

The overall objective of this study is to understand the fermentative utilization of glycerol and sugar mixtures by *P. macerans* and the factors determining the production of ethanol. Glycerol and lignocellulosic sugars were chosen as substrates in this study because they are both inexpensive and abundant carbon sources. The difference between the two substrates is that glycerol is much more reduced carbon source than lignocellulosic sugars. This study will provide a better understanding of the fermentative utilization of these substrates by *P. macerans*, an organism which can efficiently utilize a wide array of carbon sources. The specific objectives of this study are:

Fermentative utilization of glycerol:

(i) Evaluate the ability of different strains of *P. macerans* to ferment glycerol and investigate the minimum nutrient supplementation required.

(ii) Determine the identity of products generated during fermentative utilization of glycerol.

(iii) Identify the environmental determinants responsible for glycerol utilization.

(iv) Identify the key enzymes and pathways mediating glycerol fermentation.

(v) Propose a metabolic model for fermentative utilization of glycerol with the aid of systemwide tools.

Fermentative metabolism of lignocellulosic sugars:

(i) Characterize fermentative utilization of individual sugars (glucose, xylose and arabinose) by *P. macerans*.

(ii) Characterize the fermentation of sugar mixtures by *P. macerans*.

(iii) Determine the effect of environmental factors; pH and temperature on utilization of sugar mixtures by *P. macerans.*

(iv) Identify key metabolic pathways involved in the sugar mixture fermentation by *P. macerans* through metabolic flux analysis.

1.4 Overview of results

Very few microorganisms can utilize glycerol in a fermentative manner. In these microorganisms, two models have been proposed for the metabolism of glycerol: 1,3-propanediol and ethanol-1,2-propanediol model. Fermentative utilization of glycerol by *P. macerans* in the absence of external electron acceptors through ethanol-1,2-propanediol is described in Chapter 5. Our initial results showed that *P. macerans* N234A can utilize the glycerol very efficiently with specific growth rate of 0.4 h^{-1}. Further analysis of extracellular metabolites through high performance liquid chromatography (HPLC) and nuclear magnetic resonance (NMR) identified ethanol, formate, acetate, succinate, and 1,2-propanediol (1,2-PDO) as fermentation products. Further NMR

analysis of proteinogenic amino acids from the uniformly labeled ^{13}C-glycerol fermentation showed the incorporation of glycerol in cell biomass in a culture supplemented with minimum supplementation of 1 g/l tryptone. A medium formulation with low concentrations of potassium and phosphate, cultivation at acidic pH, and the use of a CO_2 enriched atmosphere stimulated glycerol fermentation and are proposed to be environmental determinants of this process. The pathways involved in glycerol utilization and synthesis of fermentation products were identified using NMR spectroscopy in combination with enzyme assays. Based on these studies, the synthesis of ethanol and 1,2-PDO is proposed to be a metabolic determinant of glycerol fermentation in *P. macerans*. Conversion of glycerol to ethanol fulfills energy requirements by generating one molecule of ATP per molecule of ethanol synthesized. Conversion of glycerol to 1,2-PDO results in the consumption of reducing equivalents, thus facilitating redox balance. Hence, these results show the ethanol and 1,2-PDO dependent utilization of glycerol, which is the similar to the model that has been reported by our group previously for the glycerol utilization by *E. coli* [5].

The utilization of lignocellulosic sugars by *P. macerans* N234A under fermentative conditions is described in Chapter 6. First, the three sugars of this study: glucose, xylose and arabinose, which together make up more than 60% of lignocellulosic biomass, were analyzed individually for their fermentative utilization by *P. macerans*. All three sugars are efficiently utilized by this microorganism as reported in previous studies for strains ATCC7068 and DSM1574 of *P. macerans* [23, 24]. In the next step, fermentative utilization of a sugar mixture by *P. macerans* N234A was studied. Since, temperature and pH are two important environmental parameters which effect cell

growth, substrate utilization and production of desired chemical, effect of changes in these two parameters on the sugar mixture utilization was analyzed. This evaluation showed that pH 6 and 47°C temperature were the best conditions for the simultaneous consumption of the three sugars.

Since knowledge about the metabolic pathways mediating the fermentative utilization of the substrates of this study: glycerol and lignocellulosic sugars by *P. macerans*, is very important for any future engineering effort to improve the production of ethanol, metabolic flux analysis (MFA) was used as a tool to gain further insights into the metabolism of these substrates. Chapter 7, describes the application of metabolic flux analysis for the study of consumption of glycerol and sugar mixtures by this microorganism. For the two cases, metabolic reaction networks were built based on the reaction stoichiometry and intracellular fluxes were then calculated from the model and information from the measured fluxes. In both cases, the system was overdetermined and the system of equations was solved accordingly. MFA showed the conversion of pyruvate to Acetyl-CoA occurs through pyruvate formate lyase in the case of glycerol, while in the case of sugar mixtures it is through pyruvate formate lyase and pyruvate dehydrogenase.

Chapter 2

P. macerans metabolism – a review

Paenibacillus macerans is a gram positive, spore-forming bacteria. It has been also been called *Bacillus macerans* and *Bacillus acetoethylicum* in literature, but in a taxonomic reassignment in 1996 by Heyndrickx et al. [25], it was reclassified as a species of genus *Paenibacillus*. Owing to its closeness to the genus *Bacillus* and unavailability of genome sequence of *P. macerans*, this chapter will describe about the metabolic pathways and regulation mechanisms of different carbon sources in *B. subtilis*, whenever the similar information is not available for *P. macerans*.

2.1 Introduction

P. macerans is a microorganism, which can grow under aerobic as well as anaerobic conditions. The word '*Paenibacillus*' comes from Latin language, which means '*almost Bacillus*'. *B. subtilis* is the model gram positive microorganism and representative species in the *Bacillus* genera and hence used in this chapter as reference to explain the phenomena, where such knowledge in not available for *P. macerans*.

B. subtilis is the second most studied microorganism after *E. coli*. It is also the model microorganism for studying the gram positive bacteria. Although it has been studied for the last sixty years, sequencing of *B. subtilis* genome in 1997 has given a completely new perspective and directions to the microbiological community [26].

Although many studies have been done since then, still much is unknown about the cellular metabolism and its global and local control mechanisms in this microorganism.

This microorganism is generally found in the rhizosphere of several plants and has adapted to metabolize the wide variety of carbohydrates found in its environment such as monosaccharides, polysaccharides, amino sugars, glycaric acid and sugar derived polyalcohols. Since there are always some differences in metabolism for each of the carbohydrate substrates, this chapter will focus mainly on the metabolism of substrates for this study: monosaccharides: glucose, xylose and arabinose and polyalcohol: glycerol.

Utilization of carbohydrates by microorganisms requires utilization of different cellular mechanisms and controls based on the substrate and cellular environment. These mechanisms include substrate transport, channeling of substrate into central carbon metabolism, funneling of carbon into respiratory (presence of electron acceptor) or fermentative pathways (absence of external electron acceptor) based on the cellular environment, biosynthetic pathways for the synthesis of biomass and finally extracellular product transport. Since this study focuses on the fermentative utilization of the carbohydrates, only fermentative pathways are described in more detail in later sections.

Carbohydrate metabolism in microorganisms starts with the transport of the substrate into the cellular environment. In every microorganism and for every substrate there is a unique mechanism for its entry into the cell. For some substrates their entry into the cellular environment is coupled with the phosphorylation, for some there is phosphorylation right after entry and for some there is no phosphorylation during transport [27]. After the transport, the substrate is fed into the central carbon metabolism,

which includes the Embden–Meyerhof–Parnas (EMP) pathway, the pentose phosphate pathway (PPP), and fermentative pathways; all of these pathways have been described in more detail in the later sections of this chapter. Central carbon metabolism is very important for cell growth because of the different precursor metabolites being generated in these pathways for use in the synthesis of cellular building blocks and macromolecules. Precursor metabolites that come from different central carbon pathways for biosynthesis are : EMP pathway precursors [glucose-6-phosphate (G6P), fructose-6-phosphate (F6P), phosphoenolpyruvate (PEP), 3-phospho-D-glycerate (3PDGL), glyceraldehyde-3-phosphate (Gly3P)], pentose phosphate pathway precursors [sedoheptulose-7-phosphate (S7P), erythrose-4-phosphate (E4P), ribose-5-phosphate (R5P)] and fermentative pathways precursors [pyruvate, acetyl-coenzyme-A (AcCoA), α-ketoglutarate (KG), oxaloacetate (OAA)]. Since all of these precursors come from different branches of central carbon metabolism, disturbances in their formation lead to severe defects in cell growth.

The amount of carbon being fed into these pathways and the ratio of the carbon fluxes among these pathways depends mainly on the substrate being used as carbon source and cellular environment: which could be either respiratory (presence of electron acceptor) or fermentative (absence of electron acceptor) [28]. In the respiratory environment, generally the electron acceptor is oxygen, but it could also be other electron accepting species such as nitrate or fumarate. Since cells need the energy in form of ATP to grow, they need an electron acceptor to which they can transfer the electrons and produce the ATP in the process. If oxygen is present in the environment, it can readily fulfill this role and allows the cell to grow. But in the absence of an electron acceptor,

there is no external species which cells can utilize for electron transfer and hence they need to balance the redox equivalents by themselves and also generate energy. So, the fermentative conditions are of a high stress for the cells with limited resources and in this environment there should be a tight balance between redox equivalents being generated and consumed for the cells to grow efficiently. This can only be achieved with a reduced substrate which can fulfill the redox balance requirements of the cell. One substrate being used in this study, glycerol, fulfills this requirement very well and redox balance achieved by using this substrate has been explained in detail in later chapters. NADH and NADPH are the two main electron donor cofactors that are produced during the cellular metabolism and they need to be recycled during the fermentative metabolism. NADH is produced in the glycolysis and NADPH is produced in the oxidative branches of the TCA cycle and pentose phosphate pathways. Since these cofactors need to be regenerated, this is achieved through external electron acceptors in the respiratory environment and through production of reduced products in the fermentative environment.

2.2 Carbohydrates and glycerol transport

To survive in the hostile natural soil environment, *B. subtilis* is enclosed by a single lipid bilayer membrane, which plays an important role in carbohydrate uptake, metabolite transport and expulsion of toxic compounds. This communication between cells and their external environment is essential for their survival and adaptation. For this reason, the bacterial cell membrane wall has many membrane transport proteins, which selectively transport nutrients and metabolites based on the cellular requirements and nutrient availability. Membrane transporter proteins are generally made up of one or

more protein subunits. These proteins can be divided into four types: channel proteins, secondary active transporters, primary active transporters and group translocating system.

Channel proteins transport solutes in an energy independent manner and no carriers are involved in the transport. Glycerol transport protein GlpF, encoded by *glpF,* facilitates glycerol uptake through this mechanism. Secondary active transporters use chemiosmotic energy of a transmembrane ion or a solute for their transport. They can travel by different mechanisms, alone through solute uniport, together with a proton in the same direction by solute:proton symport, together with a proton in opposite directions through solute:protein antiport and together through another solute through solute:solute antiport. Uptake of L-arabinose by AraE protein, glucose transport through non-PTS protein GlcP occurs through secondary transporters. Primary active transporters generally use chemical energy gained as by hydrolysis of ATP, for solute transport. These generally act like a cassette and therefore are called ATP binding cassette (ABC) family transporters. Group translocating system transporters simultaneously transport and phosphorylate the sugar they are transporting using phosphoenolpyruvate (PEP) as phosphate donor as well as energy source. The bacterial Phosphoenolpyruvate (PEP): carbohydrate phosphotransferase system (PTS) transports sugars using this mechanism and is its main sugar transport system.

Since glycerol and sugar utilization by *P. macerans* is a major focus of this study, no genetic information is available for *P. macerans* PTS sugar transport system and *P. macerans* is a close relative of *B. subtilis*, the next section will describe the PTS sugar transport system in *B. subtilis* in more detail. It includes sugar and glycerol transport systems, the mechanism controlling metabolism of less preferred carbon source

in the presence of a preferred carbon source, central carbon metabolism and fermentative pathways.

2.2.1 PTS transport system and carbon catabolite repression

2.2.1.1 Carbon catabolite repression

Most microorganisms can use various types of compounds available in the environment as substrates for their growth. When more than one substrate is present in the environment, microorganisms can either ferment them together or one by one. To survive in the natural environment, microorganisms utilize the substrate which gives them the fastest growth and hence the best chance of survival in the competition with other microorganisms. Sequential consumption of available substrates by microorganisms had been studies since last fifty years and is called diauxic. Because glucose is readily available in the environment, it is the most preferred substrate for the most microorganisms. When there are multiple substrates present along with glucose, the presence of glucose generally represses consumption of other substrates. This type of repression, where presence of glucose inhibits the consumption of other less preferred carbon sources has been termed carbon catabolite repression (CCR). Since this phenomenon is so essential for bacterial survival, it has been found to occur in most microorganisms. However, there are some microbes where there is no carbon catabolite repression meaning substrates are consumed together with glucose, i.e., genes responsible for consumption of both substrates are expressed at the same time [29, 30]. In some other cases, there is no change in gene expression in response to changes in substrate in the environment ie these microorganisms don't have regulatory systems for controlling the

utilization of available carbon sources [31, 32]. Then, there also examples where glucose is the less preferred carbon source in presence of a preferred carbon source such as lactose [33-35].

Because of its importance for microbial growth and survival, CCR has been extensively studied in model microorganisms such as gram negative model bacteria *Escherichia coli* and gram positive model bacteria *B. subtilis* [14]. The end effect of carbon catabolite repression is quite similar in both model microorganisms: in the presence of glucose, expression of genes responsible for consumption of non preferred carbon source is repressed. But, the inherent regulatory mechanisms and proteins involved in the process are quite different, which is also true for CCR mechanisms in other groups of bacteria. In *E. coli*, the control is at the transcriptional level, where presence of glucose, prevents the formation of cAMP-CRP (an inducer of expression of catabolite genes) complex. This type of mechanism of CCR is called inducer exclusion [14]. While in the case of *B. subtilis*, the presence of glucose leads to the formation of complex of CcpA and HPr(Ser-P), which binds to '*cre*' sites upstream of catabolite genes and prevents their expression. The common regulatory element in both cases is phosphoenolpyruvate:carbohydrate phosphotransferase system (PTS), which is involved in the glucose transport and its phosphorylation [27]. In most cases, a phosphorylated protein of the PTS system is the main controller of CCR. In case of *E. coli* this protein is glucose specific protein ($EIIA^{Glc}$) and for *B. subtilis* it is HPr. In the next few sections, PTS transport system in *B. subtilis* and its controlling mechanism re explained in more detail.

2.2.1.2 PTS transport System

Phosphoenolpyruvate (PEP): carbohydrate phosphotransferase system (PTS), in *B. subtilis* is mediated by general proteins the enzyme I (EI), the histidine containing protein (HPr) and the sugar specific protein (EII^{Glc}) (Figure 2.1). Each PTS sugar has its specific EII protein, which is responsible for their transport and phosphorylation. The number of subunits and order of genes encoding those subunits is different for each EII protein complex. The EII protein responsible for glucose transport has three subunits: EIIA, EIIB and EIIC. While EIIA and EIIB are involved in steps leading to glucose phosphorylation, EIIC is a membrane spanning protein which transports the sugar through the cell membrane. Nomenclature for genes encoding for these proteins in *B. subtilis* is similar to *E. coli*: *ptsG* codes for EII protein, *ptsI* codes for the EI protein and *ptsH* codes for the HPr.

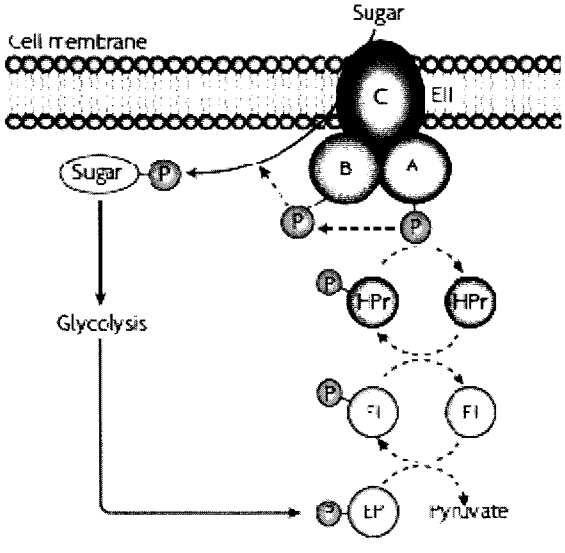

Figure 2.1: Simultaneous transport and phosphorylation of carbohydrates in bacteria by the PTS system. Figure shows the three proteins of the PTS system enzyme I (EI), histidine protein (HPr) and enzyme II (EII). [14]

The mechanism leading to glucose transport and its phosphorylation is a series of coupled reactions (Figure 2.1). It starts with the dephosphorylation of phosphoenolpyruvate (PEP) to pyruvate. This dephosphorylation is coupled with the phosphorylation of the EI protein. In the next step EI dephosphorylates and in turn phoshopyrleates HPr at His-15 residue. This P-His-HPr then in turn dephosphorylates and phosphorylates EIIA. In the next step, dephosphorylation of EIIA is coupled with phosphorylation of EIIB. In the final step dephosphorylation of EIIB is coupled with conversion of glucose to glucose-6-phosphate (G6P). In overall reaction, the PEP is converted to pyruvate and glucose is converted to G6P.

2.2.1.3 Histidine containing protein (HPr)

The histidine containing protein (HPr) plays a very important role in carbohydrate transport and metabolism in *B. subtilis*. It is the different phosphorylated forms of this protein which play a central role in regulation of carbon uptake. It is present in unphophorylated form (HPr), phosphorylated at His-15 residue in a PEP dependent reaction (P-His-HPr), phosphorylated at Ser-46 position in a ATP dependent manner (P-Ser-HPr) and phosphorylated at both both Ser-46 and His-15 positions (Figure 2.2). While phosphophyrlation at His-15 site of HPr has been reported in gram positive and gram negative microorganisms, seryl phosphorylation of HPr has been found to occur only in gram positive microorganisms. It is present in these four different forms depending on the availability of phosphate donors. Phosphorylation of HPr at the His-15 residue is mediated by the EI protein, while Ser-46 phosphorylation is catalyzed by HPr kinase/phosphatase (HprK/P). HPr kinase/phosphatase is a bifunctional enzyme [36],

which can phosphorylate HPr as well as dephosphorylate P-Ser-HPr. Its ATP dependent phosphorylation activity is increased by the increase in the intracellular concentration of fructose-1,6-biphosphate (FBP), which is produced when preferred carbon source the glucose is metabolized. In the presence of glucose, higher intracellular concentrations of the FBP have been reported, which increases the phosphorylation of HPr at Ser-46 residue (Figure 2.2). The effect of FBP concentration on HPr phosphorylation at Ser-46 is more pronounced, when there is lower concentration of ATP. The same distinct effect is also seen when there is a small amount of inorganic phosphate (Pi) present [37]. Also, the increased concentration of the phosphate donor, pyrophosphate (PPi) has also been reported for the cells growing on glucose, which in turn helps in the phosphorylation of HPr at Ser-46 [38]. HprK/P activity is also affected by concentrations of phosphate donor ATP. The effect of concentrations of ATP, Pi, PPi and FBP on the kinase and dephosphorylation activities of HPrK/phosphatase varies with microorganisms, with some of them like *B. subtilis* showing strong effects of their concentrations [37], while others show very low or no effect at all [39, 40]. It has also been reported that EI protein competes with HPr kinase for the phosphorylation of HPr protein and phosphorylation of HPr by EI reduces the affinity of HPr kinase for phosphorylation of HPr.

2.2.1.4 Control of PTS transport by P-Ser-HPr

It has been shown that in presence of preferred carbon source, the HPr is present mostly as either P-Ser-HPr or in its doubly phosphorylated form. Since there is little HPr, and PTS protein EI has a low affinity for P-Ser-HPr, there is a very little P-His-HPr present in the system (Figure 2.2) [41]. In *B. subtilis* mutants, where Ser-46 of

HPr was replaced with Ala, no increased glucose uptake was seen, suggesting that even low amounts of P-His-HPr are enough for efficient glucose transport by PTS system [42, 43]. But, when there is another PTS sugar present in addition to glucose in the media, there is competition for this low amount of P-His-HPr, which leads to the inhibitory effect of glucose on the transport of the other sugar. In mutants where Ser-46 of HPr was replaced with Ala, which increased the amount of P-His-HPr available, there was a marked increase in the transport of other PTS sugar in presence of glucose [42, 44].

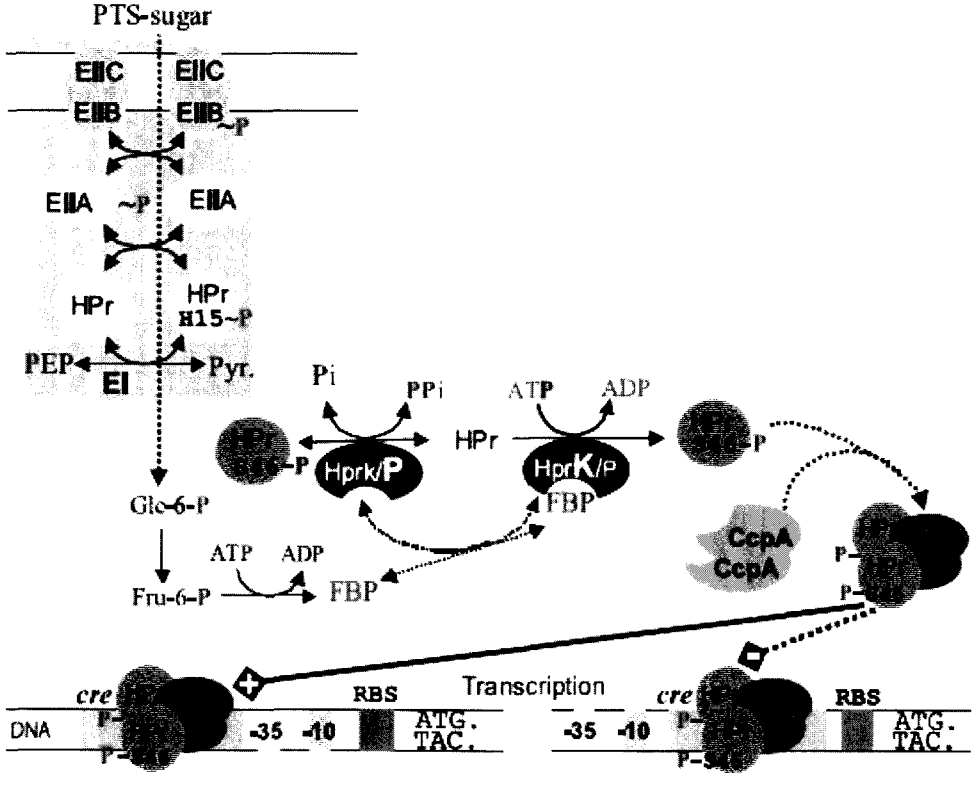

Figure 2.2: Mechanisms for the CCR and CCA in B. subtilis. Uptake of glucose leads to dephosphorylation of the PTS proteins. High concentrations of FBP simulate the HPr kinase activity of the bifunctional HprK/P and the formation of P-Ser-HPr. P-Ser-HPr interacts with CcpA, and the protein complex binds to the cre operator sites on the DNA (modified from [27])

In another experiment showing tight regulation of PTS sugar transport by P-Ser-HPr, *B. subtilis* mutants carrying a mutation which knocks out the dephosphorylation capacity of HprK, excess production P-Ser-HPr leads to complete cessation of growth on PTS sugars including glucose. This happens as a result of reduced PTS phosporyl group transfer, which results in lower sugar transport [43]. In the same experiments, when Ser-46 of HPr was replaced with Ala, PTS transport of sugars was restored because no P-Ser-HPr is formed as a result of mutation.

2.2.1.5 Importance of P-Ser-HPr

CCR is a global regulatory mechanism found in most microorganisms, where uptake and metabolism of the less preferred carbon source is significantly hindered in the presence of the preferred carbon source. P-Ser-HPr, which is formed as result of ATP dependent phosphorylation of HPr at Ser-46, plays a major role in the regulation of CCR in the *B. subtilis* (Figure 2.2). In the mutants, where Ser-46 of HPr was replaced with Ala, the repression of several enzymes involved in the metabolism of less preferred carbon source is relieved, which shows P-Ser-HPr mediated CCR in *B. subtilis* [42]. Use of the above mutant strain and its derivates has been shown to be relieved from CCR in various studies on several genes and operons. [45-48]. In some other cases use of nutrient rich media was necessary to show the effect of the mutation on relief from CCR [42, 49]. The effect of the corresponding mutations in other gram positive bacteria has also shown the relief from CCR [50-52].

In the gram positive bacteria such as *B. subtilis,* metabolism of the preferred carbon source is very important for the CCR, which is different from gram negative

bacteria, where PTS transport of preferred carbon source is sufficient for CCR. Since FBP, a glycolytic intermediate, has been found to stimulate the HprK/phosphatase catalyzed conversion of HPr to P-Ser-HPr, its formation by sugar metabolism is very important for the CCR to occur [42, 53, 54].

Another phenomenon, carbon catabolite activation (CCA), has also been found to occur in microorganisms. It occurs when expression of specific genes and operons is increased in the presence of the preferred carbon source. In the *B. subtilis*, this has been shown to be true with the expression of genes encoding alpha acetolactate synthase [55], acetate kinase [56] and phosphotransacetylase [57]. Again, in HPr mutants, because of loss of Ser-46 residue, no CCA was observed.

2.2.1.6 Catabolite responsive elements (cre)

Catabolite responsive elements are generally ~14 bp, cis acting, mostly imperfect palindromic operator sites, which are located in the promoter region of the CCR affected genes (Figure 2.2). There is a lot of variability in the location of the *'cre'* sequence among different catabolite repressed genes; in some cases it is located inside the promoter region, in some between the promoter and start codon, while in some inside the gene itself. In the specific case of *B. subtilis* arabinose operon, there are two *'cre'* sites present in the promoter region. One *'cre'* site is present in front of the *araA* gene, while the second *'cre'* site is within *araB* gene [58].

From experimental analysis of *'cre'* sequences of many carbon catabolite repressed genes in *B. subtilis*, Chambliss and coworkers proposed TGWNANCGNTNWCA as consensus *'cre'* sequence [59], although slightly different

consensus sequences have also been proposed by some other researchers [60, 61]. By using the sequence similarity search for the *'cre'* sequence in *B. subtilis* genome, about 160 *'cre'* sites were identified, which amounts to about 10% of genes in *B. subtilis* genome. This finding was similar to the other reports that as much as up to 10% genes are regulated by CCR using advanced high throughput systemwide tools such as transcriptomics and proteomics. [62-64].

2.2.1.7 CcpA:CCR/CCA protein

CcpA is a trans-acting, LacI/GalR type carbon catabolite repressor protein, which is called catabolite control protein A or CcpA [65]. It has been reported to mediate both CCR and CCA (Figure 2.2). Mutations in gene sequence of this protein lead to relief from carbon catabolite repression in many CCR repressed genes in *B. subtilis* [42, 66-68], but not all CCR or CCA affected genes change expression despite of these mutations [69].

Whole genome transcriptomics analysis of *B. subtilis ccpA* mutant has identified even more genes regulated by CcpA [63, 64]. Using another high throughput tool, two dimensional gel electrophoresis for comparative protein expression analysis, between wild type and *ccpA* mutants showed that seven tricarboxylic acid cycle (TCA) enzymes (CitC, CitG, CitH, CitZ, OdhA, SdhA, SucC/SucD) were relieved from CCR in *ccpA* mutants [70]. Further analysis of gene sequence of these enzymes showed that some of them had a potential *'cre'* sequence preceding the gene, which implicated a connection between the *'cre'* sites and CcpA protein [71, 72]. Also, in the *ccpA* mutant higher concentration of P-Ser-HPr, lower glucose uptake [73] and lower expression of enzymes

affected by CCA has been reported [73-75]. In the same mutant, it was also reported that expression of some of the carbon catabolite repressed genes remains unchanged [42], whose regulation is reported to also occur through a second CcpA independent mechanism.

CcpA also controls many other genes that are not involved in carbon catabolism like *ilv-leu* operon which encodes the enzymes catalyzing the synthesis of branched chain amino acids in *B. subtilis* by stimulating its expression [76, 77]. In another example of its control, CcpA represses some of the genes involved in the repression of genes involved in the utilization of nitrogen sources [78, 79]. Again, using systemwide analysis of transcriptional changes using DNA microarray on *ccpA* and *hprK* mutants showed that expression of even large number of genes involved in nitrogen and phosphorus metabolism is controlled by CcpA [80].

Characteristics of the protein structure of the CcpA, is unique sequences located in the DNA binding domain and in the core protein domain, which have been shown to be important for its activity [81]. The homology search in all sequenced gram positive bacteria and experimental validation of CCR activity in some of those have shown that CcpA is a common protein in all gram positive bacteria [82, 83].

Two mechanisms have been proposed for the binding of the CcpA protein to *'cre'* sites in gram positive microorganisms; in the first case CcpA can act by itself in binding to the *'cre'* sites of the catabolite controlled gene. In this case, regulation of *ccpA* expression and CCR through CcpA occurs by autoregulation through a *'cre'* site upstream of *ccpA* [84-86]. In second case, including in *B. subtilis*, expression of *ccpA*

itself is not regulated, but CcpA needs another corepressor to bind to the *'cre'* sites of carbon catabolite repressed genes [68].

2.2.1.8 P-Ser-HPr: a carbon catabolite corepressor

The first evidence of need of the corepressor for binding of CcpA to the *'cre'* sites was obtained by comparing CCR affected genes in *ccpA* mutant and *ptsH* mutant (Figure 2.2). In these mutants, it was found that CCR genes which are affected by *ptsH* mutation were also affected by *ccpA* mutation, suggesting a common mechanism of their CCR [42]. Formation of CcpA:P-Ser-Hpr complex was confirmed by the NMR study [87]. It was also found that in addition to the conserved residue: His-15 and regulatory region from 46 to 56 (which includes Ser-46) in HPr, there is also conserved region of amino acids between 21 and 27 positions in most gram positive microorganisms, which is the interaction domain between CcpA and P-Ser-HPr. Because of the large size of the CcpA molecule, its interaction domain could not identified by NMR. Instead it was identified by the indirect method: studying the effect of *ccpA* mutations on CcpA:P-Ser-HPr complex formation. It was found that Tyr-89, Tyr-295, Ala-299 and Arg-303 residues of CcpA participate in the interaction with P-Ser-Hpr [81]. Crystal structure of this complex in *B. megaterium* confirmed the residues participating in this complex: Tyr-295, Ala-299, Val-300, Arg-303, and Leu-304 of CcpA form tight interface with Ile-47, Met-48 and Met-51 of HPr [88].

Phosphorylation of HPr plays an important role in the interaction of HPr with CcpA. While its phosphorylation at Ser-46 makes it affinity for CcpA 50 times greater than unphosphorylated form [87], phosphorylation at His-15 makes its interaction

with CcpA weaker by weakening the interaction between regulatory domain of CcpA and P-Ser-HPr [88]. While phosphorylation at His-15 in HPr lowers the affinity of HPr for CcpA, His-15 residue itself is important for CcpA:HPr interaction as it interacts through hydrogen bonding at this position with Asp-296 residue of CcpA [89].

There have been some reports where mutations in the HPr, CcpA or HprK/phosphatase proteins have led to the permanent repression of genes affected by CCR. This phenomenon implies that these mutations lead to the formation of CcpA:Ser-P-HPr complex even in the absence of repressing sugar. For HPr, replacing Ser-46 with Asp causes the partial CCR in the absence of repressing sugar [42]. For CcpA, mutations in the core binding domain such as changing Glu-77 to Leu lead to the CCR even in the absence of repressing sugar [90]. For the HprK/phosphatase case, replacing Val-265 with Phe results in increased concentration of P-Ser-HPr because of loss of phosphatase activity as the result of mutation. This increased concentration of P-Ser-HPr leads to permanent repression of CCR affected genes [43].

The binding of the CcpA:P-Ser-HPr complex occurs at the *'cre'* sites of the CCR affected gene or the operon. For *B. subtilis gnt* operon, the *'cre'* site at the 5' end was found to be protected in the presence of CcpA and P-Ser-HPr, while no protection was observed with CcpA or P-Ser-HPr alone and in the presence of both CcpA and HPr [91]. Binding of CcpA:P-Ser-HPr to *'cre'* sites of CCR affected genes was also proven by analyzing the effect of mutations in the gene sequence of *'cre'* site on the CCR, which led to relief from CCR. Further studies into the binding affinities of this complex with *'cre'* sites identified that it is ternary complex with cre:CcpA dimer:P-Ser-HPr structure and no interaction with *'cre'* sites was observed if HPr was not

phosphorylated at Ser-46 [87]. With the determination of crystal structure of this ternary complex in *B. megaterium*, it was further confirmed that along with the CcpA dimer, two molecules of P-Ser-HPr participate in the complex formation with *'cre'* site of CCR affected gene [88]. The determination of crystal structure also identified the interaction domains of CcpA dimer:P-Ser-HPr complex with *'cre'* sites. In the same study, comparison of CcpA dimer:P-Ser-HPr with CcpA monomer revealed the conformational changes that occur in this complex formation that prepare it for the binding with the *'cre'* sites.

In gram positive bacteria, *'cre'* sites in the upstream of promoter regions of corresponding gene have also been found for the genes that are activated by the presence of preferred carbon source. Also, similar to CCR mechanism, binding of CcpA:P-Ser-HPr complex to *'cre'* sites activates the expression of CCA affected gene or operon. For *B. subtilis*, *'cre'* sequences in front of promoters of CCA activated *ackA*, *glg* and *pta* genes [56, 57] have been found.

Indirect control of CCR affected genes has also been reported for gram positive bacteria. In these CCR affected genes; *'cre'* site interacting with CcpA:P-Ser-HPr is located in the promoter region of the transcriptional regulator of the corresponding gene. This is true for *B. subtilis citZ* and *citB* genes, which are regulated by CcpC and *acoABCL* operon which is regulated by AcoR [71, 92].

2.2.1.9 Catabolite repression HPr (Crh)

Catabolite repression HPr (Crh) is a corepressor protein that is found in

some gram positive microorganism like *B. subtilis* (Figure 2.3). It is similar to the previously discussed protein HPr that it contains Ser-46 residue, but it doesn't contain the His-15 residue, so it can not participate in PTS sugar transport, but it acts corepressor together with CcpA protein in CCR or CCA of affected genes.

First indications of existence of a corepressor protein other than HPr was found in the mutant containing (Ser46Ala)HPr mutation. Based on previous knowledge this mutation should have relieved this mutant from CCR, but this effect was not seen in completeness in the studies. While some genes and operons were relieved from CCR or CCA [42, 47, 93-95] in this mutant, it was not quite true for some other genes and

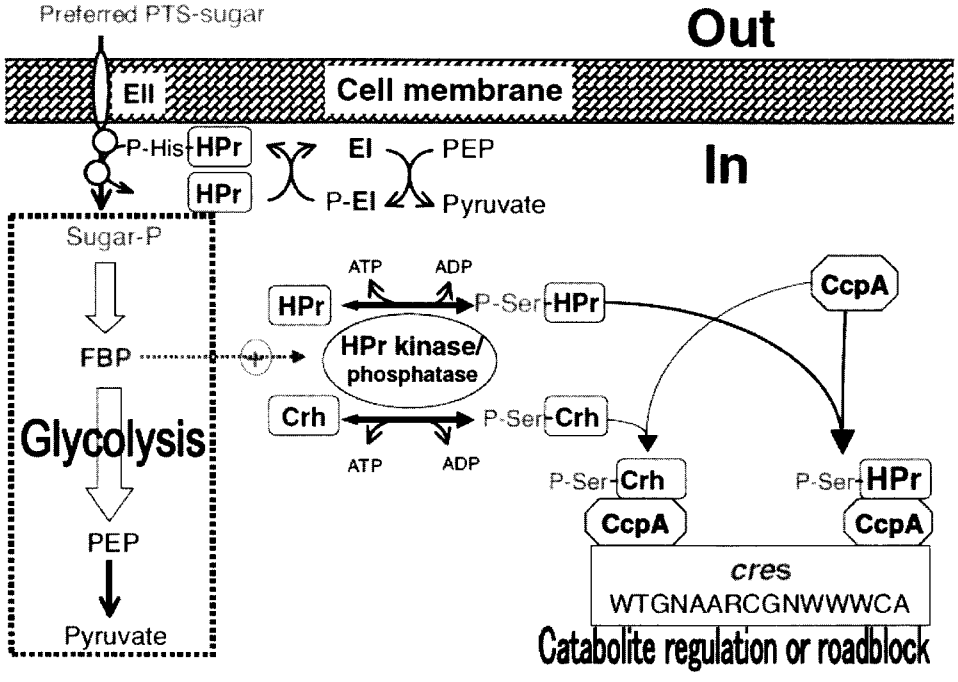

Figure 2.3: The molecular mechanism of CCR and CCA in B. subtilis. Figure shows ATP dependent phosphorylation of HPr and Crh at Ser-46 and their binding to CcpA and formation of P-Ser-HPr/CcpA and P-Ser-Crh/ccpA complexes, which can bind to 'cre' sites and cause CCR or CCA depending on the location of 'cre' sites. [26].

operons such as *gutB*, *acsA*, *ackA* [42, 56, 96]. But knocking out *ccpA* gene itself relieved CCR of CCA affect completely. This mystery wasn't solved until the sequencing of *B.*

subtilis genome, which found a protein similar to HPr, containing a region of sequence similar to HPr protein around Ser-46 residue. Further studies showed that this protein can also be phosphorylated in a similar manner as HPr by HprK/ phoshphatase [47]. Role of Crh in CCR became clear by studying mutants carrying either Crh mutation (*crh* knockout) or both Crh (*crh* knockout or Ser46Ala replacement) and HPr (Ser46Ala replacement) mutations. Mutants carrying both mutations showed complete relief from CCR, while single mutant Crh has no effect on CCR [46, 47, 95-97]. This shows that Crh only complements the CCR exerted by HPr, but it can not replace CCR of HPr by itself.

Structurally Crh is little different from HPr. In difference to HPr, it can form dimer in vitro, which was confirmed by its crystal structure and NMR [98, 99]. In similarity, replacement of Gln15His in Crh enables it to participate in its PEP dependent phosphorylation and PTS sugar transport [100].

Since single mutation of Ser46Ala in HPr did not completely relieved all CCR affected genes from CCR, *'cre'* sites of the genes not fully relieved from CCR by this mutation were compared for binding by CcpA:HPr or CcpA:Crh complexes. For all of these genes, both repressor:corepressor complexes had similar effects in protecting *'cre'* sites and positive stimulation of their binding to DNA sequences by FBP [46, 57]. Among the differences between the two complexes, P-Ser-Crh:CcpA couldn't bind to all the *'cre'* sites of CCR affected genes and had 10 times lower binding affinity as compared to Ser-46-HPr for CcpA itself. This difference in interaction with different *'cre'* sites could be attributed to the tiny differences between the DNA binding structures of P-Ser-HPr and P-Ser-Crh. While, in HPr 15^{th} and 20^{th} residues are His and Thr, these are Gln and Ala in Crh. These small differences cause changes in their interaction with

CcpA [101], which could in turn be responsible for differences in interaction of P-Ser-Crh:CcpA complexes with different *'cre'* sites.

Among gram positive microorganisms, 'Crh' is present in most *Bacillus* species [47, 102], although it has also been found in few other gram positive microorganisms. This protein exhibits higher sequence similarity among themselves as compared to their respective HPr's.

In summary, although 'Crh' can act as corepressor for some genes and operons in some carbon catabolite repression affected gram positive microorganisms including *Bacillus subtilis*, it is not essential for CCR in the presence of HPr. But it has been conserved in these microorganisms all along evolution. So, there might be some other essential role for Crh in these microorganisms, other than CCR.

2.2.1.10 Non-PTS glucose transport

Glucose utilization in *B. subtilis* is dependent on the uptake and phosphorylation by PTS system. Knocking out *ptsG* gene of PTS system encoding EII^{Glc}, makes *B. subtilis* unable to utilize glucose [103]. Other than PTS, glucose can also be transported through proton motive force dependent facilitator protein glucose permease, which is encoded by *glcP* [104]. But glucose transport by this facilitator requires an active PTS system as PTS- cells were unable to utilize glucose. After transport, glucose needs to be phosphorylated to glucose-6-phosphate to be further utilized in glycolysis. Although glucose kinase encoded by *glcK* has been identified in *B. subtilis*, it can only phosphorylate intracellular glucose produced by the hydrolysis of disaccharides or through non-PTS transport in an ATP dependent manner [105].

2.2.2 Pentose sugar transport and metabolism

2.2.2.1 Arabinose

Fermentative utilization of arabinose by *P. macerans* under fermentative conditions was first reported by Northrop et al. in 1919 [106]. In another study in 1987, involving sugar mixture utilization by *P. macerans*, consumption of arabinose in the presence of glucose was reported [24], but no information is yet available regarding the pathways involved in the arabinose utilization by this microorganism. Also, faster arabinose utilization than xylose in the sugar mixture fermentation was not explained in that study. Since no genetic information is available for the arabinose utilization by this microorganism, knowledge available from *B. subtilis* is described in this section.

. *B. subtilis* can utilize arabinose as sole carbon source. Arabinose transport in *B. subtilis* can occur through ATP binding cassette transporters (ABC) and secondary active transporters (symporters). AraN, AraP and AraQ proteins encoded by *araN*, *araP* and *araQ* respectively, in the *B. subtilis araABDLMNPQ-abfA* operon are the ABC transporter proteins (Figure 2.4) [107, 108] and AraE protein encoded by *araE* is the symporter protein, which is the main transporter of arabinose in *B. subtilis* [109]. While gene product of *araL* and *araM* genes is unknown, product of gene *abfA* encodes for the α-L-arabinofuranosidase. Genes *araA*, *araB* and *araD* of *ara* operon code for L-arabinose isomerase, L-ribulokinase and L-ribulose-5-phosphate 4-epimerase respectively and are involved in arabinose utilization. Knocking any one of these three genes leads to Ara- strain, which can not grow on arabinose; hence these three proteins are essential for the

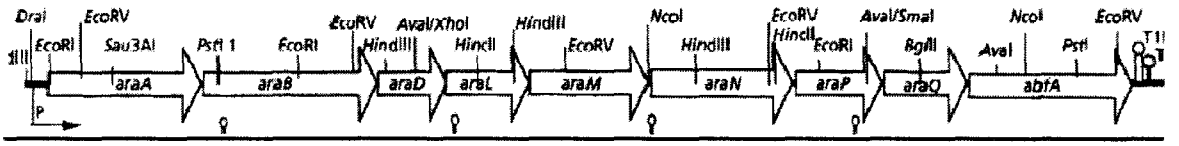

Figure 2.4: Genetic map of the ara region in the B. subtilis chromosome. Figure shows nine ORFs: araA, B, D, L, M, N, P, Q and abfA [107]

arabinose utilization by *B. subtilis*. After transport, arabinose is first converted to L-ribulose by L-arabinose isomerase, L-ribulose is then converted to L-ribulose 5-phosphate by L-ribulokinase, L-ribulose 5-phosphate is further converted to D-xylulose 5-phosphate by L-ribulose-5-phosphate 4-epimerase. After the last step, D-xylulose 5-phosphate further goes into central carbon metabolism through pentose phosphate pathway.

Expression of genes of *ara* operon and gene *araE* is induced by L-arabinose and repressed by glucose through carbon catabolite repression. The AraR protein, encoded by *araR* and located on a divergent transcriptional unit to *araE,* is the main transcriptional regulator of the *ara* operon [110]. Expression of *ara* operon and *araE* gene is negatively regulated by AraR and this regulation is modulated by the arabinose [111]. In the absence of arabinose, AraR binds to the operator sites located in the promoter regions of these operon and genes and blocks their expression. In the presence of arabinose, binding of arabinose to AraR leads to conformational changes in it such that it can no longer bind to the operator sites [112].

In the presence of glucose, CcpA, the master regulator of CCR in *B. subtilis*, together with phosphorylated HPr (P-Ser-HPr) binds to the two *'cre'* sites located in the *araABDLMNPQ-abfA* operon and blocks the expression of this operon. Out

of these two *'cre'* sites *cre araA* is located between *araA* gene and its promoter region, while *cre araB* is located within the *araB* gene [58].

2.2.2.2 Xylose

Xylose is a one of the most abundant pentose sugar found in the lignocellulose and can be utilized by many bacteria as a sole source of carbon and energy.

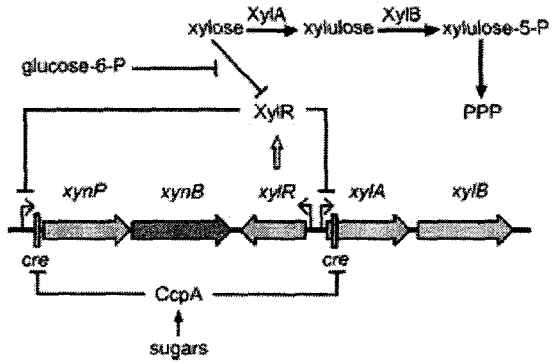

Figure 2.5: Xylose utpake and regulation in B. subtilis. Xylose is first converted to xylulose-5-P by the functions encoded in the adjacent xylAB operon. Xylulose-5-P finally enters the pentose phosphate pathway (PPP). The xylAB operon is repressed by binding of the Xyl repressor (XylR) to operator site in the absence of the inducer xylose. xylAB operon is subject to global CCR, which is mediated by binding of CcpA to 'cre' sites downstream of the promoters. In addition, glucose-6-phosphate contributes to CCR by acting as an anti-inducer for XylR [113].

Fermentative utilization of xylose utilization by *P. macerans* has been reported by Northrop et al. [106] and Schepers et al [24]. These studies showed that this microorganism can utilize xylose as sole source of carbon and energy. Although metabolic pathways involved in the xylose utilization were proposed based on the product profiles and enzyme activities in these studies, no genetic information is

available regarding the xylose utilization by this microorganism. Hence next few sections describe the knowledge available for xylose metabolism in *B. subtilis*.

It has been believed for long time that *B. subtilis* can not grow on xylose as a sole carbon source [114] because of absence of xylose specific transporter. Absence of any xylose specific transporter in *B. subtilis* is quite interesting as genes encoding proteins required for xylose metabolism after its transport have been known in this microorganism for a long time. Although no xylose transporter has been identified in its genome, constitutive expression of *araE* gene in *B. subtilis* mutants lead to the xylose utilization by this microorganism [109, 115, 116]. Further studies proved that AraE, whose expression is induced by arabinose can also nonspecifically transport xylose, but only in the presence of arabinose [116]. This finding seems consistent with earlier knowledge of presence of xylose metabolism genes in *B. subtilis* and both xylose and arabinose being found together in most natural compounds.

Xylose metabolism in *B. subtilis* occurs through conversion of xylose to D-xylulose 5-phosphate via D-xylulose through D-xylose isomerase and xylulokinase, which are encoded by *B. subtilis xylA* and *xylB* genes respectively (Figure 2.5). Then similar to arabinose utilization, D-xylulose 5-phosphate enters into pentose phosphate pathway to be further metabolized [117]. In *B. subtilis*, *xylR* is located in the same region as *xylA* and *xylB* and is transcribed divergently.

Regulation of these genes, responsible for xylose metabolism occurs at the transcriptional level. Expression of these genes is induced by xylose and repressed by glucose. In the absence of xylose, xylose repressor XylR (encoded by *xylR*) binds to the *xyl* operator sites, upstream of *xylA* transcription start site and terminates the transcription

of *xyl* operon, hence causing the repression of genes of *xyl* operon. In the presence of xylose, xylose binds to XylR causing a conformational change that makes it unable to bind to the operator site of *xyl* operon.

Glucose repression of *xyl* operon occurs by binding of P-Ser-HPr:CcpA complex on the *'cre'* site upstream of *xylA*. It has been reported that this catabolite repression also requires active XylR. In addition, glucose 6 phosphate, an intermediate of glucose utilization, is a *xyl* operon anti-inducer and can participate in carbon catabolite repression by glucose.

2.2.3 Glycerol transport and metabolism

Fermentative utilization of glycerol by *P. macerans* was reported by Northrop et al. [106]. No further study has been done since then for the utilization of

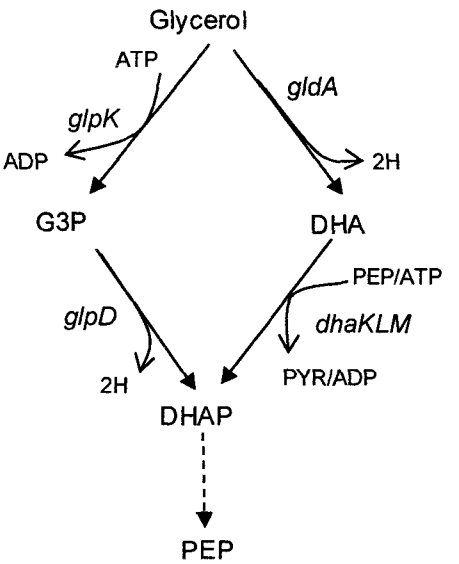

Figure 2.6: Glycerol utilization pathways under respiratory and fermentative conditions in bacteria. Left side of the diamond shows the glycerol utilization through G3P, where glycerol is converted to DHAP (respiratory pathway). Right side shows the conversion of glycerol to DHAP through DHA (fermentative pathway). (Adapted)

glycerol as a carbon source by this microorganism. Gram positive bacteria *B. subtilis* can utilize glycerol as sole source of carbon and energy. Glycerol uptake in *B. subtilis* occurs through energy independent diffusion process by a membrane channel protein GlpF of aquaporin family, which facilitates glycerol uptake. This protein is encoded by gene *glpF* and this gene is located on the *Bacillus glpPFKD* region [118]. Other genes in this region are involved in glycerol metabolism and its regulation. After glycerol uptake, it can be further metabolized by two pathways forming a diamond to make for same final intermediate metabolite dihydroxyacetone phosphate (DHAP) (Figure 2.6). On one side of diamond, intracellular glycerol is converted to glycerol-3-phosphate (G3P) by glycerol kinase (GK) in ATP dependent phosphorylation, G3P is then oxidized to DHAP by

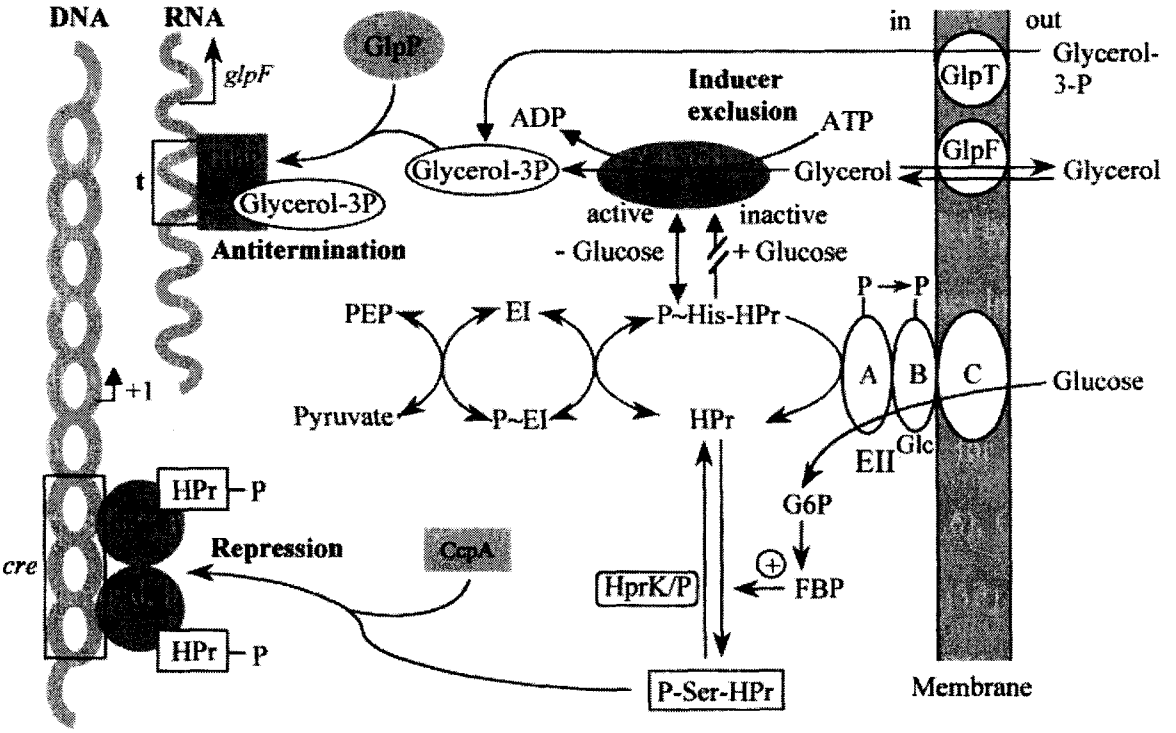

Figure 2.7: Mechanisms regulating expression of the B. subtilis glpFK operon at the DNA and RNA level. Similar to P-Ser-HPr, P-Ser-Crh can also interact with CcpA and therefore substitute for P-Ser-HPr in CCR of the glpFK operon. [45].

glycerol-3-phosphate dehydrogenase (G3PDH) [119]. In *B. subtilis* glycerol kinase is encoded by *glpK* and G3PDH is encoded by *glpD*. Expression of *glpK* and *glpD* is induced by glycerol-3-phosphate and repressed by glucose. Since P-His-HPr protein of PTS system phosphorylates glycerol kinase at its His residue and causes tenfold increase in its activity, phosphorylation of $EIIA^{Glc}$ by P-His-HPr residue partly controls the glycerol metabolism. In the presence of preferred carbon source such as glucose, there is a competition for the P-His-HPr and there is little phosphorylated glycerol kinase and very little glycerol is metabolized. Also, it has been reported that CcpA:P-Ser-HPr complex binds to the *'cre'* sites of the *glpFK* operon and causes partial CCR (Figure 2.7) [45, 120]. The remaining protein of the *glpPFKD* region, *glpP* codes for GlpP protein, which is positively acting regulatory protein. It mediates the antitermination of *glpD* transcription in the presence of G3P by preventing immature termination of *glpD* transcription, [121]. It can also participate in carbon catabolite repression through *glpFK* terminator mediated CCR in *B. subtilis* [45, 122]

Glycerol can also be metabolized through other side of the diamond through conversion of glycerol to dihydroxyacetone (DHA) by glycerol dehydrogenase; DHA is further converted to dihydroxyacetone phosphate (DHAP) by dihydroxyacetone kinase. Although genes responsible for glycerol metabolism through this part of diamond have not characterized, enzyme activities for these enzymes have been reported [123-125].

2.3 Central carbon metabolism

Although, metabolic model for the pathways and enzymes involved in the carbohydrate utilization by *P. macerans* has been proposed based on the product

stoichiometry and enzyme activities [23, 24], no genetic information is available in this microorganism for these pathways. Hence this section will describe the central carbon metabolism pathways in *B. subtilis*, which are very similar to the proposed pathways in the *P. macerans.*

After transport microorganisms metabolize carbohydrates through three pathways: EMP pathway, pentose phosphate pathway and ED pathway. Out of these pathways, while ED pathway is present and active in the *E. coli* during utilization of substrates such as gluconate, it is absent in the *B. subtilis*. EMP pathway and pentose phosphate pathway are the two main pathways, by which *P. macerans* and *B. subtilis* metabolizes carbohydrates.

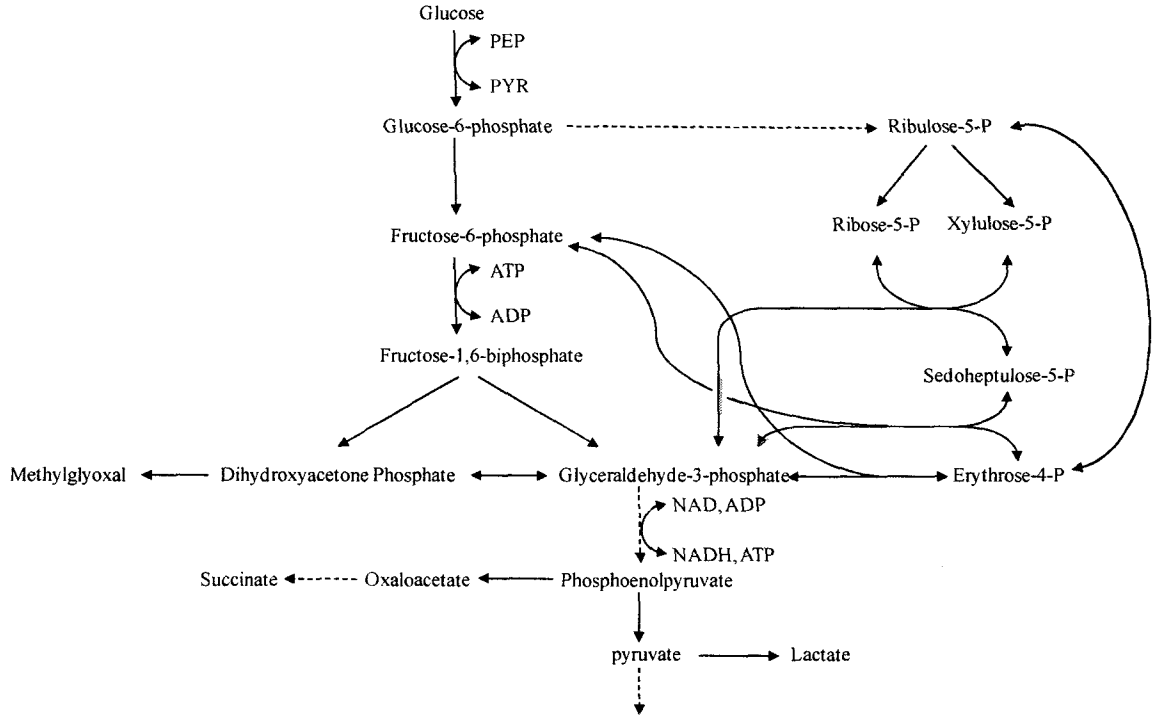

Figure 2.8: Central carbon metabolism pathways in B. subtilis. After transport, glucose is converted into fructose-1,6-biphosphate, which is further metabolized to pyruvate through glyceraldehyde-3-phosphate and phosphoenolpyruvate. Right side of the figure shows the pentose phosphate pathway. Routes for conversion of glucose to succinate or lactate are also shown in the figure.

During transport and phosphorylation by PTS system, the preferred carbon source glucose is converted to glucose-6-phosphate (G6P) (Figure 2.8). From G6P it enters into EMP pathway, in the first step it is converted in a reversible reaction to fructose-6-phosphate (F6P) by phosphoglucoseisomerase encoded by *pgi*. Mutants lacking this gene grow very slowly on glucose as pentose phosphate pathway, which can alternatively convert G6P to F6P is very inefficient. After that, F6P is converted to fructose 1,6-biphosphate (F-1,6-P) in an ATP dependent manner by phosphofructokinase (Fructose-6-phosphate-1-kinase) coded by *pfkA*. F-1,6-P is then can be converted to dihydroxyacetone phosphate (DHAP) or glyceraldehyde-3-phosphate (Gly3P). DHAP and Gly3P can be inter converted among themselves by triphosphate isomerase (encoded by *tpiA*). At this step, accumulation of DHAP is harmful for the cells as it can be easily converted to methylglyoxal by methylglyoxal synthase, which is very toxic to the cells. Then, through a series of steps Gly3P is converted to phosphoenolpyruvate (PEP). PEP can then be converted to pyruvate or succinate. Succinate produced can be found in the extracellular medium and pyruvate enters into fermentative metabolism after that. In overall, through glycolysis glucose is converted to two molecules of pyruvate with the production of two ATPs and two reducing equivalents.

Other than EMP pathway, glucose can also be metabolized through pentose phosphate pathway. Although this is not the main pathway for glucose utilization, it is still very important because three of the precursor metabolites required for biosynthesis are produced through this pathway. Pentose phosphate pathway is generally divided into two parts: initial oxidative branch and non oxidative later part. In oxidative branch G6P is converted to D-glucono-1,5-lactone-6-phosphate (G-1,5L6-P) by glucose-6-phosphate-1-

hydrogenase encoded by *zwf* in a NADP dependent and irreversible manner. G-1,5L6-P is further converted into 6-phospho-D-gluconate (6PG) by a still uncharacterized enzyme in *B. subtilis*. Further, 6PG is converted to ribulose-5-phopshate (RL5P) by 6 phosphogluconate dehydrogenase in a NADP dependent manner with liberation of one mole of CO_2. Although, three isozymes of above enzyme have been found in *B. subtilis*, only one coded by *gndA/yqjI* has been found active in pentose phosphate pathway. Further in the non-oxidative branch, R5P is converted to glyceraldehyde-3-phosphate (Gly3P) and fructose-6-phopshate (F6P) in a series of reactions. These F6P and Gly3P join the main carbon metabolism pathway EMP as shown in the figure, to be further metabolized.

Other carbohydrates including pentoses such xylose and arabinose are converted to xylulose-5-phosphate through a series of steps. These pentoses then enter the central carbon metabolism through the non-oxidative branch of the pentose phosphate pathway through the xylulose-5-phosphate. Further xylulose-5-phosphate is converted to fructose-6-phosphate or glycerldehyde-3-phosphate in a sequence of reactions as described before.

2.4 Fermentative metabolism

Fermentative utilization of glucose and xylose by *P. macerans* has been reported in previous studies [23, 24]. These studies show that ethanol and acetate are the main fermentation products of sugar utilization by this microorganism, while formate and acetone are minor products. In the fermentative utilization of sugars by its close relative *B. subtilis*, no formate and acetone is detected in the culture media, while we see the

production of lactate and 2,3 butaendiol. This shows that although *P. macerans* is close relative of *B. subtilis*, there are major differences in the fermentative pathways between the two microorganisms. Since no genetic information is available for the fermentative utilization of sugars by *P. macerans*, this section will talk about fermentative pathways in bacteria.

Phosphoenolpyruvate (PEP) produced in the glycolysis is generally goes through two routes in microorganisms depending on cellular requirements. In the first route, it can convert to succinate through oxaloacetate (OAA) in a series of reactions with consumption of CO_2 and reducing equivalents. This pathway has been shown to exist in gram negative model microorganism *E. coli*, but no corresponding enzyme converting PEP to OAA, has been found in *B. subtilis*. Since some of the intermediates involved in the conversion of PEP to succinate, also participate in TCA cycle as explained in the next section, there presence doesn't imply that they are produced as result of the conversion of PEP to OAA. Also, in the gluconeogenesis OAA can be converted to PEP by PEP carboxykinase (encoded by *pckA*) in an irreversible manner. In the second route, PEP is converted to pyruvate with the generation of one ATP, by pyruvate kinase encoded by *pyk*.

Pyruvate can go through several routes after that. In the first one it is converted to lactate with the consumption of one reducing equivalent by lactate dehydrogenase (encoded by *lctE*) (Figure 2.9). In the second route pyruvate is converted to Acetyl coenzyme A (AcCoA) with the production of CO_2 and one reducing equivalent by pyruvate dehydrogenase. Although this pathway generates one more reducing

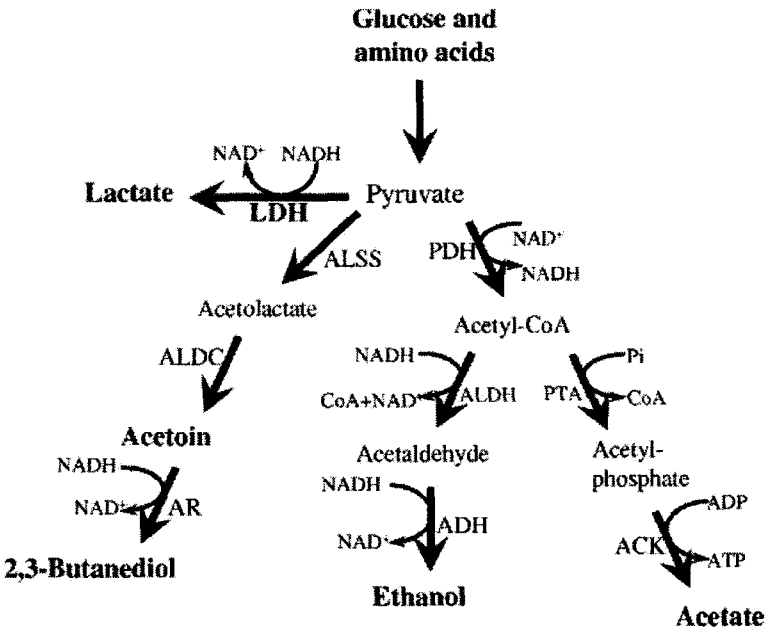

Figure 2.9: Bacillus subtilis fermentation pathways. ALDC, acetolactate decarboxylase; AR, acetoin reductase; PDH, pyruvate dehydrogenase; CoA, coenzyme A; ALDH, acetaldehyde dehydrogenase; PTA, phosphotransacetylase; ACK, acetate kinase. (Adapted from [126])

equivalent in addition to the two produced during glycolysis and there is no electron acceptor present during fermentation, it has been found active during fermentative metabolism in *B. subtilis*.

In the third route, pyruvate is converted to AcCoA together with production of formate by pyruvate formate lyase (PFL). This formate is either secreted extracellularly or is converted to hydrogen and CO_2 by formate hydrogen lyase (FHL), depending on the pH of the medium. Since conversion of AcCoA through this pathway does not generate any reducing equivalents, this is the main pathway for conversion of pyruvate in fermentative metabolism of microorganisms such as *E. coli*. No corresponding enzymes have been reported for the *B. subtilis*, although PFL activity and formate production has been reported in the case of *P. macerans*.

B. subtilis also have the pathway to convert pyruvate to 2,3-butanediol (BDO) through acetolactate and acetoin. First, pyruvate is converted to acetolactate and CO_2 by acetolactate synthase (encoded by *alsS*), then acetolactate is converted to acetoin by acetolactate decarboxylase (encoded by *alsD*) together with the production of CO_2. In the presence of oxygen, unstable acetolactate can convert to diacetyl spontaneously and then diacetyl is converted to acetoin by acetoin dehydrogenase with a consumption of one reducing equivalent. Conversion of acetoin to BDO occurs in a reversible manner by a single enzyme. Enzyme for forward reaction has been called acetoin reductase and for the reverse reaction has been called 2,3-butanediol dehydrogenase. Gene coding for this enzyme (*bdhA*) has been reported recently [127]. Pyruvate can also converted to the TCA cycle intermediate OAA by pyruvate carboxylase (encoded by *pycA*).

AcCoA, coming from pyruvate can be converted to two products: acetate and ethanol. Conversion of AcCoA to ethanol occurs via acetaldehyde along with the consumption of two reducing equivalents. First, AcCoA is converted to acetaldehyde by acetaldehyde dehydrogenase and then acetaldehyde is further converted to ethanol by alcohol dehydrogenase. Consumption of reducing equivalents in this pathway is very important for the overall redox balance during the fermentative utilization of glucose as there is no electron acceptor such as oxygen is present and by consuming the reducing equivalents generated during the glycolysis this pathway helps in maintaining redox balance. In the second energy generating pathway, AcCoA is converted to acetate via acetyl phosphate. First, AcCoA is converted to acetyl phosphate by phosphotransacetylase (encoded by *pta*) (PTA) and then acetyl phosphate is converted to acetate by acetate kinase (ACK) (encoded by *ackA*) and generating one mole of ATP

along the way. Formation of acetone (not seen in sugar fermentation by *B. subtilis* and *E. coli*) in the case of sugar fermentation by *P. macerans* has been proposed to occur through the conversion two moles of acetate to acetone via acetoacetate.

Similar to *E. coli*, there are few global anaerobic regulators, which control the expression of genes during the fermentative metabolism. FNR (Fumarate-Nitrate reduction regulator), one of these regulators, partially controls the expression of *lctE*, *alsS* and *alsD* by inducing their expression under anaerobic conditions [128]. This induction and subsequent consumption of reducing equivalents in these pathways balances the redox equivalents generated during the glycolysis. Opposite to this, expression of *pta* gene, involved in the energy generation pathway for the cell is unaffected by global redox regulator FNR, but its expression is induced by the carbon catabolite repressor CcpA in the presence of glucose [129, 130]. Out of the four pathways for the dissimilation of pyruvate into lactate, BDO, ethanol and acetate; deletions of *lctE* of lactate pathway and *pta* of acetate pathway severely reduce the cell growth significantly, while *alsSD* deletion doesn't affect the cellular growth [131]. These observations clearly show the intricate mechanisms involved in the cellular requirements of energy generation in the form of ATP and redox balance during the fermentative metabolism.

2.5 TCA cycle

Tricarboxylic acid (TCA) cycle has been generally associated with the aerobic growth and provides energy and reducing equivalents in this environment. It also plays another very important role of providing intermediates for the production of several

amino acids for cellular metabolism. TCA cycle can be divided into two parts, oxidative branch on the right side of the cycle and reductive branch on the left of the cycle. At the

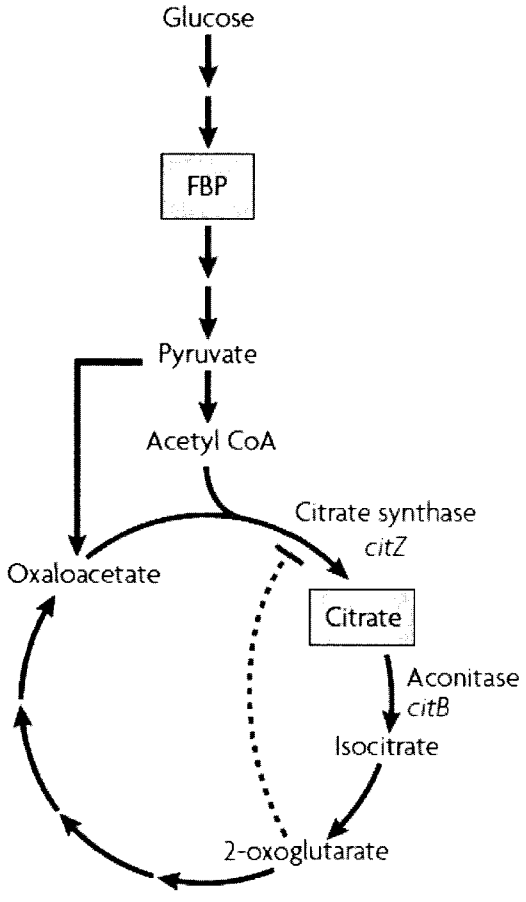

Figure 2.10: TCA cycle in B. subtilis. Figure shows the conversion of Acetyl-CoA to citrate, which converts to icocitrate, 2-oxyglutarate and oxaloacetate in a sequential manner. Since B. subtilis doesn't have glyoxylate shunt, it is not shown in the figure. (Adapated from [132])

start of the oxidative branch, AcCoA coming from pyruvate reacts with OAA to form citrate, in a reaction catalyzed by citrate synthase (encoded by *citA* and *citZ*). Citrate is then converted to α-ketoglutarate (KG) via isocitrate with the production of CO_2 and reducing equivalents along the way. In the next step, KG is converted to succinyl CoA by 2-keto glutarate dehydrogenase (encoded by *odhAB* and *pdhD*). Succinyl CoA is further

converted to succinate by succinyl CoA synthetase (encoded by *sucCD*) and producing one ATP. The reductive branch of left side can work in both directions depending on the carbon source and presence of oxygen. This branch starts with succinate converting to fumarate by succinate dehydrogenase (encoded by *sdhCAB*). Fumurate is further converted to malate by fumarase (encoded by *citG*). Malate is then converted to OAA by malate dehydrogenase (encoded by *citH*) and completing the TCA cycle.

Regulation mechanism of expression of TCA cycle genes is different among various microorganisms. In gram negative *E. coli*, expression of genes of KG to succinate pathway is regulated by global redox regulators and is impaired during fermentative metabolism. Hence TCA cycle can not be completed through this pathway. Instead during fermentative growth, in the reductive branch, OAA is converted to succinyl CoA in a reverse direction and produces all the intermediates of the reductive branch of the TCA cycle. *B. subtilis* is different to *E. coli* for TCA cycle in two respects: the regulation of gene expression as well as reductive pathway itself. First, most the TCA cycle genes in *B. subtilis* are regulated by CcpA, which is main signal molecule for the carbon catabolite repression. Hence, in the presence of glucose, expression of TCA cycle genes is repressed. As a result, when both glucose and glutamate are present in the media, although oxidative branch genes are not expressed, there is no effect of it on cell growth as cells already have necessary precursors for making macromolecules [133, 134]. In the reductive pathway of TCA cycle during anaerobic growth, fumarate needs to be converted to succinate by fumarate reductase, but no gene encoding for this enzyme has been found in *B. subtilis*. As a result, reductive branch can not be completed under anaerobic conditions.

Another important part of the TCA cycle is glyoxylate shunt, which connects isocitrate to succinate by bypassing KG and succinyl CoA. In this pathway, isocitrate from the oxidative branch dissociates into succinate and glyoxylate by isocitrate lyase. Further, glyoxylate together with one mole of AcCoA are converted to malate by malate synthase. Although, glyoxylate shunt has been found in many gram positive and gram negative microorganism, it does not exist in the *B. subtilis*. As a result, while many microorganisms can grow on acetate or fatty acids as sole carbon source using glyoxylate shunt, *B. subtilis* can not grow on these substrates.

2.6 Synthesis of building blocks and macromolecules

Proteins, nucleic acids and lipids are major macromolecules of the microbial cell. Synthesis of these macromolecules through building blocks in the cell occurs from the precursor metabolites, energy and reducing equivalents. The main macromolecule of the cellular environment, proteins is made up of the twenty different amino acid monomers. The number of amino acids used and in the order which are they used to form the protein molecule determines the various properties of proteins such as their structure and function. The twenty amino acids have been divided into the six families based on their common precursor metabolites. Incorporation of nitrogen in the amino acids occurs via biosynthesis of glutamate from α-ketoglutarate in the TCA cycle. Addition of a molecule of ammonia and ATP converts glutamate to glutamine. Hence, oxidative branch of TCA cycle is very important for the cell maintenance and generation of building blocks. Another important point is the distribution of amino acid precursors in the metabolic reactions; these precursors are distributed at different points throughout the

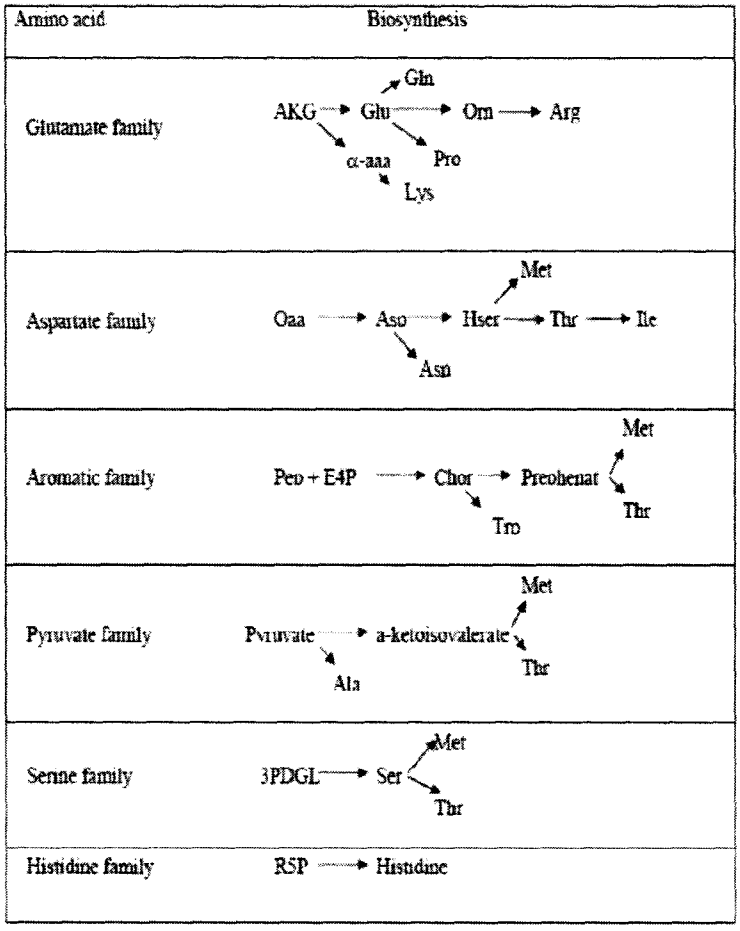

Figure 2.11: Overview of amino acids formation according to family [28].

glycolysis and TCA cycle and their production as well as consumption for the amino acids biosynthesis is tightly regulated at different points of cellular cycle.

Second macromolecule, nucleic acids are made by polymerization of nucleotides: Ribonucleotides (AMP, GMP, UMP and CMP) and their deoxy form deoxyribonucleotides (replacement of 2'-OH group in ribonucleotides with hydrogen) (dAMP, dGMP, dUMP, dCMP). Polymerization of nucleotides leads to the production of ribonucleic acids (RNA) or deoxyribonucleic acids (DNA). Nucleotides are made from three components: a nitrogenous base (a purine (adenine(A) or guanine(G)) or pyrimidine (cytosine(C) or uracil(U) or thymine(T))), pentose sugar (D-ribose or 2-deoxyribose) and

phosphate groups (mono, di or triphosphates). Precursors for purines are ribose-5-phosphate and 3-phospho-D-glycerate and for pyrimidines are OAA, which are formed in pentose phosphate pathway, glycolysis and TCA cycle respectively. Nucleotides are also part of cofactors like NAD, FAD or Coenzyme A (CoA).

Lipids are the third important macromolecule of the cell and are made from fatty acids. Lipids are used for energy storage, cell wall and vitamins synthesis. In contrast to *E. coli*, *B. subtilis* synthesizes both even and odd numbered saturated and unsaturated fatty acids. Another major difference is the occurrence of branched chain fatty acids as compared to straight chain fatty acids, which are the main type of fatty acids in *E. coli*.

Chapter 3

Metabolic flux analysis: a review

Metabolic flux analysis (MFA) is an important tool for the study of cell physiology and insights gained from this analysis can be used in different ways to achieve the desired outcome. In industrial biotechnology, often the objective is the production of desired chemical or fuel at high productivities with no byproducts. MFA is a very useful tool in such a scenario as it provides the information about the roles different cellular pathways and reactions play in the production of a specific product. Many attempts have been made to model cellular behavior for a long time, dating back to year 1979 [135], but knowledge of the cellular physiology is still incomplete today because of its inherent complexity. Metabolic fluxes which are defined as "the rate at which material is processed through a metabolic pathway" [22] are the basis for the MFA. In any biological study, it is important to carryout MFA because it gives a direct knowledge about the role each metabolic pathway plays in the utilization of a given substrate. Knowledge gained from this analysis is very useful in development of metabolic engineering strategies.

MFA is most useful in finding the differences in metabolic fluxes between two different conditions, which could be two different growth conditions for the same strain or two different strains under same growth conditions [28]. Comparison of the metabolic fluxes obtained through this analysis provides the knowledge about the intracellular reactions and pathways, which is not available through other tools. Such a comparative analysis offers the information about the critical branch points in the

metabolic network and how fluxes around such a branch point change with the environmental or genetic changes. Some of these branch points could be rigid, while others might be more flexible [136]. It is harder to change fluxes around the rigid branch points as compared to flexible ones. This kind of knowledge helps in formulating rational design strategies for improving the production of the desired product.

MFA can also be used a pathways discovery tool. This analysis is based on the mass balances around the intracellular metabolites based on the reaction stoichiometry. Building such a model requires the knowledge of the all the routes leading to an intracellular metabolite, which is not always available. In those cases, mass balances around an intracellular metabolite can provide the clues about possible missing pathways, which were not included in the model. In a different scenario, MFA can identify alternate routes between two intracellular metabolites, which might not be visible otherwise [28]. Although, these alternate routes may or may not be feasible under the given conditions. MFA can also find the pathways considered in model, which will not satisfy the requirements of material balances around intracellular metabolites [135]. These pathways can then be eliminated from the model as a result of MFA. This analysis also provides the maximum theoretical yield values for the desired product from a given substrate through various possible pathways, which can be used to decide, which pathway or substrate to use to maximize the production of desired metabolite.

One of the main reasons for using the MFA in any study is that it is a quantitative analysis, in which the values for the intracellular fluxes are calculated from the experimentally measured fluxes. First, mass balance equations for each of the intracellular metabolites are written based on the reaction stoichiometry. Then these

equations are used to create the reaction network model, which is solved for the intracellular fluxes. The extracellular fluxes are often the substrate uptake rates or the production rates of extracellular metabolites. By solving the reaction network model, we get the flux values for each step of the reaction network model. Then, a metabolic reaction diagram is created and fluxes values are written for each of step in the diagram.

Another advantage of MFA is that it is an *in vivo* analysis, compared to the flux balance analysis (FBA), which is an *in silico* analysis. In the FBA, a reaction network model is build based on the reaction stoichiometry [137], but instead of using extracellular measurements, an objective function is optimized for a cellular characteristic such as cell growth [138] or substrate consumption. Since without the measured extracellular flux values, this system of equations will have a large solution space, additional constraints on some of the fluxes are added to solve this system [139]. As FBA doesn't use any experimental data, it is important to have comprehensive information about the metabolic reactions in this analysis. Since it is very difficult to have such detailed information about any microorganism, fluxes obtained through FBA are often erroneous.

In the case of MFA, extracellular measurements play the role of the constraints, but since these are the *in vivo* values, fluxes obtained from this analysis are inherently more accurate than the FBA calculated fluxes. Other than extracellular measurements, information about the cofactors utilization in the reaction network can provide additional constraint for the reaction network. In case of well studied organism such as *E. coli* such information is readily available and in these cases balance on the cofactors $NADH/NAD^+$ can be applied to obtain additional constraint. Next section

describes the development of reaction network and mathematical formulation of the model for the MFA.

3.1 Theory and metabolic fluxes

The first step in the MFA is knowledge of stoichiometry of each reaction of the various metabolic pathways in the given microorganism. This includes all the steps in the conversion of the substrate to an extracellular metabolite or biomass. In this context, it is important to define the main constituents of this analysis as it is very important for writing balance equations later on. Here, substrate is defined as any compound present in the medium, which can be utilized by cells as carbon, energy or nitrogen source [28]. Extracellular metabolite is any compound secreted by cells in the medium. Intracellular metabolite is any compound, which remains inside the cell and therefore not excreted. During the utilization of a given substrate, distinction between intracellular metabolites and extracellular metabolites is not always clear, as metabolites such as formate can be inside the cell or excreted as well. In such cases, intracellular and extracellular portions are considered as two different entities.

Detailed knowledge about the reaction stoichiometries of metabolic reactions of the well studied microorganisms is available in public and can be found in the databases such as (ECOCYC, KEGG, WIT, etc.) [140-142]. When considering these reactions it is important to keep in mind the growth conditions and the substrate of your study, as not all metabolic reactions are active under a particular condition and eliminating such reactions from the start reduces the model complexity later on. Writing all the possible reactions under a given condition in the microorganism of study gives a

metabolic reaction network, which can be written in general terms as follows [28]. If we have N substrates (S_i), M extracellular products (P_i), Q biomass constituents ($X_{macro,i}$) and K intracellular metabolites ($X_{met,i}$) in the J reactions, we can write the jth reaction in general terms as follows:

$$\sum_{i=1}^{N} \alpha_{ji} S_i + \sum_{i=1}^{M} \beta_{ji} P_i + \sum_{i=1}^{Q} \gamma_{ji} X_{macro,i} + \sum_{i=1}^{K} g_{ji} X_{met,i} = 0 \qquad (3.1)$$

Where α_{ji} is the stoichiometric coefficient for i^{th} substrate in j^{th} reaction, β_{ji} is the stoichiometric coefficient for i^{th} product in j^{th} reaction and so on. Writing stoichiometry for all the J reactions in matrix form gives:

$$AS + BP + \Gamma X_{macro} + GX_{met} = 0 \qquad (3.2)$$

Where A, B, Γ and G are stoichiometric matrices containing stoichiometric coefficients in the J reactions for the substrates, products, biomass constituents and pathway intermediates, respectively. Because of the generic nature of equation 3.2, a large number of stoichiometric coefficients are generally zero in these matrices.

The rate of reaction of a specific reaction is defined as the rate at which a particular compound is being consumed or produced. Generally when reactions are written, stoichiometric coefficient of one of the compound in that reaction is made one and that rate of formation or consumption of that compound is defined as rate of reaction, v. In cellular reactions, this rate is specific rate of formation or consumption with unit mol/g DW hr. By convention, rates of formation are considered positive and rates of

consumption negative. In general terms, rate of formation of i^{th} product in j^{th} reaction can be written as $\beta_{ji}v_j$, similarly rate of consumption of i^{th} substrate in j^{th} reaction can be written as $\alpha_{ji}v_j$. Hence, net of rate of production of i^{th} product can be written as

$$r_{P,i} = \sum_{j=1}^{J} \beta_{ji} v_j \tag{3.3}$$

or writing the net rates of production for all the products M in general matrix notation gives

$$r_P = B^T v \tag{3.4}$$

3.2 Development of metabolic flux model

During the cell growth, mass balance around intracellular metabolites at any given time t gives:

$$\frac{dX_{met}}{dt} = r_{met} - \mu X_{met} \tag{3.5}$$

where r_{met} is the vector representing the net rate of formation of metabolites and μ is the maximum specific growth rate of cells. In this equation the term 'μX_{met}' represents the consumption of intracellular metabolites due to the cell growth [28]. In the exponential phase of cell growth, intracellular metabolites are consumed at high rates and they are at pseudo steady state in this period. This makes the left hand side of the equation 3.5 zero. Also, second term of the equation 3.5 is a dilution term, but since the concentrations of

intracellular metabolites during initial growth phase are relatively small, this term can be neglected in the equation 3.5. After these assumptions, this equation becomes

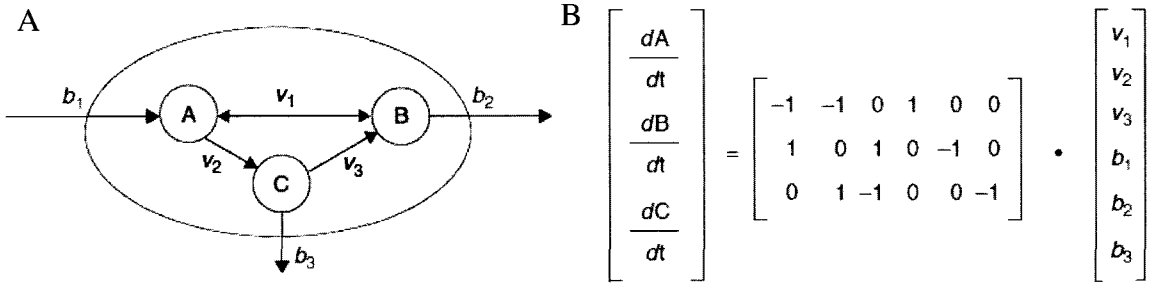

Figure 3.1 (A) A reaction network consisting of three metabolites (A, B, and C), three transport reactions, and three enzymatic reactions is constructed. v_i indicates the flux through reaction i and b_j represents the flux through transport reaction j. (B) stoichiometric matrix for the system shown in (A). Adapted from [143]

$$r_{met} = 0 \tag{3.6}$$

From the notation used in the equation 3.4, r_{met} can also be written that

$$r_{met} = G^T v \tag{3.7}$$

Figure 3.1 shows the mathematical formulation of a typical reaction network in the form of equation 3.7. Combining the equations 3.6 and 3.7 gives us the following equation, where G^T is the matrix of stoichiometric coefficients of all the intracellular metabolites and v is the matrix of all the reaction rates.

$$G^T v = 0 \tag{3.8}$$

Since some of rates in the reaction rate matrix are known, through the rates of formation of extracellular metabolites, stoichiometric matrix G^T can be divided into two parts: calculated part (G_c^T and ν_c) and measured part (G_m^T and ν_m). Applying this nomenclature to equation 3.8 gives

$$G_c^T \nu_c + G_m^T \nu_m = 0 \tag{3.9}$$

Since our aim is to calculate the intracellular fluxes ν_c, rearranging the equation 3.9 gives

$$\nu_c = - (G_c^T)^{-1} (G_m^T \nu_m) \tag{3.10}$$

where $(G_c^T)^{-1}$ is the matrix inverse of G_c^T. In the above equation since G_m and G_c are already known from reaction stoichiometry and ν_m is known through extracellular measurements, intracellular flux matrix ν_c can be easily calculated. To solve this system of equations there are couple of conditions, first is that all the rows of the matrices G_c and G_m should be linearly independent, which means that no row should be linear combination of two other rows in the matrix. Second condition is that to obtain inverse of matrix G_c^T, it should be square and its determinant should be non zero.

Another important point to remember in solving this system of equation is that the system should be exactly determined, which means that the number of unknown fluxes should be equal to the number of intracellular metabolite balance equations. If the number of calculated fluxes is more than the number of balance equations, the system is underdetermined and can not be solved without extra equations. In that case, additional

constraints are added on the calculated fluxes and system of equations is solved through optimization routines. In cases, when number of calculated fluxes is less than the number of intracellular metabolite balance equations, system is overdetermined [28] and solution matrix v_c is obtained through Moore-Penrose pseudo inverse, which gives

$$v_c = - (G_c^T)^{\#} G_m^T v_m \tag{3.11}$$

$$\text{where} \quad (G_c^T)^{\#} = (G_c G_c^T)^{-1} G_c \tag{3.12}$$

This method of solving overdetermined system is suited for the cases, where there is little noise in the system and these noises are equally distributed. The solution in the overdetermined case represents the least square estimate for the nonmeasured fluxes under these assumptions. If this is not the case, mass balances around some of the nodes in the metabolic network will not be exactly satisfied. Another method for solving overdetermined systems is Tsai and Lee method [144], which provides the better estimates for both measured as well calculated fluxes.

3.3 Identifiability of fluxes

One of the important issues with solving the system of equations for calculating unknown fluxes is that the equation 3.10 should have solution. As discussed in above paragraphs, this equation has a solution only if the system is exactly determined, which can be easily found out through the matrix operations on the G_c^T. If it has full rank, which means rank of this matrix is equal to the number of metabolite balances, then the

matrix is invertible and no row of the matrix is linear combination of other two rows in the matrix [28]. Calculation of rank of matrix G_c^T, helps in identifying any redundant equations in the system of reactions and removing such equations from the system helps in solving it. IF after applying this method system is underdetermined, then it is solved by applying constraints and optimization routines.

3.4 Consistency of data

Since MFA is a very useful tool in the decision making for the metabolic engineering strategies, it is extremely important that the results obtained from this analysis are accurate and reliable, which depends on the accuracy of the model being used to calculate the fluxes for intracellular metabolites as well as on the extracellular measurements. Since MFA analysis is based on the mole balances of intracellular metabolites, other type of balances such as elemental balances can be used to check the consistency of the data. One of the popular elemental balance is around carbon, where number of carbon atoms going into the system through substrate are balanced against the number of carbon atoms coming through the extracellular products. As chemical structures of substrates and extracellular products are already known, it is very easy to carbon atoms in these compounds, but similar information is often not available about the carbon atoms going into the biomass and hence it is very difficult to perform accurate carbon balances. Same arguments cam also be made for other elemental balances such as nitrogen, oxygen, sulfur and hydrogen. Another method, which can be used to check the consistency of the data, is the redox balance analysis. In this, sum of the multiplications

of the products moles into their oxidation states should be equal to the multiplication of moles of substrate into its oxidation state.

Chapter 4

Materials and methods

4.1 Strains

Wild-type *P. macerans* Northrop 234A (LMG 13285: referred to as N234A here) was obtained from Belgian Co-ordinated Collections of Microorganisms (BCCM/LMG, Gent, Belgium) and used throughout this study, unless otherwise specified. *P. macerans* strains B-394 (NRRL collection, Peoria, IL) and ATCC 7068 (American Type Culture Collection, Mannassas, VA) were also tested for their ability to ferment glycerol. Wild-type K12 *E. coli* strain MG1655 was obtained from the University of Wisconsin *E. coli* Genome Project (www.genome.wisc.edu) [145]. The strains were kept in 32.5% glycerol stocks at -80 ^{0}C. Plates were prepared using Luria Bertani (LB) medium containing 1.5% agar.

4.2 Culture medium and cultivation conditions

4.2.1 Media

The following medium compositions were used for the various culture conditions described later. These media were sterilized by either autoclaving or using 0.22 μm syringe filters prior to use. All chemicals were obtained from Fisher Scientific (Pittsburgh, PA) and Sigma-Aldrich Co. (St Louis, MO).

Solid media plates: The LB plates were prepared by first making a solution consisting of 25.0 g/l LB broth (Fisher Scientific) and 15.0 g/l agar (Fisher Scientific) in nanopure water. This solution was then sterilized by autoclaving for 15 minutes at 121°C. Subsequently, the solution was poured into Petri dishes (Fisher Scientific, Pittsburgh, PA) in a sterile hood and left to cool for about 10 minutes at room temperature. The liquid media solidified upon cooling in the Petri dishes, was kept overnight at room temperature for drying and then were stored in 4°C for later use.

Glycerol stock media: The media for glycerol stock had the following composition: 65% glycerol (v/v), 0.1 M $MgSO_4$ and 0.025 M Tris-HCL, pH 8.0. 0.5 mL of this media was added to 0.5 mL of cell culture in LB media and subsequently stored at -80°C.

Glycerol fermentation media: The minimal medium described by Schepers et al. [24] was used with minor modifications. The medium contains the following components (per liter final volume): 6.8 g KH_2PO_4, 3 g NH_4Cl, 1 g KCl, 0.2 g $MgSO_4.7H_2O$, 30 mg $MnSO_4.H_2O$, 30 mg Ethylendiamintetraacetate (EDTA), 10 mg $CaCl_2.2H_2O$, 5 mg Na_2MoO_4, 5 mg $FeSO_4.7H_2O$, 5 mg H_3BO_3, 3 mg $CoCl_2.6H_2O$, 1 mg $CuSO_4.5H_2O$, 1 mg $ZnSO_4.7H_2O$, 1 mg Nicotinic acid, 2 mg biotin, 2 mg p-amino benzoic acid, and 2 mg thiamine hydrochloride. Unless otherwise specified, the medium was supplemented with 10 g/L glycerol, 0.5 g/L sodium citrate and 1 g/L tryptone for glycerol fermentation. Experiments in "low phosphate and potassium" medium were conducted by replacing KH_2PO_4 and KCl with 0.35 g NaH_2PO_4 and 8.37 g MOPS (morpholino-propanesulfonic acid), on per liter basis. All chemicals were obtained from Fisher Scientific (Pittsburg, PA) and Sigma Aldrich (ST. Louis, MO).

Sugar fermentation media: Minimum media described above was also used in the sugar fermentations. This medium was supplemented with 10 g/l tryptone and 5 g/l yeast extract and respective sugar (glucose, xylose or arabinose) at a concentration of 10 g/l in the individual sugar experiments. For the sugar mixture fermentations, all three sugars were used at concentration of 10 g/l each, with total concentration of 30 g/l.

4.2.2 Culture conditions

Glycerol fermentation: Fermentations were conducted in a 750 mL fermentation system from Ward's Natural Science (Rochester, NY), with a working volume of 500 mL and independent control of temperature, pH, and stirrer speed. The pH was controlled at the desired set points using a Jenco 3671 pH controller fitted with a Jenco 600p pH probe (Jenco, San Diego, CA). Base (2M NaOH) for pH control was added by gravity flow using a pinch valve (Bio-Chem Inc., Boonton, NJ) connected to the pH controller. The stirrer speed was maintained at 200 rpm by using a Fisher Scientific Isotemp stirring plate (Pittsburg, PA). Anaerobic conditions were maintained by sparging the medium with ultrahigh purity argon (Matheson Tri-Gas, Inc., Houston, TX). Sterile conditions were achieved by using 0.2 mm and 0.45 mm HEPA filters (Millipore, Billerica, CA) to fit the inlet and outlet lines, respectively. Experiments conducted in tubes (specified in each case) were carried out using 17-ml Hungate tubes (Bellco Glass, Inc., Vineland, N.J.), which were modified by piercing the septa with two luer lock needles, one for oxygen-free argon sparging (20G × 2", Hamilton Company-USA, Reno, Nevada) and one for gas efflux (20G × 8", Hamilton Company-USA, Reno,

Nevada). Mixing was achieved through the rising gas bubbles. The working volume of these modified Hungate tubes was 10 ml.

Prior to use, the cultures (stored as glycerol stocks at -80 °C) were streaked onto LB plates and incubated at 37 °C. Single colonies were used to inoculate 17.5 mL modified Hungate tubes (see above) containing 10 ml of the medium described above supplemented with 10 g/L tryptone, 5 g/L yeast extract, and 5 g/L glycerol. The tubes were incubated at 37 °C until an OD_{550} of ~0.4 was reached. An appropriate volume of this actively growing pre-culture was centrifuged and the pellet washed and used to inoculate 500 mL of medium in the fermenter, with a target starting optical density of 0.05 at 550 nm.

Sugar fermentation: For the sugar mixture fermentations, similar setup as described above was used. In this case, high purity argon was only sparged into the medium before the inoculation, after inoculation argon was passed in the headspace to reduce the foaming and evaporation. For the preparation of pre-culture, cells were grown in 17 ml closed Hungate tubes with culture volume of 10 ml. This pre-culture was made anaerobic by passing the argon initially into the tubes through needle set up described above and then closing the tubes immediately. These tubes were filled with the minimum media described above and supplemented with 10 g/l tryptone, 5 g/l yeast extract and 10 g/l glycerol and were kept at 37°C in a tube rotator for mixing.

4.3 Analytical methods

Optical density was measured at 550 nm and used as an estimate of cell mass (1 O.D. = 0.41 g dry weight/L). After centrifugation, the supernatant was stored at -20 °C

for HPLC (High Performance Liquid Chromatography) and NMR (nuclear magnetic resonance) analysis. Glycerol, organic acids, ethanol, and hydrogen were quantified as previously described [146, 147].

4.4 NMR experiments

4.4.1 Fermentation product identification

The identity of the fermentation products was determined via NMR. Sixty µl D_2O and 1 µl of 600 mM NMR internal standard TSP (3-(Trimethylsilyl) propionic acid-D4, sodium salt) were added to 540 µl of the sample (culture supernatant). The resulting solution was then transferred to a 5mm-NMR tube and 1D proton NMR spectroscopy was performed at 25°C in a Varian 500MHz Inova spectrometer equipped with a Penta probe (Varian, Inc., Palo Alto, CA). The following parameters were used: 8,000 Hz sweep width; 2.8 s acquisition time; 256 acquisitions; 6.3 µs pulse width; 1.2 s pulse repetition delay; and presaturation for 2 s. The resulting spectrum was analyzed using the software packages FELIX 2001 (Accelrys Software Inc., Burlington, MA) and MestRe Nova 5.0.3 (MESTRELAB RESEARCH SL, Santiago de Compostela, Spain). Peaks were identified by their chemical shifts and J-coupling values, which were obtained in separate experiments where samples were spiked with metabolite standards (2 mM final concentration).

4.4.2 Determination of glycerol incorporation into cell biomass

An experiment with 100% U-^{13}C-labeled glycerol was conducted to assess the incorporation of glycerol into proteinogenic biomass and to verify that fermentation

products originated from glycerol and not from tryptone components. This experiment was carried out using modified Hungate tubes as described in the section 4.2.2. After 30 hours, cultures were harvested and the fermentation broth was centrifuged. The cell pellets were washed twice with 9 g/l NaCl solution and centrifuged again. The resulting cell pellets were hydrolyzed with 6N constant boiling HCl at 110°C for 24 hours using the Reacti-Therm hydrolysis system (Pierce, Rockford, IL). To remove HCl, the resulting solutions were subjected to rapid vaporization at 75°C under vacuum for 2 hours using the CentriVap system (Labconco Corp., Kansas City, MO). The dried samples were reconstituted in 1 ml D_2O (Cambridge Isotope Laboratories, Cambridge, MA), frozen to -80°C, and subsequently freeze-dried in the 4.5L FreeZone freeze dry system (Labconco Corp., Kansas City, MO) for 24 hours. The samples were then reconstituted in 600 µl D_2O and filtered to remove cell particulates. One µl TSP standard was added to each sample, and the contents were transferred to NMR tubes. To determine ^{13}C enrichment, the samples were analyzed using 1D proton spin echo with and without concurrent 90° pulse on carbon [148]. The 90° pulse on carbon refocused the ^{13}C carbon atoms, thereby suppressing the ^{13}C satellites arising due to proton-carbon spin coupling. This phenomenon did not occur for the ^{12}C carbon atoms. For these experiments, we used the commercially available pulse sequence *pwxcal* on 500 MHz Varian Innova spectrometer (Varian, Inc., Palo Alto, CA). The following parameters were used: 8,000 Hz sweep width; 2.7 s acquisition time; 256 transients; and pwx1 0 and 90° at 25 °C. Individual amino acids were identified based on chemical shifts and the fine structure of the spectra [149]. 1D proton NMR spectroscopy (performed as described above) was also used to analyze the supernatant of the 30-hour culture to assess whether the fermentation

products were synthesized from glycerol or tryptone components. Sample preparation and acquisition parameters were those described above for the analysis of fermentation broth through 1D 1H NMR spectroscopy.

4.5 OD_{550} vs. dry weight calibration

During fermentation experiments, the cell concentration at different time points was measured by measuring the optical density of the growth media. However, this experimental quantity could not be used directly for flux calculation and needs to be correlated to the cell concentration in terms of g/l. Hence, experiments were carried out to determine the relationship between cell dry weight and OD. Cells were grown anaerobically and after significant growth (OD550 ~1); the broth was distributed in several flasks and diluted to different extents. Optical densities of the resulting broths were measured and then these broths were filtered through pre-weighed filter papers with pore size of 0.2 μm. 50 ml nanopure water without cells was filtered through one of the filter papers. This was done to take the moisture content of filter papers into account. These filter papers containing cells were then kept in an oven at a temperature of 70°C for 24 hours and then weighed again. The difference between new weight (with cells) and old weight (without cells) gave the weight of the cells. Thus knowing weight of the cells, OD of the broth and volume of broth used, relationship between OD and cell dry weight was found by plotting the cell concentration in terms of dry wt. (g/l) vs cell density (in terms of OD) and calculating the slope of the resulting straight line. The calibration experiment showed that relationship between optical density and cell concentration was: 1OD = 0.41 g dry weight/l.

4.6 Enzyme activities

For enzyme assays, cells were grown at specified culture conditions and medium composition. Actively growing cells were harvested by centrifugation, washed twice with a saline solution (9 g/L NaCl), and stored as cell pellets at -80 °C until use. The pellets were resuspended in the same saline solution to obtain ~1 mg dry cell weight/ml and sonicated in a Branson 500 sonifier (NJ, USA) for 15 minutes at 4 °C. The microtip configuration with power rating 7 and 50% pulse duration was used.

Glycerol kinase activity was assayed as described by [150], by measuring the change in absorbance at 340 nm and 25 °C in a 1 mL reaction mixture containing 0.15 M glycine, 11 mM $MgCl_2$, 0.27 M hydrazine, 1.2 mM NAD^+, 5 mM ATP, 2 mM glycerol, 20 U of α-glycerophosphate dehydrogenase, and 50 μL crude cell extract prepared as described above. The assay for measuring anaerobic glycerol-3-phosphate dehydrogenase (G3PDH) activity is a modification of the assay described by [150], using the following final concentrations/amounts: 3-(4,5-dimethyl-2-thiazolyl)-2,5-diphenyl-2H-tetrazolium bromide (MTT), 75 μM; phenazine methosulfate, 600 μM; DL-glycerol 3-phosphate, 10 mM; Triton X-100, 0.2%; flavine adenine dinucleotide (FAD), 10 μM; flavine mononucleotide (FMN), 1 mM; and crude cell extract, 50 μL. The aerobic G3PDH activity was determined in the same way, except that flavines were omitted and sodium cyanide (10 μM) was included in the assay. The assays were monitored spectrophotometrically at 570 nm. The extinction coefficient of reduced MTT was 17 $mM^{-1}cm^{-1}$.

The activity of glycerol dehydrogenase in the oxidation of glycerol was measured as reported by [151] by following the change in absorbance at 340 nm and 25°C in a 1 ml

reaction mixture containing 2 mM $MgCl_2$, 500 μM NAD^+, 100 mM glycerol, 100 mM of potassium carbonate buffer (pH 9.5), and 30 μl crude cell extract. Reductive glycerol dehydrogenase activity (i.e., toward hydroxyacetone, HA) was measured in a similar mixture, but with HA and NADH replacing glycerol and NAD^+, respectively. Measurement of dihydroxyacetone kinase activity involved two different procedures for preparation of cell extracts, depending on whether the ATP- or the phosphoenolpyruvate (PEP)-dependent enzyme was assayed. Cell extracts for the ATP-dependent assay were prepared as described above and a coupled assay for ATP-dependent conversion of dihydroxyacetone (DHA) to DHA-phosphate (DHAP) and then NADH-dependent conversion of DHAP to glycerol-3-phosphate (G3P) was performed [152]. The assay mixture contained 50 mM potassium bicarbonate (pH 9), 2.5 mM ATP, 0.4 mM NADH, 15 mM $MgCl_2$, 2 mM dithiothreitol (DTT), 18 U G3PDH from rabbit muscle, 10 mM DHA, and 30 μl crude cell extract. 15 mM alpha-alpha dipyridyl was added to stop any secondary reaction. The PEP-dependent DHAK was assayed using the method reported by [153] with minor modifications. In this case, cell pellets were washed with decryptification buffer (0.1 M-sodium-potassium phosphate, pH 7.2, and 5 mM $MgCl_2$) and stored at -80°C. The pellets were resuspended in decryptification buffer to obtain ~1 mg dry cell weight/ml. A portion of the ice-cold cell suspension was placed in a test tube, vigorously mixed for one minute, and 0.2 volume of toluene-ethanol (1:9, v/v) added. The assay was conducted in a 1 ml reaction mixture containing 1 mM PEP trisodium, 0.1 mM NADH, 2U lactate dehydrogenase, and 50 μg dry weight of toluene-ethanol treated cells. The assay mixture was incubated at 30°C for 15 min. Dihydroxyacetone was added to a concentration of 1 mM and the decrease in absorbance was followed at 340 nm.

Alcohol dehydrogenase activity was determined by following the NADH-dependent reduction of acetaldehyde at 340 nm [154]. The assay mixture contained 0.1 M MOPS-KOH buffer (pH 7.5), 6 mM DTT, 5 mM $MgSO_4$, 0.3 mM $Fe(NH_4)_2(SO_4)_2$, 0.4 mM NADH, 10 mM acetaldehyde, and 30 µl crude cell extract. Coenzyme A linked acetaldehyde dehydrogenase was assayed as previously reported [155]. The reaction mixture contained 25 µM CoA, 0.5 mM NAD^+, 50 mM acetaldehyde, 20 mM DTT, 23 mM potassium phosphate buffer (pH 7.0), and 30 µl crude cell extract.

The activity of methylglyoxal synthase was determined using a colorimetric assay [156]. The reaction mixture contained 0.4 ml of 50 mM imidazole–HCl buffer (pH=7.0), 25 µl of 15 mM DHAP and 50 µl distilled water at 30°C. The assay was initiated by adding 25 µl of crude enzyme extract. After 2.5 min, 5 min and 10 min, 0.1 ml aliquots were removed from the reaction mixtures and added to the appropriate detection mixture vials. The detection mixture contained 0.9 ml distilled water and 0.33 ml 0.1% 2,4-dinitrophenylhydrazine dissolved in 2 N HCl. After incubating the detection mixtures with the aliquots at 30°C for 15 min, 1.67 ml of 10% NaOH was added to each vial to produce a purple color. This mixture was incubated at room temperature for 15 min and the absorbance at 550 nm was recorded. In this system 1 µmol of methylglyoxal has an absorbance at 550 nm of 0.145. Methylglyoxal (MG)-reducing activities (e.g., MG reductase and aldo-keto reductases) were measured in a 1 ml reaction mixture containing 10 mM MG, 0.1 mM NAD(P)H, and 100 mM potassium phosphate buffer (pH 7.0) [157]. 1D proton NMR spectroscopy was used to identify the products of MG- and HA-reducing reactions. NMR measurements were carried out after cell debris were removed from a reaction mixture containing cell extract (30 µl), MG/HA (10 mM), coenzymes (1

mM NADH or 1 mM NADPH), buffer (100 mM potassium phosphate, pH 7.0), and D_2O. The NMR data were collected 4 h after incubation at 25°C.

Linearity of the reactions (protein concentration and time) was established for all preparations. All spectrophotometric measurements were conducted in a BioMate 5 spectrophotometer (Thermo Scientific, MA, USA). The nonenzymatic rates were subtracted from the observed initial reaction rates. Enzyme activities are reported as μmol of substrate/minute/mg of cell protein and represent averages for at least three cell preparations.

4.7 Calculation of fermentation parameters

Maximum specific growth rates (μ_M, h^{-1}) were estimated by plotting total cell concentration versus time in a log-linear plot. The slope of the curves thus obtained (a straight line during exponential growth) was used as the average specific rate. Data for cell growth, glycerol/sugar consumption, and product synthesis were used to calculate volumetric rates (mmol/L/h) during active growth (i.e. from time zero until the cultures reached stationary phase). Growth and product yields (weight or molar basis) were calculated as the amount of cell mass or product synthesized per amount of glycerol/sugar consumed once the cultures reached the stationary phase. In the above calculations, an average molecular weight of 25.1 was used, which corresponds to an average microbial cell of a molecular formula $CH_{1.81}O_{0.52}N_{0.21}$ [158] .

For the calculation of extracellular fluxes for metabolic flux analysis, sample time points were chosen in the exponential phase, which had good carbon balance. For calculating the specific rates for extracellular flux calculations, the change in

concentration of a species between the two time points in a sample pair was divided by the time interval and then by the time-averaged cell density to calculate the flux for that species.

4.8 Metabolic flux analysis

For the calculation of flux values for extracellular metabolites, concentrations data obtained through HPLC needs to be transformed to the respective flux values. For this purpose, two sample points which had good carbon balance were chosen from the exponential phase of the respective fermentation. To calculate measured fluxes, the change in concentration of a species between the two time points in the chosen sample pair was divided by the time interval and then by the time-averaged cell density. These fluxes were then converted to mM/hr/g dry weight by multiplying by 1000. This calculation was performed for all the external fluxes calculated for different sample pairs within the exponential growth phase and an average of resulting fluxes was calculated. Based on these extracellular fluxes and stoichiometric matrix, the reaction network model for *P. macerans* was developed as described in Appendix A and B. This model was used for calculation of intracellular fluxes using experimental measurements in the case of glycerol as well as sugar fermentations (see Chapter 3 for detailed theory). The stoichiometric matrix was divided into measured (G_m^T) and calculated (G_c^T) matrices and the intracellular fluxes (v_c) were calculated from measured fluxes (v_m) using equation 3.10 or 3.11.

Chapter 5

Fermentative utilization of glycerol by *P. macerans*

Glycerol has become an inexpensive and abundant carbon source due to its generation as inevitable by-product of biodiesel fuel production. Given the highly reduced state of carbon in glycerol, its conversion to fuels or reduced chemicals could result in yields higher than those obtained with the use of common sugars [3]. Fully realizing this potential, however, would require the fermentation of glycerol in the absence of external electron acceptors.

Although many microorganisms are able to metabolize glycerol in the presence of external electron acceptors (respiratory metabolism), few are able to do so fermentatively (i.e., absence of electron acceptors). Fermentative metabolism of glycerol has been reported in species of the genera *Klebsiella*, *Citrobacter*, *Enterobacter*, *Clostridium*, *Lactobacillus*, *Bacillus*, *Propionibacterium*, and *Anaerobiospirillum* but has been studied more extensively in a few species of the *Enterobacteriaceae* family, namely *Citrobacter freundii* and *Klebsiella pneumoniae* [4, 159]. Glycerol fermentation in these organisms is mediated by a two-branch pathway, which results in the synthesis of glycolytic intermediate dihydroxyacetone-phosphate (DHAP) and fermentation product 1,3-propanediol (1,3-PDO) (Figure 5.1A) [159]. In the oxidative branch, glycerol is dehydrogenated to dihydroxyacetone (DHA) by a type I, NAD-linked glycerol dehydrogenase (glyDH-I). DHA is then phosphorylated by ATP- or PEP-dependent DHA kinases (DHAK) to generate DHAP. Through the parallel reductive branch, glycerol is dehydrated by glycerol dehydratase (glyD) to form 3-hydroxypropionaldehyde (3-HPA).

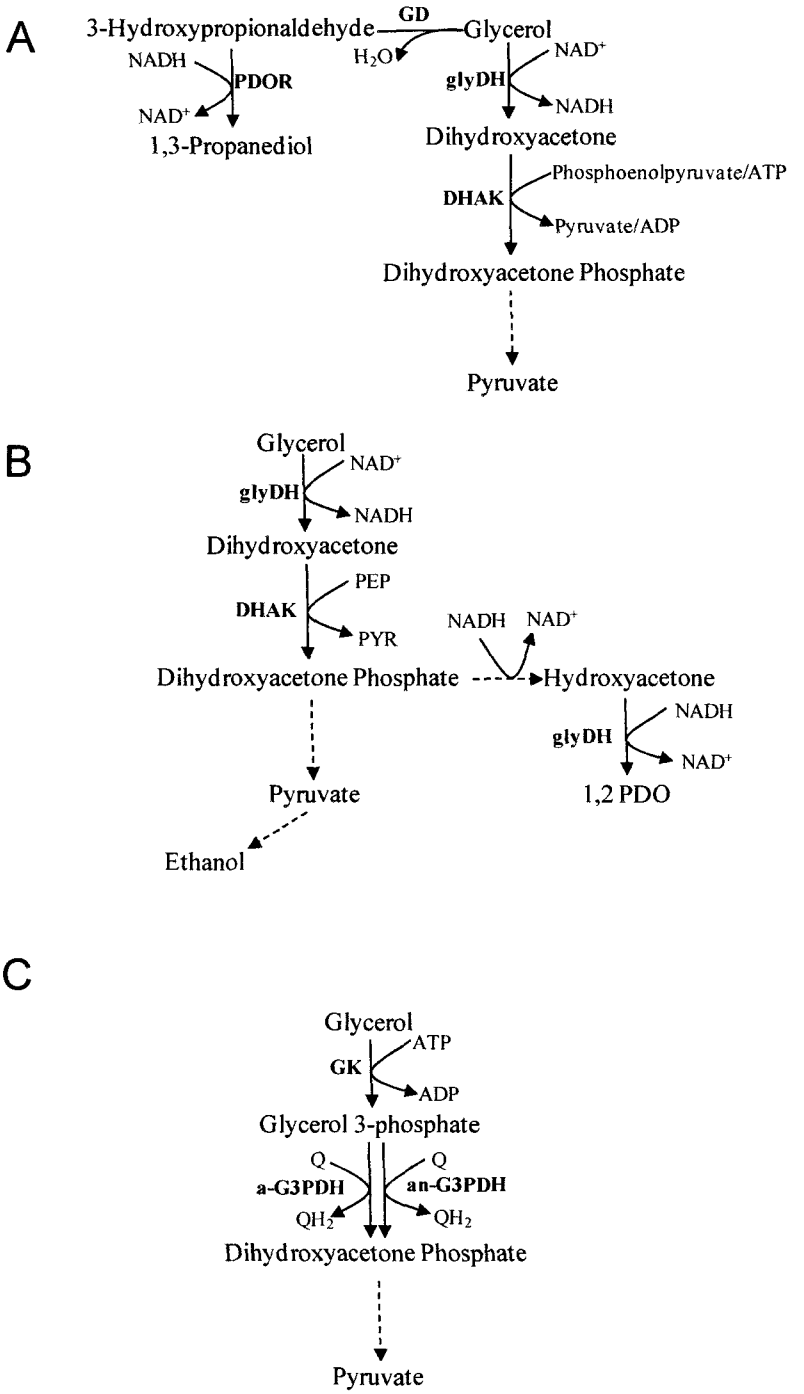

Figure 5.1: Glycerol metabolism in bacteria. (A) 1,3-PDO model for the fermentative utilization of glycerol. (B) 1,2-PDO–ethanol model for the fermentative utilization of glycerol. (C) Respiratory metabolism of glycerol (i.e., metabolism in the presence of an electron acceptor). Dashed lines indicate multiple steps. GD: Glycerol dehydratase; glyDH: Glycerol dehydrogenase; PDOR: Propanediol oxireductase; DHAK: Dihydroxy acetone kinase; GK: Glycerol kinase; a-G3PDH: Aerobic Glycerol 3 phosphate dehydrogenase; an-G3PDH: Anaerobic G3PDH

3-HPA is then reduced to the major fermentation product 1,3-PDO by an NADH-linked 1,3-PDO dehydrogenase (1,3-PDODH), thereby regenerating NAD^+ (Figure 5.1A).

In a comprehensive study of glycerol fermentation in the *Enterobacteriaceae* it was shown that only eight taxa grew fermentatively on glycerol; in all cases, they produced 1,3-PDO and possessed the enzymes glyDH-I and 1,3-PDODH [4]. Organisms that lack the capacity to synthesize 1,3-PDO have been deemed unable to utilize glycerol in a fermentative manner [4, 159, 160]. The metabolism of glycerol in these organisms is thought to require the presence of an electron acceptor and takes place through a respiratory pathway that involves a glycerol kinase and two respiratory (aerobic and anaerobic) glycerol-3-P dehydrogenases (G3PDHs) [124, 161-164] (Figure 5.1C). A recent development in this area is the finding that the synthesis of ethanol and 1,2-propanediol can enable glycerol fermentation in *E. coli*, an organism lacking the ability to produce 1,3-PDO (Figure 5.1B) [5, 165]. In this model, it is proposed that a type-II glyDH and a PEP-dependent DHAK mediate the conversion of glycerol to glycolytic intermediates. The former enzyme (glyDH) also catalyzes the last step in the synthesis of the key fermentation product 1,2-PDO (Figure 5.1B).

Glycerol is considered a non-fermentable carbon source for *P. macerans*. The "non-fermentable status" of glycerol has been used to determine whether certain electron acceptors such as fumarate, trimethylamine N-oxide, nitrate, and nitrite can mediate anaerobic respiration in this organism [166]. That study established that *P. macerans* strains are unable to metabolize glycerol in the absence of the aforementioned electron acceptors.

Despite the reports described above, we have found that several *P. macerans* strains are able to ferment glycerol in the absence of external electron acceptors. Moreover, the fermentation of glycerol in *P. macerans* strain N234A took place at high metabolic rates and in the absence of an active 1,3-PDO pathway. Given the availability, low prices, and high degree of reduction of carbon in glycerol, these high metabolic rates are of paramount importance for the development of processes to convert glycerol to fuels and chemicals. Therefore, the environmental and metabolic determinants of glycerol fermentation were investigated. A medium formulation with low concentrations of potassium and phosphate, cultivation at acidic pH, and the use of a CO_2-enriched atmosphere facilitated glycerol fermentation and are proposed here as environmental determinants of this metabolic process. The pathways involved in the utilization of glycerol and the synthesis of fermentation products were identified through the use of different NMR techniques in combination with enzyme assays and metabolic flux analysis. The synthesis of ethanol and 1,2-PDO are proposed as metabolic determinants of glycerol fermentation as these pathways enable redox balance and ATP synthesis, respectively.

5.1 Anaerobic fermentation of glycerol by *P. macerans*

Despite previous reports of the inability of *P. macerans* to ferment glycerol [166], we have found that several strains of this species are able to utilize glycerol in the absence of external electron acceptors. Commonly used strains such as N234A, B-394, and ATCC 7068 all showed efficient growth and glycerol utilization under fermentative conditions (Table 5.1).

Strain	Cell growth (optical density at 550 nm)	Amt of glycerol utilized (g/liter)	Amt of ethanol produced (g/liter)
B-394	1.12 ± 0.10	8.56 ± 0.53	4.18 ± 0.34
N234A	1.24 ± 0.11	9.92 ± 0.74	4.84 ± 0.36
ATCC 7068	0.98 ± 0.08	6.05 ± 0.46	2.97 ± 0.18

Table 5.1: Glycerol fermentation by P. macerans strains[a]
[a]*Cells were grown for 24 h in modified Hungate tubes using minimal medium supplemented with 10 g/liter glycerol, 10 g/liter tryptone, and 5 g/liter yeast extract, as described in Chapter 4. The values are averages ± standard deviations for three different cultures.*

A typical fermentation profile for strain N234A is shown in Figure 5.2, which also includes as a reference the results reported for the fermentation of glycerol by *E. coli* MG1655 in a similar medium [147]. Although the fermentative metabolism of glycerol in these two organisms share several similarities (to be discussed in detail later), it is noteworthy that glycerol utilization by *P. macerans* takes place at a much higher rate: 9.4 g/L of glycerol fermented and 4.8 g/L of ethanol produced in 15 hours while it takes *E. coli* 96 hours to ferment about 8 g/L of glycerol and produce 2.6 g/L of ethanol (Figure 5.2). This translates into 7- and 12-fold higher rates of glycerol utilization and ethanol production in *P. macerans*, respectively. Since the conversion of glycerol to ethanol and other products via anaerobic fermentation has been proposed as a means of achieving economic viability for the biodiesel industry [3], the high metabolic rates exhibited by *P. macerans* are of paramount importance. To further investigate the fermentative metabolism of glycerol in *P. macerans*, we conducted experiments in a low-

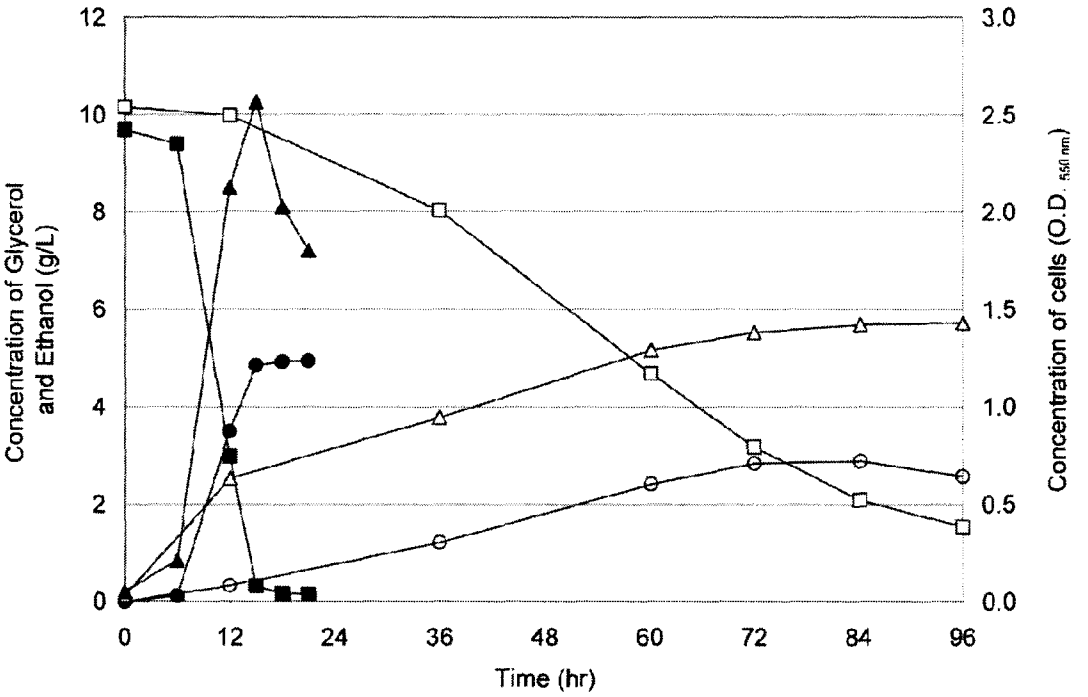

Figure 5.2: Comparison of cell growth, glycerol consumption and ethanol produced between E. coli and P. macerans. Open triangles and open squares show cell growth and glycerol consumption for glycerol fermentation in E. coli. Closed triangles, closed squares and closed circles show cell growth, glycerol consumption and ethanol produced for glycerol fermentation in P. macerans respectively. Medium was supplemented with LB in both cases. pH was maintained at constant value of 6 for both fermentations.

supplemented medium: i.e. supplementation with 1 g/L of tryptone instead of the 10 g/L of tryptone and 5 g/L of yeast extract used in the experiments described above. While this minimum supplementation with tryptone was required to observe significant utilization of glycerol, it is noteworthy that similar levels of rich supplements have been used in the study of the fermentative and respiratory metabolism of *P. macerans* [23, 166, 167]. Figure 5.3A shows a typical fermentation profile for strain N234A in this low-supplemented medium. Exponential growth was observed for a period of 4 hours (Figure

5.3A, inset: note the excellent fitting to a straight-line model in the log-linear plot between 6 and 10 hours). The maximum specific growth rate during exponential growth (μ_M) for the profile shown in Figure 5.3A was 0.402 h^{-1} (0.40±0.03 h^{-1} for three independent fermentations). This μ_M is about ten times that reported for *E. coli* MG1655 in a similar medium and culture conditions [165]. The growth yield once the cells reached stationary phase was 78.4 mg cell/g glycerol, which is about 2.4 times that reported for *E. coli*. It is noteworthy that no cell growth was observed when glycerol was

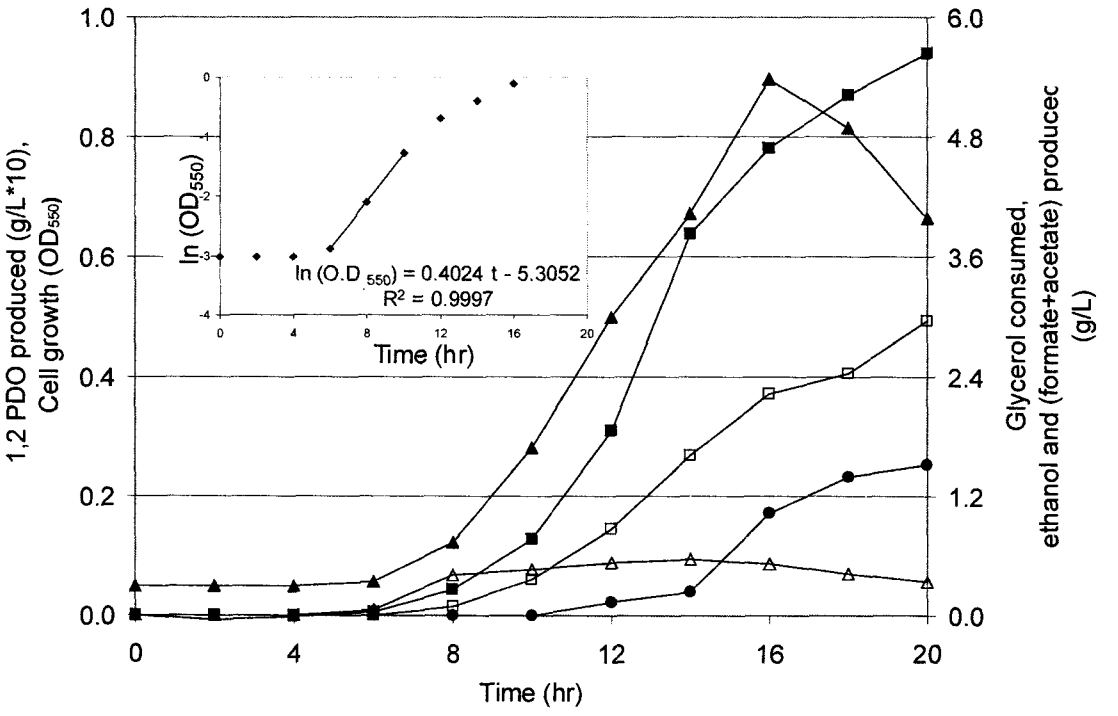

Figure 5.3 (A): Fermentation of glycerol by P. macerans in minimal media with supplementation of 0.5 g/L citrate and 1 g/L tryptone. Optical density at 550 nm (▲), Formic + Acetic Acid (Δ), Ethanol (□), 1,2 PDO (●), Glycerol consumed (■). Inset: Specific cell growth is being shown in the log-linear plot, along with their fitting to a straight-line model (least-squares method)

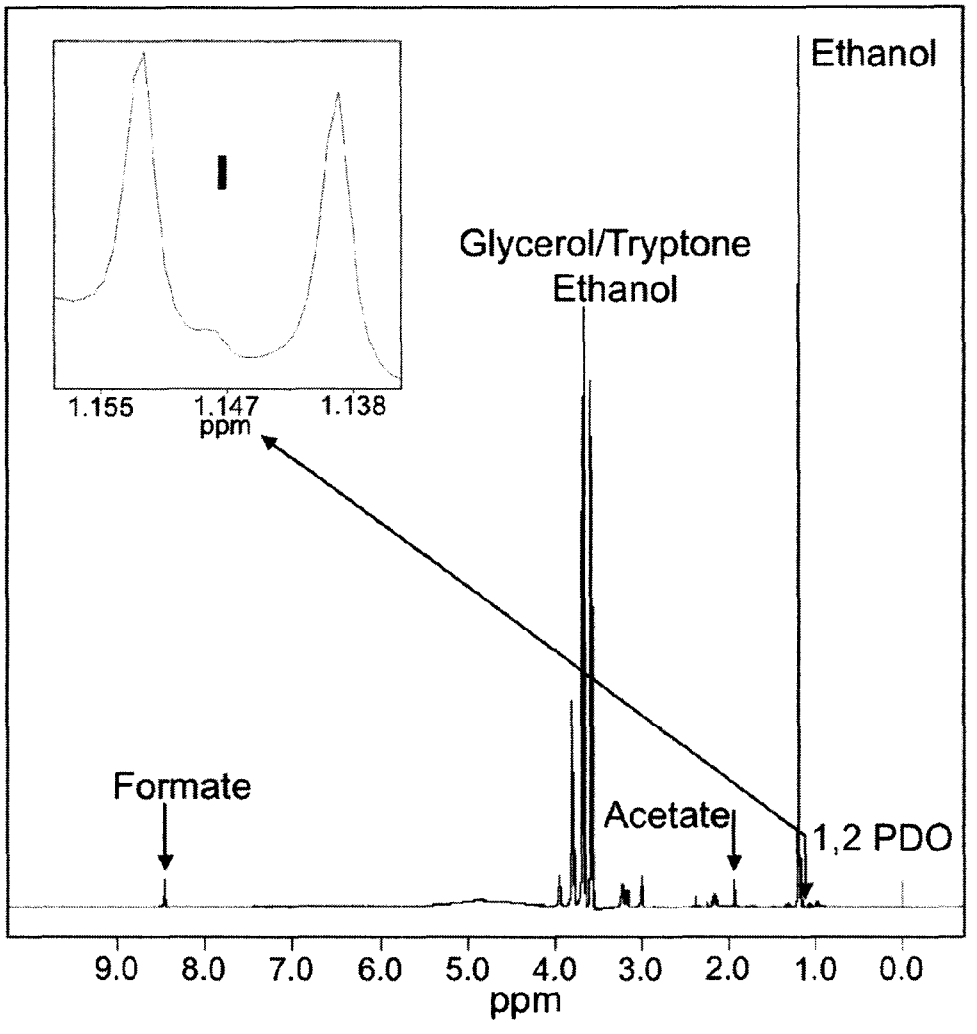

Figure 5.3(B): 1D ^{1}H NMR spectrum of the culture medium in a late fermentation sample. Arrows indicate the corresponding compound in the spectra. (Inset I) Two peaks at the same chemical shifts as those of methyl protons of 1,2-PDO (doublet at 1.15 ppm) are shown.

omitted from the medium formulation (optical density at 550 nm increased by less than 0.01). The identity of the products found in the fermentation broth was determined through the analysis of the medium via 1D 1H-NMR spectroscopy. Products identified include ethanol (two multiplets at 3.66 and 1.19 ppm) and acetic (1.93 ppm) and formic (8.46 ppm) acids (Figure 5.3B). While succinic acid (2.444 ppm) was found in fermentations conducted at basic pH (e.g. pH 8: see next sections), no lactic acid was

detected in the extracellular medium. A doublet was observed in the spectra of late fermentation samples at a position with the same chemical shift as that of methyl protons of 1,2-propanediol (1,2-PDO) (doublet at 1.15 ppm: Figure 5.3B, inset). The same doublet has been found in the spectra of fermentation samples of *E. coli* [165] and, upon further investigation via 2D 1H-1H COSY (COrrelation SpectroscopY) NMR, the peaks were unambiguously identified as originating from 1,2-PDO methyl protons [5]. Our findings represent the first report of 1,2-PDO production during the metabolism of glycerol in *P. macerans*. 1,2-PDO synthesis by *P. macerans* had only been reported as a

Substrate consumed or product formed	Mol of product/ mol of glycerol consumed[a]	Oxidation state[b]	Redox balance[c]	Carbon recovery (no. of C atoms)[d]
Substrate				
Glycerol		−2	−2	3
Products				
Acetic acid	0.011 ± 0.001	0.00	0.000	0.022
Formic acid	0.210 ± 0.011	2.00	0.420	0.210
Carbon dioxide	0.801 ± 0.036	4.00	3.205	0.801
Hydrogen[e]	0.801 ± 0.036	−2.00	−1.602	
1,2 PDO	0.005 ± 0.001	−4.00	−0.007	0.028
Ethanol	1.000 ± 0.023	−4.00	−4.000	2.000
Total			−1.985	3.061

Table 5.2: Calculation of fermentation balance for growth of P. macerans on glycerol at pH 6 and 37 °C. Data corresponds to 16 hr sample from figure shown in Figure 5.3A.
[a] Values are net mol produced per mol of glycerol consumed.
[b] The oxidation state of carbon atoms was calculated assuming oxidation states of 2 and 1 for oxygen and hydrogen, respectively [168].
[c] Data in this column were obtained as (mol of product/mol of glycerol) × oxidation state of carbon atoms.
[d] Carbon recovery was calculated as (mol of product/mol of glycerol) × no. of carbon atoms in molecule.
[e] Moles of hydrogen generated in the dissimilation of pyruvate were calculated assuming that moles of "CO_2 plus formate" equals moles of "ethanol plus acetate".

product of the fermentation of 6-deoxyhexose sugars fucose and rhamnose [167]. The concentration of glycerol and the products identified in the NMR spectrum, including 1,2-PDO, were determined via HPLC, and the results are included in Figure 5.3A. This data was used to conduct a fermentation balance analysis, which included both carbon and degree of reduction balances (Table 5.2). The carbon recovered as fermentation products was close to 100% of the carbon consumed as glycerol (3.049/3 = 1.02; see Table 5.2). Similarly, about 99% of the reducing equivalents generated during the fermentation of glycerol were captured in the synthesis of fermentation products (-1.985/-2 = 0.99; see Table 5.2). This represents an excellent closure of both redox and carbon balances. Glycerol fermentation was also observed when the growth medium was supplemented with a mixture of proteinogenic amino acids at levels similar to those provided by the tryptone supplementation: i.e. an $O.D._{550}$ of 0.5 and 3.8 g/L of glycerol fermented. However, amino acid supplementation resulted in lower cell density and slower fermentation kinetics, compared to those shown in Figure 5.3A.

5.2 Identification of the origin of carbon in fermentation products and cellular components

Since glycerol metabolism required supplementation of the medium with small amounts of tryptone, we conducted experiments to investigate whether cellular components and fermentation products were synthesized from glycerol or tryptone components. To this end, cells were grown on 100% U-^{13}C-labeled glycerol. Selected areas of the NMR spectrum of the supernatant of a 30-hour sample from this culture are

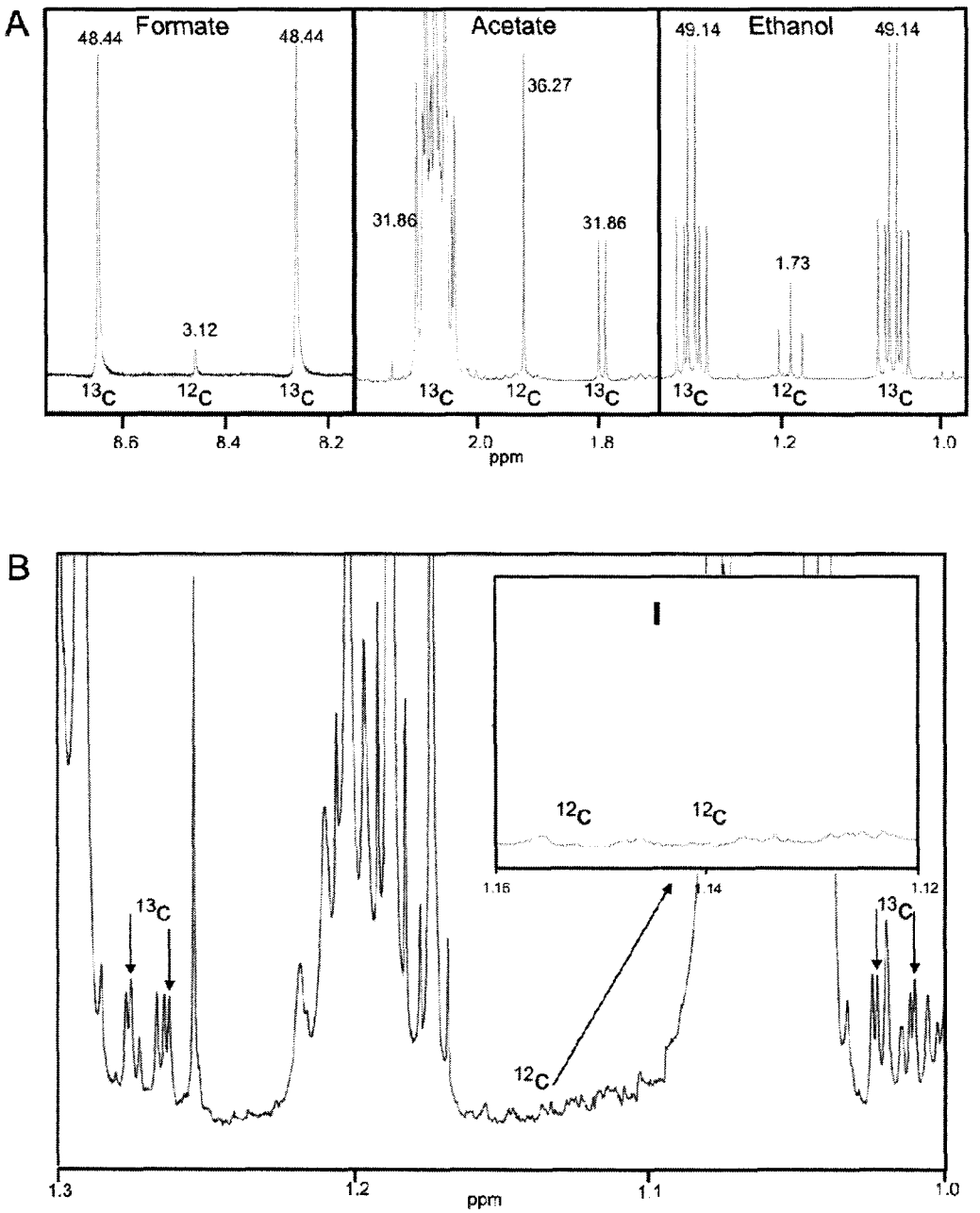

Figure 5.4: (A) $^{1}D\ ^{1}H$ NMR spectra of the fermentation broth from a 30-h culture grown on 100% U-^{13}C-labeled glycerol. The percentage of area of each peak to that of total area (i.e., sum of all peaks) is shown. (B): Splitting of methyl protons of 1,2-PDO attached to ^{12}C or ^{13}C atoms (doublet for ^{12}C atoms and no signal for ^{13}C atoms at 1.15 ppm) in $^{1}D\ ^{1}H$ NMR spectra of the fermentation broth from a 30-h culture grown on 100% U-^{13}C-labeled glycerol. Figure shows the splitting between (Inset I) Location of ^{12}C carbon atom peaks of 1,2-PDO (doublet at 1.15 ppm) in 100% U-^{13}C-labeled glycerol experiment.

shown in Figure 5.4. 1D 1H-NMR spectroscopy was used in these experiments to distinguish between ^{13}C and ^{12}C atoms (see Chapter 4 for more details).

Since ^{13}C is magnetic, protons attached to ^{13}C carbons have two different chemical shifts due to positive and negative energy levels of these carbon atoms. Protons attached to ^{12}C atoms will have chemical shifts in between those of ^{13}C because all ^{12}C atoms will be at neutral state. Thus, protons attached to ^{12}C carbon atoms lead to a central peak structure flanked by two satellite peak structures that arise from those protons attached to the ^{13}C atoms. The percentage area of ^{13}C satellite peaks to that of total area then reflects the ^{13}C enrichment of that carbon atom. As can be seen from Figure 5.4A, the ^{13}C enrichment in ethanol and formic acid approaches 100%, demonstrating that all carbon atoms in these products originated from glycerol. ^{13}C enrichment was also observed in the case of acetic acid, although it appears that only about 64% of the carbon in this product originates from glycerol (Figure 5.4A).

Given the complexity of the area of the spectrum where the 1,2-PDO doublet was observed, and the importance of 1,2-PDO as a product of glycerol fermentation, the area of the spectrum corresponding to the methyl protons of this compound is shown separately in Figure 5.4B. While the ^{13}C signals were identified (down arrows), no signal was observed at the ^{12}C positions. The inset of Figure 5.4B shows a magnification of the area of the spectrum where a doublet due to the protons attached to ^{12}C carbons should appear. When this inset is compared to the inset of Figure 5.3B, which shows the ^{12}C doublet observed with the use of unlabeled (naturally labeled) glycerol, it becomes evident that 1,2-PDO is exclusively synthesized from glycerol.

In the same experiment described above, the ^{13}C enrichment of proteinogenic biomass was assessed as a way to determine whether glycerol was used in the synthesis of cell mass. For this purpose, the ^{13}C enrichment of biomass in cells grown on U-^{13}C-labeled glycerol was compared to a reference culture in which cells were grown on unlabeled glycerol. The cells from the two cultures were hydrolyzed to obtain a cocktail of their proteinogenic amino acids, which was subsequently analyzed via NMR. ^{13}C enrichment was determined using 1D proton spin echo with and without concurrent 90° pulse on carbon as described in Chapter 4. The 90° pulse on carbon refocuses the ^{13}C carbon atoms, thereby suppressing the ^{13}C satellites arising due to proton-carbon spin coupling. The nucleus of ^{12}C is non-magnetic and thus protons attached to ^{12}C would not experience any difference between the two situations. Therefore, ^{13}C satellite peaks could be easily identified upon comparison of the spectra obtained via these two methods. The 1D NMR spectra thus obtained for the two samples (with and without labeled carbon) contained small ^{13}C satellite peaks, which in several cases were hidden below bigger peaks. However, many of them were well resolved with visible ^{13}C satellites. Parts of the NMR spectra depicting two of these resolved areas from a sample in which ^{13}C-labeled glycerol was used are shown in Figure 5.5.

The depicted amino acid carbon atoms are threonine-γ (left panels) and alanine-β (right panels); the down arrows point the ^{13}C satellites for these carbon atoms. Each panel contains an inset that magnifies the region of the spectra corresponding to the ^{13}C satellite signals and which also includes (up) arrows that indicate the peaks of interest. Since the signal for these satellites were small, their identity (as peaks arising due to labeled carbon) was confirmed by performing a ^{13}C-decoupled experiment where the ^{13}C signals

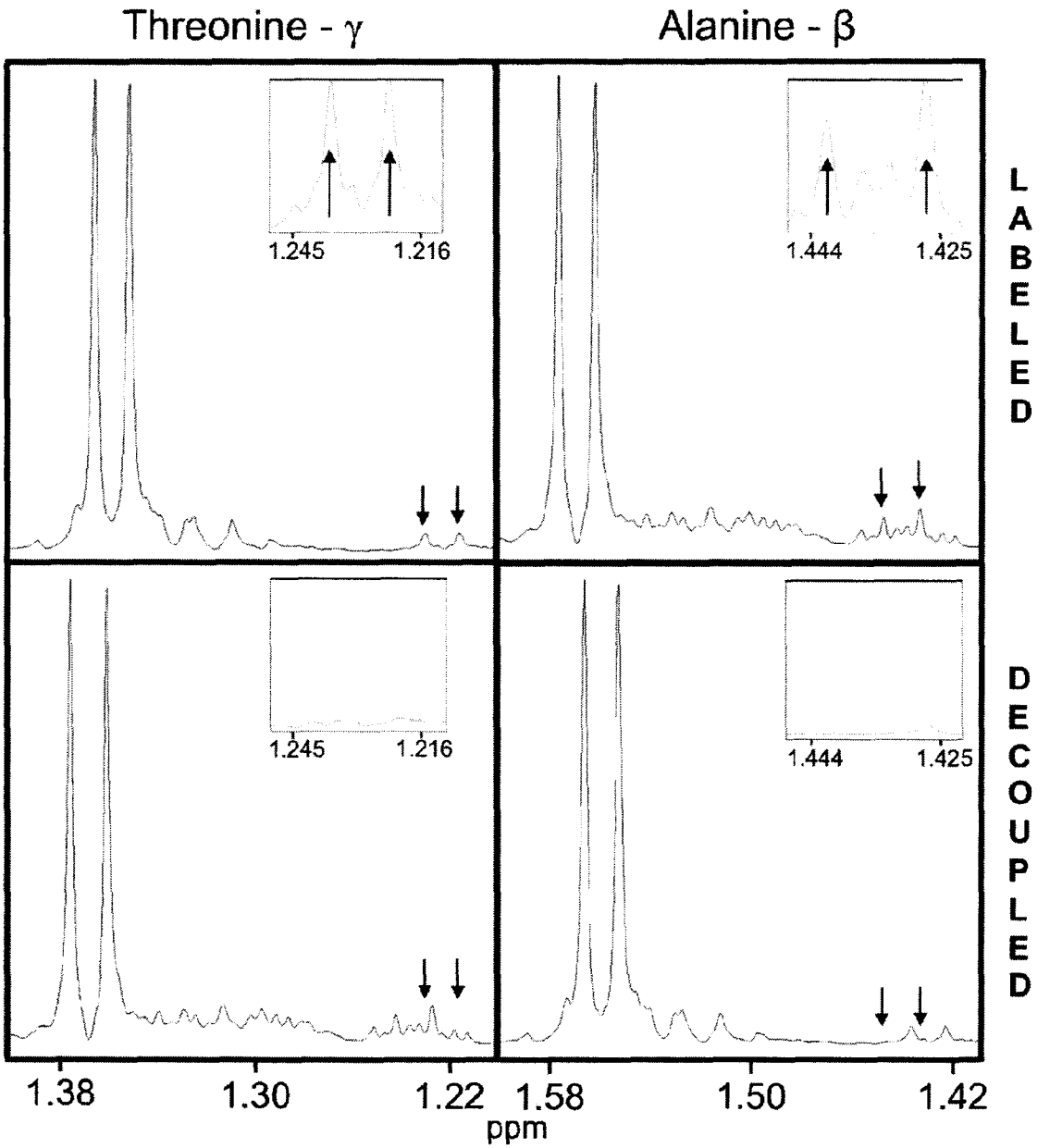

Figure 5.5: NMR spectra of proteinogenic amino acids in cell biomass obtained from experiments with 50% U-^{13}C-labeled glycerol. The identity of ^{13}C satellites as peaks arising due to labeled carbon was confirmed by performing a ^{13}C-decoupled experiment in which the ^{13}C signals were suppressed (bottom panels). Marked peaks (arrows) illustrate the incorporation of labeled carbon into threonine-γ (left panels), alanine-β (right panels).

were suppressed (Figure 5.5, bottom panels). In the case of unlabeled glycerol, the ^{13}C satellite peaks constituted about 1% of the total signal (data not shown), which represents the natural abundance of this isotope. However, when 100% U-^{13}C-labeled glycerol was used (Figure 5.5, top panels), the ^{13}C satellites constituted about 22% of the total signal indicating that about 20% of these amino acids in biomass originated from glycerol. Although not shown here due to space limitations, similar spectra were obtained for many other carbons corresponding to amino acids in proteinogenic biomass. The requirement of tryptone supplementation could also raise the question of whether glycerol utilization is truly fermentative or compounds present in the tryptone, or generated from it, serve as electron acceptors. The almost exclusive synthesis of reduced product ethanol (Figure 5.3A, Table 5.2) is interpreted as a strong indication that glycerol is in fact metabolized in a fermentative manner: i.e. the presence of an electron acceptor would otherwise consume the reducing equivalents generated from glycerol, and significant amounts of oxidized products (such as acetate) would be produced instead of ethanol. The excellent closure of the redox balance (~99%) is yet another indication that glycerol metabolism is mediated by fermentative pathways (Table 5.2). More direct evidence of the fermentative nature of this metabolic process was provided by experiments in which cell growth and glycerol utilization were observed despite the use of respiratory inhibitors that block general respiratory processes. Specifically, the use of respiratory inhibitors cyanide and azide did not prevent cell growth or glycerol utilization by *P. macerans* N234A (data not shown).

5.3 Metabolic pathways involved in the fermentation of glycerol by *P. macerans* N234A

Two pathways have been reported to mediate the microbial conversion of glycerol to glycolytic intermediate dihydroxyacetone phosphate (DHAP) [3, 124, 159] (Figure 5.1). In one route, glycerol is directly oxidized by the enzyme glycerol dehydrogenase (glyDH) generating DHA, which in turn can be converted to DHAP by the action of DHA kinase (DHAK). A second route involves the conversion of glycerol to glycerol-3-phosphate (G3P) and G3P to DHAP, catalyzed by the enzymes glycerol kinase (GK) and

Activity Assayed	Enzyme Activity Value(Mean ± SD)[a]
Glycerol dissimilation	
Glycerol dehydrogenase (toward glycerol)	0.014±.001
ATP dependent dihydroxyacetone kinase	0.035±.001
PEP depdendent dihydrixyacetone kinase	0.026±.001
Glycerol kinase	ND[b]
Glycerol 3 phosphate dehydrogenase	ND[b]
1,3 propanediol synthesis	
1,3 propanediol oxireductase	ND[b]
1,2-Propanediol synthesis	
Methylglyoxal Synthase	0.067±.004
Aldo-keto reductase/ Methyglyoxal reductase with NADPH	0.013±.001
Aldo-keto reductase/ Methylglyoxal reductase with NADH	0.022±.002
Glycerol dehydrogenase (toward hydroxyacetone)	0.198±.002
Ethanol synthesis	
Alcohol dehydrogenase	0.035±.001
CoA linked aldehyde dehydrogenase	0.015±.001

Table 5.3 : Enzyme activity values of key enzymes in glycerol dissimilation
Cells were grown as described in Chapter 4 at pH 6 and the culture was harvested in the late exponential phase for enzyme assays.
[a] All activities were measured as described in Chapter 4 and activity values are reported in μmol of substrate/min/mg protein. Reported values are averages ± standard deviation of triplicate assays.
[b] ND denotes that no activity was detected

G3P dehydrogenase (G3PDH), respectively. We assayed crude cell extracts of *P. macerans* N234A obtained from a 16-hour sample of the culture shown in Figure 5.3A. All the aforementioned activities were assayed and the results indicate that the GK-G3PDH route is inactive as no activity was detected for these enzymes (Table 5.3). It is noteworthy that both anaerobic and aerobic G3PDH were assayed. On the other hand, significant activity of glyDH and DHAK were found, indicating that the glyDH-DHAK route mediates the utilization of glycerol in *P. macerans* N234A (Table 5.3). These activities were absent in cultures grown on LB but detected upon inclusion of glycerol (Table 5.4), which suggests their inducibility by this carbon source. The glyDH activity was found to be NAD+ specific, as it was undetectable when NADP+ was used as cofactor. The four types of bacterial glyDH reported to date can be clearly differentiated

Enzyme	Activity under different growth conditions[a]			
	LB	LB + Gly	LB + DHA	LB + HA
Glycerol dissimilation				
Oxidative glyDH	ND	0.014 ± 0.002	ND	0.002 ± 0.001
ATP-dependent DHAK	ND	0.033 ± 0.001	0.008 ± 0.001	NM
PEP-dependent DHAK	ND	0.007 ± 0.001	ND	NM
1,2-PDO synthesis				
MG synthase	ND	0.096 ± 0.005	NM	NM
MG reductase	ND	0.022 ± 0.002	NM	NM
Reductive glyDH	ND	0.070 ± 0.003	0.066 ± 0.005	0.043 ± 0.002

Table 5.4: Effect of glycerol, DHA, and HA on the activities of selected enzymes involved in glycerol fermentation. [a]Oxidative and reductive glyDH and MG reductase activities were measured using NAD(H) as a cofactor, and the enzyme activities are expressed in μmol/min/mg of cell protein. Cells were grown in closed Hungate tubes using the minimal medium described in Chapter 4 supplemented with 10 g/liter tryptone and 5 g/liter yeast extract (LB medium) and with 5 mM glycerol (Gly), DHA, or HA, as indicated. Crude cell extracts were prepared as described in Chapter 4 using cell pellets from actively growing cultures. ND, no activity detected; NM, not measured.

on the basis of their inducibility by glycerol, dihydroxyacetone, and hydroxyacetone [4]. The glyDH activity detected in *P. macerans* N234A extracts was induced by both glycerol and hydroxyacetone, but not by dihydroxyacetone (Table 5.4). Type II glyDHs from enteric bacteria are induced by glycerol and hydroxyacetone [4], and therefore glyDH from *P. macerans* N234A appears to be a type II enzyme. The DHA generated by the action of glyDH is converted to DHAP by the action of both ATP- and phosphoenolpyruvate (PEP)-dependent DHAKs, as can be inferred from the enzyme assay results (Table 5.3). Both enzymes were induced by glycerol but dihydroxyacetone was only able to induce the ATP-dependent activity. Taken together, these results agree with current models for the microbial metabolism of glycerol in which the glyDH-DHAK pathway is associated with the fermentative utilization of this carbon source (Figure 5.1) [3, 5, 124, 159].

The pathways involved in the synthesis of fermentation product 1,2-PDO were also investigated through enzyme activity measurements, characterization of enzymatic reactions via NMR, and supplementation of intermediates in the postulated pathways. Based on previous studies in bacteria, the pathways that could mediate the synthesis of 1,2-PDO from DHAP are summarized in Figure 5.6A [5, 151, 157, 167, 169-173].

It is noteworthy that DHAP is a glycolytic intermediate generated during the utilization of glycerol via the glyDH-DHAK route discussed above. Since the synthesis of methylglyoxal (MG) from DHAP is a common step in the 1,2-PDO pathway, regardless of the branch used for the conversion of MG to 1,2-PDO (Figure 5.6A), MG synthase (MGS) was assayed and significant activity of this enzyme was found (Table

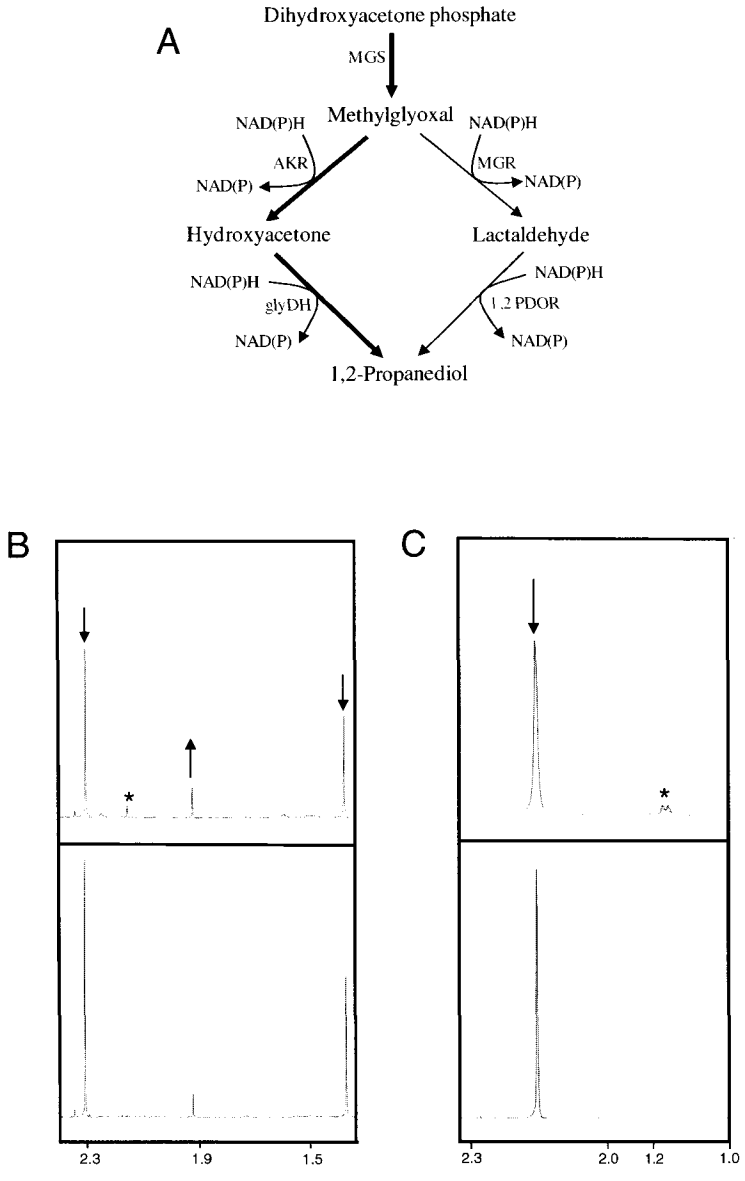

*Figure 5.6: (A) Proposed pathways for synthesis of 1,2 PDO from DHAP in P. macerans. Enzyme names are given based on similar pathways in E. coli and shown in red. (B) ^{1}D ^{1}H NMR spectra of products of enzyme assay for conversion of methylglyoxal to acetol. Upper spectra shows NMR of products four hours after the assay and lower one shows at the start of the assay. Arrows pointing downwards indicate methylglyoxal peaks and * represents acetol peak. Arrow pointing upwards indicate Acetate an impurity in methylglyoxal. (C): ^{1}D ^{1}H NMR spectra of products from enzyme assay for conversion of acetol to 1,2 PDO by glycerol dehydrogenase. Lower spectra is at the beginning of assay and upper spectra is after four hours. Arrow pointing downwards indicate acetol and 1,2 PDO is shown by *. Abbreviations: AKR, aldo-keto reductase; MGR: Methylglyoxal synthase; glyDH: glycerol dehydrogenase; 1,2 PDOR: 1,2 propanediol reductase; MG: methylglyoxal; 1,2 PDO: 1,2 propanediol; DHAP: dihydroxy acetone.*

5.3). MGS was undetectable in the absence of glycerol (Table 5.4), which indicates its inducibility by this carbon source. When cell extracts were assayed for MG-reducing enzymes (MGR), significant activity in the presence of either NADH or NADPH was found. Since these activities could be involved in the conversion of MG to either HA or LAL, 1D 1H NMR spectroscopy was used to characterize the reaction(s). Figure 5.6B shows that the product of the MG-reducing activities is indeed HA (no LAL was detected).

We also demonstrated that cells fermenting glycerol exhibit significant HA-reducing activity (Table 5.3). The enzyme(s) catalyzing this conversion was (were) able to use NADH or NADPH as cofactors. Further characterization of the reaction(s) via 1D 1H NMR spectroscopy showed that the product of HA reduction is 1,2-PDO (Figure 5.6C). Both MGR and HA-reducing activities were induced by glycerol (Table 5.4).

The above results suggest that the synthesis of 1,2-PDO during glycerol fermentation occurs through the conversion of DHAP to MG to HA to 1,2-PDO (represented by thick lines in Figure 5.6A). We further investigated the relevance of 1,2-PDO synthesis for glycerol fermentation. An experiment in which amplification of the 1,2-PDO pathway allowed glycerol fermentation in the absence of rich supplements provided evidence of the important role of this pathway. The experiment involved supplementation of the growth medium with 20 mM HA, upon which glycerol fermentation was observed in the complete absence of tryptone: cells grew to an OD_{550} of 0.48 and fermented 3.72 g/L of glycerol in 48 hours. Externally provided HA was completely converted to 1,2-PDO. These results suggest that the synthesis of 1,2-PDO enables the fermentation of glycerol by *P. macerans* N234A. The conversion of glycerol

to 1,2-PDO results in the consumption of reducing equivalents and has been proposed to facilitate glycerol fermentation in *E. coli* by enabling redox balance in the absence of external electron acceptors [5, 165].

1,3-propanediol (1,3-PDO), a structural isomer of 1,2-PDO, is known to be a metabolic product that enables the fermentative utilization of glycerol in enteric bacteria [3, 124, 159]. 1,3-PDO is synthesized in those microorganisms via a reductive pathway in which glycerol is dehydrated by the coenzyme B_{12}-dependent glycerol dehydratase (glyD) to form 3-hydroxypropionaldehyde (3-HPA), which is then reduced to 1,3-PDO by an NADH-linked 1,3-PDO dehydrogenase (1,3-PDODH) (Figure 5.1A). We did not find 1,3-PDO in the supernatant of *P. macerans* N234A cultures and 1,3-PDODH activity was not detected in cell extracts (Table 5.3). These results indicate the lack of an active 1,3-PDO pathway in *P. macerans* N234A during glycerol fermentation.

The almost homoethanologenic nature of glycerol fermentation (Figures 5.2 and 5.3) reflects the highly reduced state of carbon in glycerol and suggests a central role for this pathway. Ethanol is synthesized in microorganisms through the reduction of acetaldehyde, a reaction catalyzed by alcohol dehydrogenase [168, 174]. Acetaldehyde, in turn, originates from either the oxidation of pyruvate (catalyzed by pyruvate decarboxylase, PDC) or the reduction of acetyl-CoA (catalyzed by acetaldehyde dehydrogenase) [168, 174, 175]. In previous studies it has been reported that the dissimilation of pyruvate in *P. macerans* strains during fermentative metabolism of sugars is mediated by pyruvate formate-lyase (PFL), an enzyme that converts pyruvate to acetyl-CoA and formate [23, 24, 167]. We then postulate that the route to ethanol synthesis should involve the consecutive reduction of acetyl-CoA to acetaldehyde to

ethanol. To verify this hypothesis, we assayed cell extracts of *P. macerans* N234A grown on glycerol for acetaldehyde and alcohol dehydrogenase and both activities were present at significant levels (Table 5.3).

5.4 Effect of culture conditions and medium composition on the fermentative metabolism of glycerol

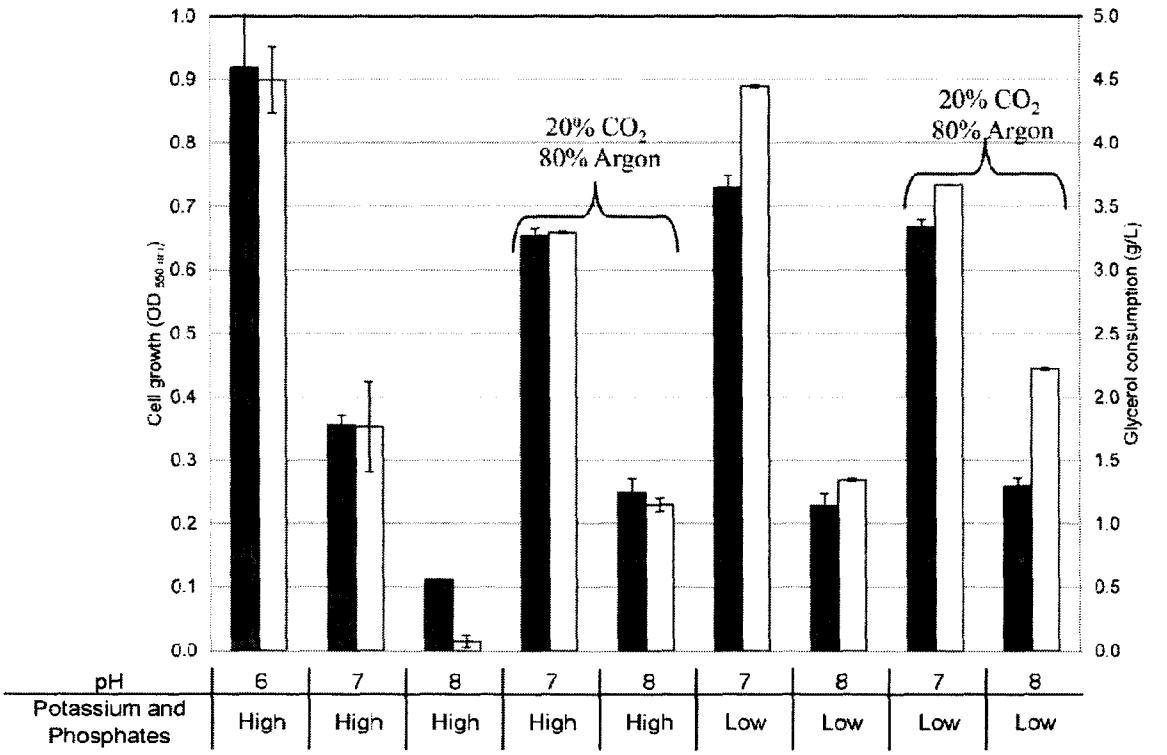

Figure 5.7: Effect of pH, carbon dioxide, and concentrations of potassium and phosphate on cell growth (filled bars) and glycerol fermentation (open bars) by P. macerans N234A. The basal medium used in this study contained 6.8 g/liter KH2PO4 and 1 g/liter KCl (See Chapter 4) ("high potassium and phosphates"). A low-potassium and low-phosphate medium was prepared by replacing KH_2PO4 and KCl in the basal medium with 0.35 g/liter of Na_2HPO4 and 8.36 g/liter of MOPS ("low potassium and phosphates"). Experiments were conducted at 37°C, using the media described above supplemented with 10 g/liter glycerol and 1 g/liter tryptone. The gas atmosphere and pH used are indicated. The bars indicate the means and the error bars indicate the standard deviations for three samples taken once the cultures reached the stationary phase

A study on the effect of pH on glycerol fermentation showed that the fermentative metabolism of this carbon source by *P. macerans* N234A is negatively affected by the use of neutral and alkaline pH (Figure 5.7). Both cell growth and glycerol utilization at pH 7 were less that half of that observed at pH 6. Even more surprising was the observation that no significant cell growth or glycerol consumption was observed at pH 8. This relationship between pH and ability to ferment glycerol has recently been reported for *E. coli* and attributed to several factors [5, 147, 165], which are examined in detail below. It is noteworthy that the negative impact of alkaline conditions is much more pronounced in *P. macerans* N234A than *E. coli*.

One reason for the absence of glycerol fermentation at pH 8 could be the limited availability of CO_2 at alkaline conditions, which in turn could be caused by the low activity of CO_2-generating enzymes such as formate-hydrogen lyase at this pH [147]. The activity of oxidative enzymes, which are another source of CO_2, is also thought to be low during glycerol fermentation due to the high internal redox state created by the fermentative utilization of this substrate (i.e. high NADH/NAD+ ratio) [165]. An alternative route for the generation of CO_2 could be the conversion of acetate to acetone, but this pathway appears to be inactive during glycerol fermentation as we did not find acetone in the extracellular medium. Moreover, it has been reported that acetone production during fermentation of sugars by *P. macerans* ceases at alkaline conditions [23]. The hypothesis of CO_2 limitation was investigated by providing 20% CO_2 in the gas atmosphere. This supplementation with CO_2 had a positive impact on both glycerol utilization and cell growth (Figure 5.7). The most dramatic effect was observed at pH 8

as the cells transitioned from a glycerol-non-fermenting state in an Argon atmosphere to a glycerol-fermenting state in a CO_2-enriched atmosphere.

Another reason for the negative impact of alkaline conditions could be that a basic pH in combination with high level of potassium and phosphate is known to have a negative impact on the activity of two key pathways involved in the fermentative utilization of glycerol, namely the 1,2-PDO and glyDH-DHAK pathways [5]. While this evidence originates from studies conducted with *E. coli*, the aforementioned pathways are active in *P. macerans* N234A as well (Tables 5.3 and 5.4; Figure 5.6). More specifically, the use of basic pH in combination with high levels of potassium leads to higher toxicity of MG [159], a key intermediate in the synthesis of 1,2-PDO (Figure 5.6). High phosphate concentrations, on the other hand, have been shown to inhibit glycerol dehydrogenase [151], and this is a key enzyme in the conversion of glycerol to glycolytic intermediates (Tables 5.3 and 5.4; Figure 5.1A) and the synthesis of 1,2-PDO (Tables 5.3 and 5.4; Figure 5.6). The use of a medium with low levels of phosphate and potassium had a beneficial effect on glycerol fermentation at pH 7 and 8 (Figure 5.7). The improvement in cell growth and glycerol utilization was very similar to that observed in response to CO_2 supplementation (Figure 5.7). Low levels of both phosphate and potassium were required to observe this improvement. Interestingly, the use of a CO_2-enriched atmosphere in combination with a low phosphate and potassium medium did not lead to further improvements in cell growth or glycerol utilization (Figure 5.7). The latter result appears to indicate that both CO_2 supplementation and low levels of potassium and phosphate stimulate the fermentative metabolism of glycerol through related mechanisms.

Since the use of a CO_2-enriched atmosphere and a low phosphate-potassium medium enabled the fermentation of glycerol at basic conditions, we examined the effect of pH on the distribution of fermentation products (Figure 5.8). While at pH 6 the fermentation broth contained almost exclusively ethanol, the used of alkaline conditions led to a slight decrease in ethanol yield along with the production of significant amounts of formic, acetic and succinic acids (Figure 5.8). This variable organic acid yield with changes in pH is similar to that reported for other *P. macerans* strains during glucose fermentation [23]. However, the shift from almost homoethanologenic to mixed-acid-

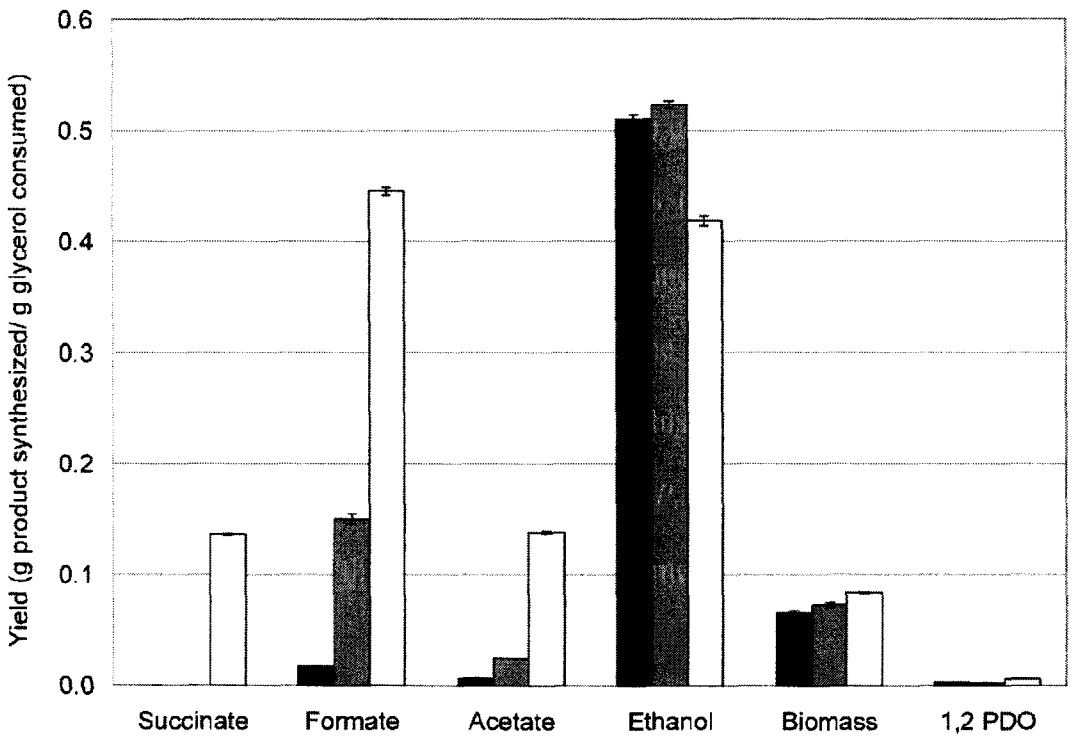

Figure 5.8: Effect of pH on product and biomass yields. Experiments were conducted using a low-potassium and low-phosphate medium. The data are for pH 6 (black bars), pH 7 (gray bars), and pH 8 (open bars). The bars indicate the means and the error bars indicate the standard deviations for three samples taken once the cultures reached the stationary phase.

type fermentation is very unique to the fermentation of glycerol. To illustrate this aspect, it is instructive to compare the ratio of organic acids to ethanol (organic acids/ethanol, w/w), which changed from 0.04 at pH 6 to 1.6 at pH 8: a 37-fold increase. Both biomass and 1,2-PDO yields were higher at alkaline conditions, which further supports the enabling role of 1,2-PDO synthesis. Another important finding was the identification of succinic acid as a product of glycerol fermentation at alkaline conditions (Figure 5.8). Previous studies on the fermentation of glucose, xylose, and deoxysugars by *P. macerans* strains did not report succinic acid as a product [23, 24, 167]. Therefore, this represents the first report of succinic acid production by *P. macerans*.

In previous studies of glycerol fermentation by *E. coli* we have shown that hydrogen, a fermentation gas co-produced along with CO_2 during the oxidation of formate, is detrimental for glycerol fermentation [165]. The effect of hydrogen was evaluated by using a 20% hydrogen (balance argon) atmosphere and by conducting the fermentation in closed vessels with no headspace. Unlike *E. coli*, no inhibitory effect due to the presence of hydrogen was observed in *P. macerans* N234A (data not shown).

5.5 Proposed model for fermentative utilization of glycerol by *P. macerans*

Although glycerol metabolism in *P. macerans* strains was thought to be restricted to respiratory conditions [166], the results reported here demonstrate that these organisms can utilize glycerol in a fermentative manner (Table 5.1 and Figures 5.3 and 5.4). The use of ^{13}C-labeled glycerol and analysis of the fermentation broth using different NMR techniques allowed identification of fermentation products and provided

evidence that they were synthesized from glycerol (Figures 5.4 and 5.5). Another NMR technique, 1D proton spin echo with and without a concurrent 90° pulse on carbon, was used to analyze the ^{13}C enrichment of proteinogenic biomass, which demonstrated that glycerol was incorporated into macromolecules. Excellent closure of redox and carbon balances was observed (Table 5.2).

Theoretical analysis			Experimental data	
Pathway	Stoichiometry (κ)[a]	ΔK (H)[b]	Concn of first product (mM)[c]	H_{HA}[d]
Glycerol → biomass	$C_3H_8O_3$ (14/3) → $3CH_{1.9}O_{0.5}N_{0.2}$ (4.3)[e]	1.1 (0.55H)	9.26	1.75
Glycerol → ethanol + CO_2[f]	$C_3H_8O_3$ (14/3) → C_2H_6O (6) + CO_2 (0)	2 (1H)		
Glycerol → ethanol + formate[g]	$C_3H_8O_3$ (14/3) → C_2H_6O (6) + CH_2O_2 (2)	0 (0H)	32.56	0.00
Glycerol → acetate + formate[g]	$C_3H_8O_3$ (14/3) → $C_2H_4O_2$ (4) + CH_2O_2 (2)	4 (2H)	0.63	1.27
Glycerol → 0.5 acetone + formate + 0.5 CO_2	$C_3H_8O_3$ (14/3) → $0.5C_3H_6O$ (16/3) + CH_2O_2 (2) + $0.5CO_2$ (0)	4 (2H)	3.46	13.82
Glycerol → 1,2-PDO	$C_3H_8O_3$ (14/3) → $C_3H_8O_2$ (16/3)	−2 (−1H)		
HA → 1,2-PDO	$C_3H_6O_2$ (14/3) → $C_3H_8O_2$ (16/3)	−2 (−1H)	16.67	−16.67

TABLE 5.5: Generalized degree-of-reduction balances for the conversion of glycerol into cell mass and selected fermentation products.
[a] Pathway stoichiometry accounts only for the carbon balance between reactants and products. The degree of reduction per carbon (κ) was estimated as described elsewhere [158] and is indicated in parentheses. [b] The degree of reduction balance (ΔK) is estimated as follows: $\sum_{over\ i\ reactants} v_i c_i \kappa_i - \sum_{over\ j\ products} v_j c_i \kappa_j$, *where v and c are the stoichiometric coefficient and the number of carbon atoms for each compound, respectively. The net number of redox units (H) is expressed per mole of glycerol (H ≡ NAD(P)H = reduce flavin adenine dinucleotide =* H_2*). [c] An experiment was conducted using a medium without tryptone but supplemented with HA. The values are the concentrations of the first product in the corresponding pathway or reaction. [d] The net number of redox units (*H_{HA}*) was calculated for the experiment in which HA was included in the medium (see footnote c) as follows: net number of redox units (H) obtained in the theoretical analysis × product concentration/product stoichiometric coefficient. [e] The cell mass formula is the average reported for a microbial cell [158]. [f] Pyruvate dissimilation via pyruvate decarboxylase was assumed. [g] Pyruvate dissimilation via PFL was assumed. The same results were obtained if the conversion of formate to* H_2 *and* CO_2 *was considered.*

The most established model for the fermentative metabolism of glycerol in bacteria entails an active 1,3-PDO pathway (Figure 5.1A). However, no 1,3-PDO was found in the fermentation broth, nor was 1,3-PDODH activity detected in cell extracts of *P. macerans* N234A (Figures 5.3 and 5.4 and Table 5.3). Instead, production of 1,2-PDO,

a structural isomer of 1,3-PDO, was observed (Figures 5.4B and 5.5B), and the pathway involved in its synthesis was identified (Figure 5.6). Based on this evidence, we conclude that glycerol fermentation in *P. macerans* N234A follows the "1,2-PDO–ethanol model" previously proposed for the fermentative utilization of glycerol in *E. coli* [5, 165] (Figure 5.1B). In this model, the synthesis of 1,2-PDO and ethanol enables glycerol fermentation by facilitating redox balance and ATP generation, respectively.

The role of the 1,2-PDO pathway in glycerol fermentation is better illustrated by performing a generalized degree-of-reduction balance analysis, as shown in Table 5.5. The synthesis of 1,2-PDO allows the cells to attain redox balance by consumption of the reducing equivalents generated during the incorporation of glycerol into cell mass and oxidized products. In agreement with the importance of this pathway, we found that stimulation of 1,2-PDO synthesis by addition of the pathway intermediate HA allows glycerol fermentation in the absence of tryptone. In this experiment, 42.1 mM glycerol was consumed, which resulted in the synthesis of 32.6 mM ethanol, 16.7 mM 1,2-PDO, 3.5 mM acetone, and 0.6 mM acetate (Table 5.5). Table 5.5 shows the calculated reducing equivalents generated or consumed in the synthesis of biomass and the products described above. Overall, the analysis of the degree of reduction shows that the reducing equivalents consumed in the synthesis of 1,2-PDO (16.7 mM) account for 99% of the reducing equivalents generated in the synthesis of cell mass and the fermentation products acetate and acetone (16.8 mM).

The results of the generalized degree-of-reduction analysis also supported the assumption that pyruvate dissimilation during glycerol fermentation takes place via PFL. Pyruvate dissimilation via any other known pyruvate-dissimilating enzyme (e.g.,

PDC, pyruvate dehydrogenase, or pyruvate oxidase) would result in the generation of one reducing equivalent per pyruvate molecule dissimilated. The degree of reduction for ethanol synthesis via PDC is shown in Table 5.5 ("glycerol → ethanol + CO_2" pathway). If the analysis described above were conducted with the assumption that pyruvate dissimilation occurs via PDC, only 34% of the reducing equivalents generated during the metabolism of glycerol would be accounted for by the 1,2-PDO pathway. These results indicate that the operation of the PDC pathway results in a significant redox imbalance that prevents the fermentative metabolism of glycerol. The PFL route avoids this situation by "storing" the "excess" reducing equivalents as formate or "releasing" them as hydrogen. Further evidence for the operation of PFL was obtained in the analysis of the composition of fermentation products for experiments conducted under alkaline conditions. Since a high pH inhibits the enzyme formate hydrogen lyase [176], which converts formic acid to CO_2 and hydrogen, the operation of the PFL route implies that the molar amount of formic acid accumulated in the extracellular medium should approach the sum of the amounts of ethanol and acetic acid. Using the data obtained at pH 8 (Figure 5.8), the number of moles of formic acid was calculated to be equivalent to 92% of the sum of the numbers of moles of ethanol and acetate.

The degree-of-reduction analysis presented above was more difficult to determine in experiments in which tryptone was included in the culture medium because of the lack of precise information about the relative contributions of glycerol and tryptone to the synthesis of biomass and acetate. However, if one assumes that the carbon from glycerol is incorporated into other cellular macromolecules in the same proportion that it is incorporated into proteinogenic biomass (i.e., 20%; Figure 5.5), 0.56 mM reducing

equivalents would be generated as a result of the cell growth shown in Figure 5.3A (0.385 g/liter). Since the conversion of glycerol to 1,2-PDO consumes 1 mol of reducing equivalents per mol of 1,2-PDO synthesized (Table 5.5), it follows that the amount of 1,2-PDO found in the fermentation broth (~0.33 mM) is close to the amount needed to provide a sink for the reducing equivalents generated in the synthesis of cell mass.

A key component of the proposed metabolic model is the operation of an oxidative pathway that channels glycerol into the glycolytic intermediate DHAP and is composed of three enzymes, namely a glyDH and PEP- and ATP-dependent DHAKs. The reaction catalyzed by glyDH is the first step in the fermentative metabolism of glycerol in all microorganisms in which this metabolic process has been characterized to date [3, 124, 159]. Although PEP-dependent DHAK is the most common DHAK found in glycerol-fermenting organisms [5, 124, 159], *P. macerans* N234A also possesses a second DHAK, ATP dependent DHAK.

The pathways described above provide a framework to explain the observed changes in cell growth and glycerol fermentation as a function of the pH and the concentrations of potassium and phosphate (Figure 5.7). High levels of phosphate promote the decomposition of both DHA and HA, two key intermediates in these pathways, and have also been shown to negatively affect the activity and inducibility of glyDH in other bacteria [151]. glyDH is one of the most important enzymes in the proposed pathways (Figure 5.1B). Moreover, bacterial MG synthases, which are key enzymes in the synthesis of 1,2-PDO (Figure 5.6A), are inhibited by high levels of phosphate [172, 177, 178]. High concentrations of potassium, on the other hand, increase the toxicity of MG in *E. coli* [159], and MG is a key intermediate in the synthesis of 1,2-

PDO (Figure 5.6). The effect of pH on glycerol fermentation (Figure 5.7) can also be related to its impact on the pathways mentioned above. DHA, an intermediate in the glyDH-DHAK pathway, is very unstable in alkaline environments. The higher toxicity of MG under alkaline conditions [159] also limits the synthesis of 1,2-PDO. Interestingly, the conditions described here as conditions that negatively affect glycerol fermentation (i.e., alkaline pH and high concentrations of potassium and phosphates) were used by other investigators during studies of glycerol metabolism in *P. macerans* [166]. This may be one of the reasons why the fermentative utilization of glycerol by this organism was not observed previously.

Finally, the proposed model suggests that the small amount of tryptone (or amino acids) required for glycerol fermentation to proceed is a consequence of the low activity of the 1,2-PDO pathway. The synthesis of 1,2-PDO appears to be the only pathway in *P. macerans* N234A able to "dispose of" the "excess" reducing equivalents generated during the incorporation of glycerol into cell mass; i.e., it is the only pathway that results in the net consumption of reducing equivalents (Table 5.5). The utilization of building blocks present in tryptone (e.g., amino acids) then reduces the use of glycerol in the synthesis of cell mass and, therefore, the associated redox imbalance. In agreement with this hypothesis, stimulation of the 1,2-PDO pathway (via addition of the intermediate HA) led to cell growth and glycerol fermentation in the absence of tryptone supplementation.

Chapter 6

Fermentation of lignocellulosic sugars by *P. macerans*

Production of biofuels and biochemicals from renewable sources is one way to reduce our reliance on fossil fuels [1]. Lignocellulosic biomass is one of the most abundant and inexpensive source of biomass available [15]. It is available in all parts of the world and it can be produced at faster rate than the replenishment of decaying supplies of fossil fuel. Production of ethanol, a fuel which can been used in place of gasoline as a transportation fuel, from lignocellulosic biomass has been touted as a possible way to utilize this abundant supply of biomass for production of biofuels [2].

Since the oil crisis of 1970, ethanol has been produced and marketed as an alternative to gasoline. But, even after so many years of research and government support, ethanol is not a cost effective alternative to the gasoline. There are several reasons for the failure of ethanol to take off in a cost competitive manner. One of the most important reasons is the substrate used for the industrial ethanol production: glucose. Although it is the best source of carbon and energy for growth of most microorganisms, it is often only a small part of the biomass used for the ethanol production [6]. Another major portion of the biomass is the five carbon sugars: pentoses, which mainly include xylose and arabinose. Yeast *Saccharomyces cerevisiae* has been used in the traditional production of ethanol from corn, which can not utilize these five carbon sugars and hence the productivity and yields of these processes have been low.

Another problem with the utilization of pentoses is that they can not be simultaneously consumed with glucose by most microorganisms. This has been the case

with model gram negative organism *E. coli* [179]. As described in Chapter 2, this phenomenon is called carbon catabolite repression and has been studied extensively in model microorganisms [13, 14]. As a result of these studies, several metabolic engineering based strategies have been implemented in last few years for simultaneous utilization of sugars by gram negative model microorganism *E. coli* and bioethanol producer *S. cerevisiae* [10, 15, 180-182]. Although this chapter doesn't focus on using metabolic engineering strategies for the simultaneous utilization of sugars, its focus is on traditional tools of finding the best conditions, when microorganism for this study, *P. macerans* can utilize the six carbon and five carbon sugars simultaneously.

Together with the simultaneous utilization of various sugars, another important factor for achieving higher productivity in the bioethanol production is the generation of byproducts. In the fermentative utilization of a substrate, cells naturally produce different organic acids and ethanol. These organic acids include formic acid, lactic acid, succinic acid and acetic acid. In a natural environment, cells don't have a preference for production of any of these products, so they produce them in a manner so that they can achieve optimal growth. But in industrial production, these products are side products and their production should be minimized to better achieve the substrate utilization. A popular strategy to reduce these byproducts and get higher yields of the desired products in model microorganisms has been to utilize the available knowledge of cellular pathways to knock out the genes responsible for the production of these side products [183, 184]. These metabolic engineering based strategies always lead to unintended effects on the cell growth because our knowledge of cellular pathways and their controlling mechanisms is not complete and also because with the removal of these

pathways, bacteria loses some of its flexibility to adapt to the changing environmental conditions, which could be requirements of redox balance or energy generation in the form of ATP. This chapter on sugar utilization will not focus on these metabolic engineering based strategies because of two reasons: the microorganism of this study, *P. macerans* naturally produces very low amounts of some of these byproducts as compared to many model microorganisms and also because this microorganism doesn't have a publicly available genome sequence.

Most biochemicals and biofuels, including ethanol (the focus of this chapter) are toxic to the cells above a certain concentration and most microorganisms can not survive the higher concentrations of these chemicals, which they are producing. This is one of the main reasons for use of *S. cerevisiae* in the industrial bioethanol production as it can tolerate higher concentrations of ethanol as compared to many other microorganisms [185-187].

This chapter will focus on three major sugars of the hemicelluloses portion of the lignocellulosic biomass: glucose ($C_6H_{12}O_6$), xylose ($C_5H_{10}O_5$) and arabinose ($C_5H_{10}O_5$). Although these hexose and pentose sugars have different number of carbon atoms in their chemical structures, oxidation state of carbon in all three sugars is zero (assuming the oxidation state for hydrogen as +1 and oxidation state for oxygen as -2 in three sugars) [158]. Hence in terms of reduced substrate, all three sugars are similar. As explained in Chapter 2, differences in the uptake and regulation of the three sugars of this study make *P. macerans* utilize these sugars differently. One thing that is common between any substrate utilization by microorganisms is need to maintain the energy and redox balance during their growth, which becomes more challenging for the cells in the

fermentative environment as there is no external electron acceptor present. Microorganisms achieve this by changing the ratio of extracellular products they are producing, which are ethanol, acetate, succinate, formate, and lactate. Since each of these products can be produced by multiple pathways and consumption or production of reducing equivalents is different in each possible pathway, there is always a complex balancing act going on in the cell to achieve the redox balance and to generate energy in the form of ATP for cell growth and maintenance. For example, in case of model microorganism *B. subtilis* (Figure 6.1), since conversion of glucose or pentose sugars to ethanol is not a redox balanced process (it consumes one net redox equivalent), theoretically generation of one mole of ethanol from Acetyl-CoA together with the acetic acid could achieve the redox balance. In this process, half of Acetyl-CoA will convert to ethanol and other half will go to acetic acid and coproducing one ATP. But this kind of product profile is seen very rarely experimentally because microorganisms often find other routes to achieve these balances. As an example, model microorganism *B. subtilis* achieves redox balance in a much shorter route with the production of lactic acid and still generates energy in the form of ATP through production of acetate [131, 174]. This versatility of achieving same objective through multiple routes makes cellular metabolism so challenging and complex.

Figure 6.1 depicts a simplified version of this complex central carbon metabolism in *B. subtilis*. As shown in the figure, in the first step, glucose is transported and phosphorylated by the phosphotransferase system (PTS), which has been described in detail in Chapter 2.

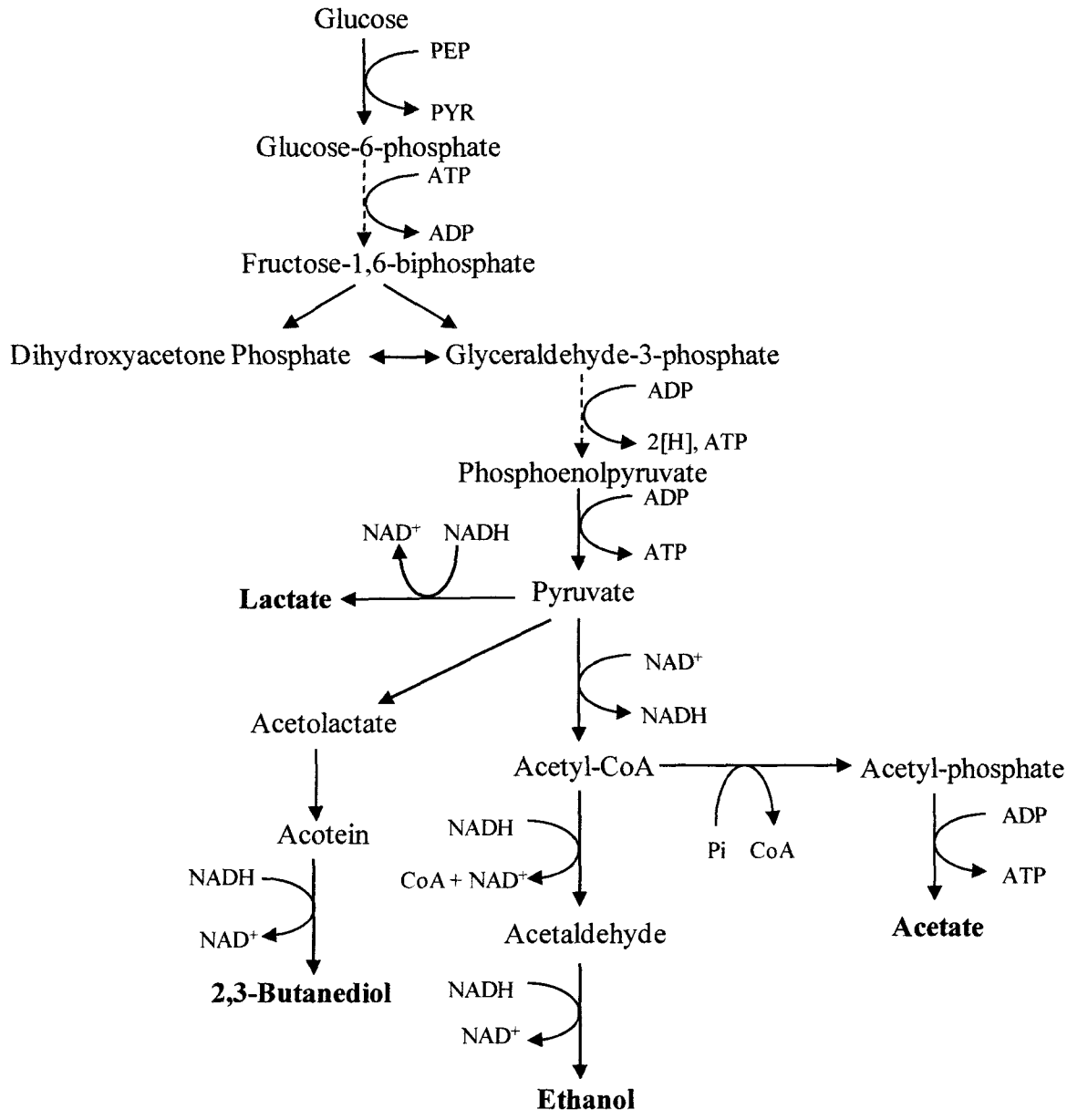

Figure 6.1: Metabolic Pathways for fermentative utilization of glucose by B. subtilis. Extracellular products have been shown in bold. (Adapted from [126, 131])

After transport, it is metabolized by Embden-Meyerhof-Parnas pathway (EMP) or pentose phosphate pathway (PPP). While EMP pathway generates energy and precursor metabolites for the cell, PPP pathway is mainly involved in the generation of cellular precursor metabolites and NADPH for the production of biomass. To balance the

dynamic cellular requirements, PPP and EMP pathways are connected through precursor metabolites fructose 6 phosphate (F6P) and glyceraldehyde 3 phosphate (Gly3P).

As explained earlier, during the complex act of balancing cellular requirements of energy and redox balance under fermentative conditions, cells try to balance redox equivalents while maximizing energy generation in the form of ATP. Pyruvate is an important intermediate in this scheme of balancing as multiple pathways originating from this intermediate lead to generation of different amounts of redox equivalents and energy. This intermediate is produced through the EMP pathway from phosphoenolpruvate (PEP). In the first pathway, pyruvate is converted to lactate in *B. subtilis* while consuming one redox equivalent. Since conversion of glucose to pyruvate through glycolysis generates one net reducing equivalent, conversion of pyruvate to lactate will balance the redox equivalents. This has been indeed the case with glucose fermentation in *B. subtilis*, where lactate, acetate and 2,3-butanediol are the main products of fermentative metabolism and blocking lactate pathway severely restricts cellular growth [131, 174]. Since the formation of 2,3-butanediol also involves consumption of one redox equivalents, it also provides a redox balanced pathway. Also, since conversion of pyruvate to acetate is one of the few pathways from pyruvate through which cells can generate ATP, acetate is a preferred product.

In general, microorganisms can convert pyruvate to Acetyl-CoA through two routes, in one route pyruvate is converted to Acetyl-CoA with the production of formate along the way by enzyme pyruvate formate lyase (PFL), and in the second route pyruvate is converted to Acetyl-CoA with generation of one redox equivalent and one mole of CO_2 by enzyme pyruvate dehydrogenase (PDH). Since the two routes result in very different

outcomes in terms of generation of redox equivalents, they are active based on the cellular redox balance requirements. In model gram negative microorganism *E. coli*, both PFL and PDH are present and they are active based on the cellular environment. During the fermentative conditions, there is no external electron acceptor present and hence the pathway in which no redox equivalent is generated (PFL), through PFL is active [188, 189]. In the respiratory conditions, when there is an external electron acceptor present, route through which redox equivalent is generated, the route through PDH is active [190]. But, in gram positive model microorganism *B. subtilis*, no gene coding for enzyme PFL has been found. Hence PDH is the only enzyme through which cells can convert pyruvate to Acetyl-CoA, which makes redox balance under fermentative conditions in this microorganism even more challenging [131, 174].

After conversion of pyruvate to Acetyl-CoA, it can go through two routes, in the first Acetyl-CoA is converted to ethanol through acetaldehyde by enzyme alcohol dehydrogenase. Generation of ethanol is accompanied by consumption of two redox equivalents, which is very good for the redox balance requirements as redox equivalents are generated in the conversion of glucose to pyruvate as well as in the conversion of pyruvate to Acetyl-CoA through PDH. In the second route, Acetyl-CoA is converted to acetate along with the generation of one ATP. This conversion is very important for the cells because of energy generation for the cells in the form of ATP. It is also one of the very few pathways through which cells can generate energy after substrate has been metabolized up to pyruvate node. Since cells always need energy for cell growth and maintenance requirements, this pathway is active in both respiratory and fermentative conditions, although level of activity is different depending on the conditions.

6.1 Fermentation of individual sugars by *P. macerans*

6.1.1 Fermentation of glucose by *P. macerans*

Glucose is the preferred carbon source for most microorganisms. It is abundant in nature and microorganisms can utilize it as a sole source of carbon and energy. Initial testing of the *P. macerans* strain N234A, with single sugars was done in tubes with a initial starting pH of 7 and with argon bubbling into the tubes to maintain an inert atmosphere, where no external electron acceptor is present. But, since this strain produced significant amount of acids (formic and acetic acid), the culture pH dropped significantly and further testing in the tubes was not possible without a pH control. Experiments with the use of buffering agents in the culture media also didn't help because of higher concentrations of acids being produced in the initial tube experiments. So further experiments were conducted under controlled conditions in the fermentor, where pH was controlled by external addition of base through a pH controller. Further evaluation in the fermentors also contributed in achieving better mixing as compared to the bubbling tubes.

Initial evaluation of growth on single sugars was done in fermentors with a culture volume of 500 ml, at 37°C and pH 6, with argon in the headspace. These conditions were chosen as our initial experiments, where initial testing in the bubbling tubes suggested that pH 6 is better than the normally used pH 7 for the glucose fermentation in *E. coli*, which could be because of several reasons that will be explained later in the pH optimization section 6.2. As can be seen in the Figure 6.2, in the nutrient rich LB medium, *P. macerans* N234A can consume 10 g/l of glucose in less than 12 hours, which is a consumption rate of ~1 g/l/hr. The main fermentation products in this

condition are formate, ethanol, acetate and acetone. The higher amounts of acids being produced cause the pH to drop and make the use of external pH control necessary. Also, sparging the argon in the fermentation media before the inoculation and in the headspace during the fermentation was done for three reasons: first use of argon itself provides an inert environment, where no external electron acceptor is present; second, by passing the argon in headspace, frothing in the fermentation media was minimized and third; by removing the bubbling in the media, the evaporation of volatile products such as ethanol and acetone was reduced. The stirrer rotation rate of 300 rpm was chosen because it provided a very good mixing without disturbing the stirrer itself. Since these were preliminary profiles, sampling was not done extensively.

It is clear from Figure 6.2(A) that product profiles for glucose fermentation by *P. macerans* N234A are unique, as there are no lactate and succinate detected in the fermentation media and formate is produced at more than 2 g/l, which is quite different from its close relative *B. subtilis* [174] and model microorganism *E. coli* [188]. In the fermentative metabolism of glucose by *B. subtilis*, lactate and acetate were main products, while in *E. coli* case succinate, formate, lactate, acetate and ethanol were detected in the fermentation media. In case of *P. macerans* N234A, ethanol and acetate are the main products of glucose fermentation, while formate is a minor product. Detection of formate in the fermentation of glucose by *P. macerans* N234A points to active pyruvate formate lyase (PFL) enzyme. No acetone was detected in the fermentation of glucose by *P. macerans*, which has been reported as one of the fermentation products in the previous studies of glucose fermentation by this

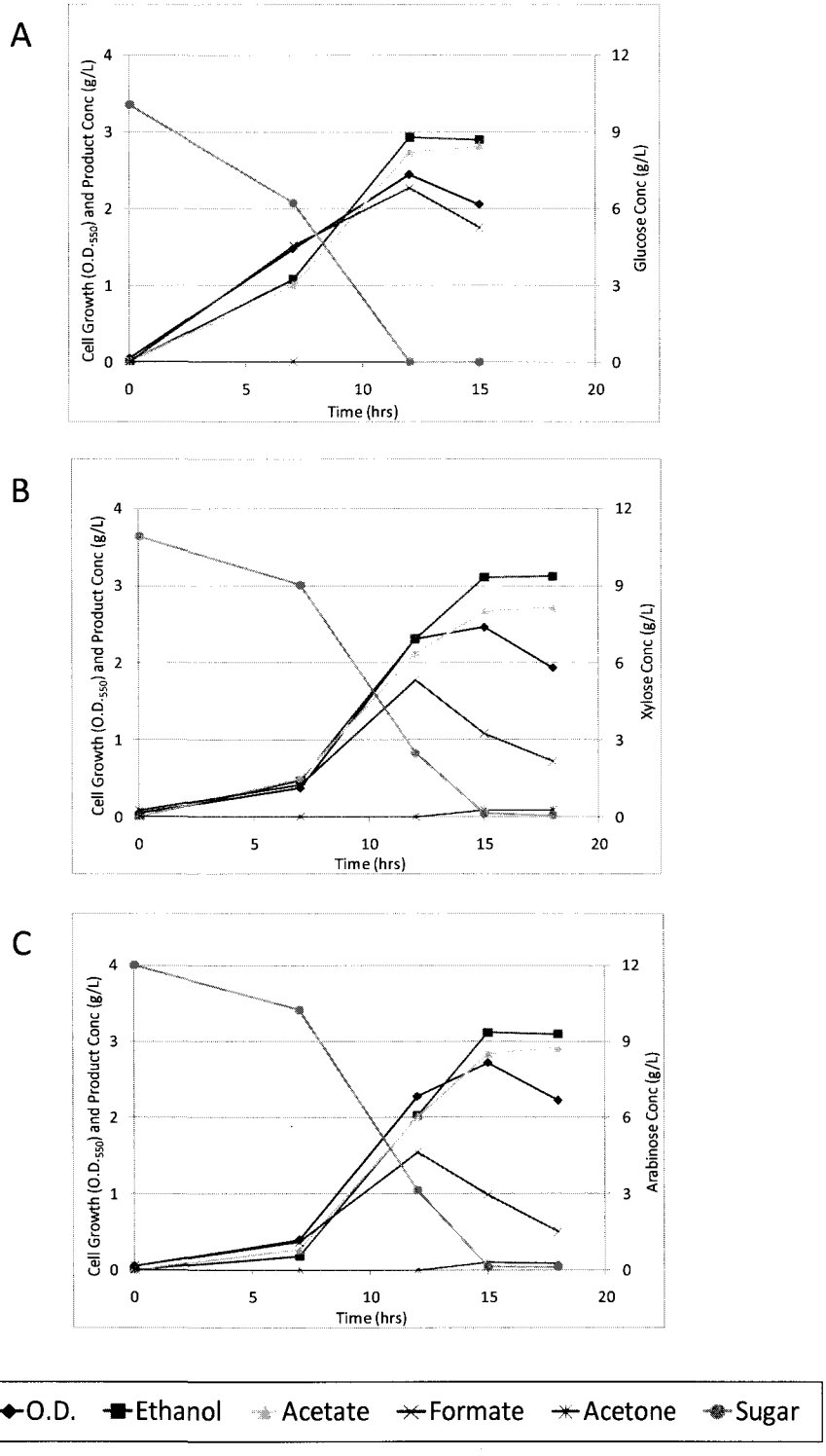

Figure 6.2: Fermentative utilization of individual sugars by P. macerans N234A in minimal media supplemented with tryptone and yeast extract and 10 g/l of respective sugar. (A) Glucose (B) Xylose (C) Arabinose. Cell growth and product concentrations are shown on left vertical axis, while sugar concentration is shown on the right vertical axis.

microorganism [23]. In terms of product yields, biomass had a yield of 0.62 mol/mol and ethanol had a yield of 1.14 mol/mol (Table 6.1).

6.1.2 Fermentation of xylose by *P. macerans*

Fermentation of xylose as sole source of carbon and energy by *P. macerans* N234A was evaluated in a similar manner as in glucose case. Since in *B. subtilis* there is no specific xylose transporter [191], it was expected that xylose metabolism will be slower than glucose, which was indeed the case. As seen in the Figure 6.2(B), *P. macerans* N234A can ferment xylose efficiently by fermenting 10 g/l xylose in 15 hours with a consumption rate of 0.66 g/l/hr. Similar to glucose fermentation, acetate and ethanol are the main products, while formate production first increases and then decreases because of possible conversion of formate into CO_2 and H_2. In a distinction from glucose fermentation, acetone was detected in the fermentation broth of xylose fermentation, although in very low concentrations. The product yields for the xylose case are 0.49 mol/mol for biomass and 0.94 mol/mol for the ethanol (Table 6.1). A lower yield for the acetate in the xylose fermentation can be attributed to the formation of acetone as acetone is produced from the condensation of two molecules of acetate.

6.1.3 Fermentation of arabinose by *P. macerans*

Fermentation of arabinose by *P. macerans* N234A as sole source of carbon and energy was very similar to the xylose fermentation, with 10 g/l of arabinose consumed in 15 hours with a consumption rate of 0.66 g/l/hr. Similar to xylose fermentation, ethanol and acetate are major products, while formate and acetone are the minor products. Again,

as seen in the Figure 6.2(C), formate concentration increases up to 1.5 g/l and then drops significantly, which could be attributed to possible dissociation of formate into CO_2 and H_2. Acetate and ethanol concentrations remain constant after reaching the maximum value at the highest cell growth. Yields of biomass and ethanol in arabinose case are 0.49 mol/mol and 0.86 mol/mol respectively, which are lower than in both glucose and xylose cases (Table 6.1).

An important aspect to consider in three individual sugars consumption is the formate profiles. Formate concentration first increases and then decreases in all three cases; in the case of xylose and arabinose, even when the cells are still growing. Also, there is sequential decrease in the highest concentration of formate produced as we go from glucose to xylose to arabinose. This increase and then decrease in the concentration of formate is distinct feature of sugar fermentation by *P. macerans* N234A as there is no formate production by its close relative *B. subtilis* under similar conditions [174], while in the case of *E. coli* there is no decrease in concentration of formate while the cells are still growing [192, 193].

Comparison of the growth curves for the three sugars shows that while final optical density value is highest in case of arabinose, growth rate on glucose is much higher (Figure 6.2). The highest cell density (OD_{550}) achieved for the case of glucose is 2.44, for xylose case it is 2.46 and for the arabinose case it is 2.72. As it is evident from the Figure 6.2, growth rate on glucose is higher than both xylose and arabinose.

Similarly the comparison of the sugar consumption profiles in the three cases shows that glucose is consumed at much faster rate as compared to the xylose and

arabinose. Since xylose and arabinose are both pentose sugars, their very similar consumption profiles point to their similar mechanisms of uptake and transport.

After the initial testing of individual sugars in the fermentors, which showed that both hexose and pentose sugars can be consumed efficiently, next step was to evaluate the consumption of sugar mixtures by *P. macerans* N234A. As discussed earlier, simultaneous consumption of lignocellulosic sugars is very important for the efficient conversion of hemicellulosic portion of the biomass, as current industrial processes only rely on conversion of glucose to ethanol. Efficient conversion of sugar mixtures to ethanol will increase the process yields of the current processes.

Given the importance of simultaneous sugars utilization, initial experiments were done to examine the metabolism of sugar mixtures by *P. macerans* N234A. As we saw in the previous section that *P. macerans* N234A was able to utilize the three sugars individually at pH 6 and 37 °C, this initial examination was done at pH 6 and 37°C. Further experiments showed that *P. macerans* N234A can utilize the three sugars simultaneously at this condition, results of which are explained in detail in section 6.2.2. Since this was very interesting result, to further evaluate the consumption of sugar mixtures by *P. macerans* N234A, two very important fermentation parameters were chosen for systemic study: first was the culture pH and second was the medium temperature. These two parameters can affect the fermentation profiles in multiple ways, including changes in enzyme activities caused by variation in these two parameters. To evaluate these two parameters, first temperature was fixed and effect of pH was studied, and then in the next part pH was fixed and temperature was studied.

6.2 Effect of pH on sugar mixture fermentation by *P. macerans*

As we saw in the case of individual sugars in bubbling tubes, culture pH had a significant effect on the sugar fermentation by *P. macerans* N234A. So based on our initial screening, we chose four pH conditions for the systemic evaluation of effect of culture pH on sugar mixture consumption: 5.5, 6, 6.5 and 7. This range of pH gives us both narrow intervals and wide enough range to evaluate the effects of medium pH on the sugar mixture fermentation.

6.2.1 Evaluation of fermentation profile at pH 5.5

Analysis of effect of change in pH on fermentation profiles was started with pH 5.5. As seen in Figure 6.3(A), as compared to individual sugars case, changing the pH to 5.5 had dramatic effect on sugar mixture consumption. For the glucose, instead of consuming 10 g/L in 12 hours, it took 36 hours to consume the same amount of glucose. As for xylose and arabinose, there was only 1 g/l consumption of both sugars before cells reached stationary phase. Maximum cell growth (OD_{550}) at this pH was 1.96, which is lower than the maximum cell growth achieved in the case of single sugar glucose fermentation. Both acetate and ethanol were produced at close to 3 g/l in the fermentation time of 36 hours. One important aspect of fermentation at this pH is the lower amount of formate produced with maximum concentrations only reaching 0.24 g/l. As for amount of acetone produced in this condition, no acetone was detected in the fermentation samples

at this pH. Yields of cell biomass and ethanol achieved in this case are 0.46 and 1.05 respectively (Table 6.3), which are both less than the single sugar glucose fermentation.

From the fermentation profile, it may be noted that this microorganism was able to utilize the three sugars of sugar mixture simultaneously at this pH. In the Figure 6.3(A), we can clearly see that presence of glucose inhibits the utilization of pentose sugars: xylose and arabinose, but it is not the complete repression usually seen in the sugar mixture fermentations. Even in the presence of glucose, xylose and arabinose consumption starts, but much more slowly than individual sugars. Other important feature to note in this case is the amount of consumption of xylose and arabinose during the fermentation. It is very clear from the profile that rate of consumption of arabinose is much faster than the xylose, which is quite different from individual sugar case, where xylose and arabinose had very similar consumption and product profiles.

6.2.2 Evaluation of fermentation profile at pH 6

This is the same pH at which single sugar consumption was evaluated as described in the previous section. From the fermentation profiles in the Figure 6.3(B), it is clear that sugar mixture consumption at pH 6 is much better than in the pH 5.5, with all three sugars consumed in less than 36 hours. Out of sugar mixtures, first glucose is finished, then arabinose and finally xylose. But, it is also clear from the profile that as in the case of pH 5.5, simultaneous consumption of sugars starts before the glucose is

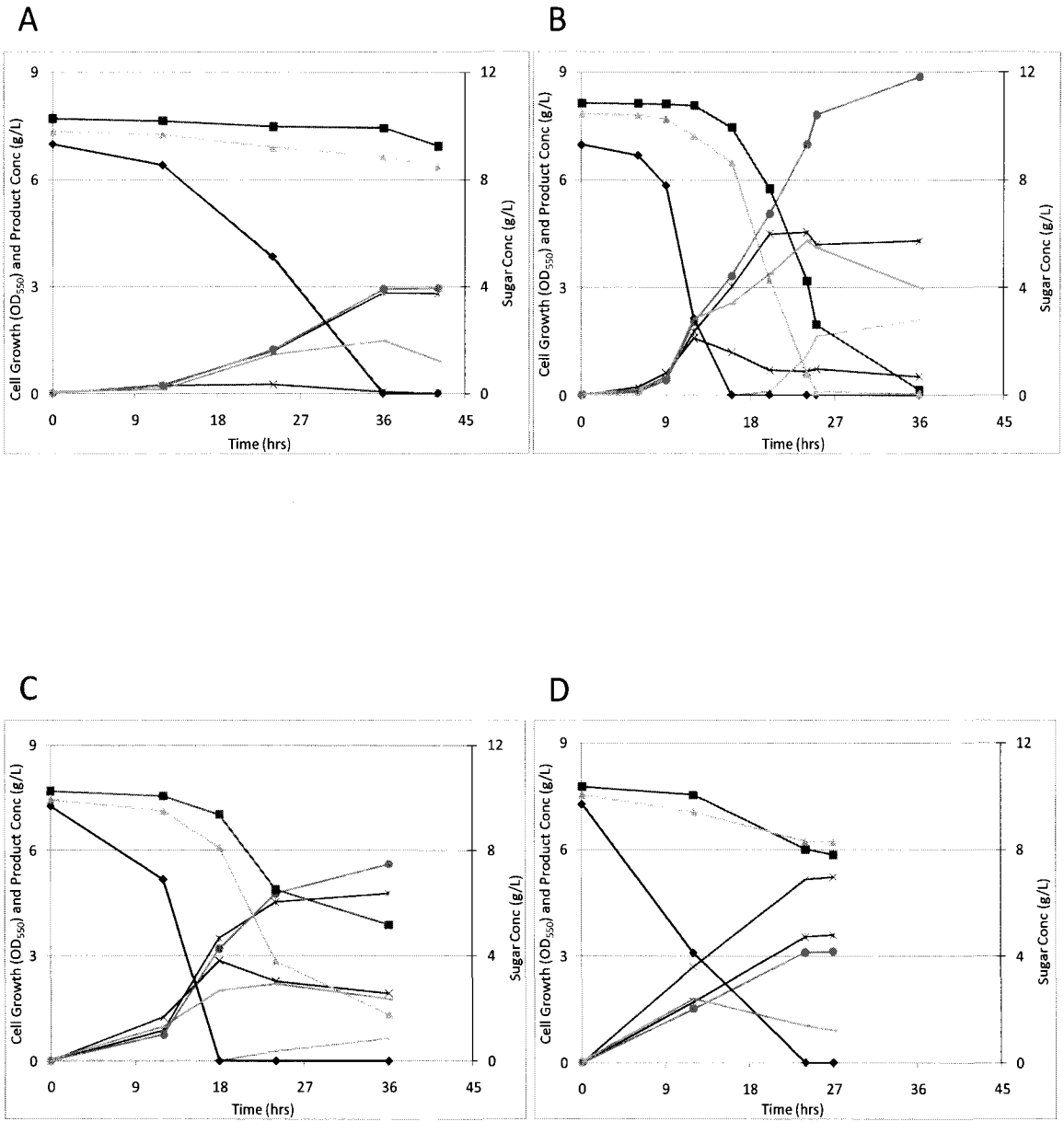

Figure 6.3: Fermentative utilization of sugar mixtures by P. macerans N234A at different culture pHs in minimal media supplemented with tryptone and yeast extract and 10 g/l each of glucose, xylose and arabinose. (A) 5.5 (B) 6 (C) 6.5 (D) 7

finished, with 1 g/l of xylose and 2 g/l of arabinose consumed, while 10 g/l of glucose is consumed, implying that there is no repression in sugar mixture fermentation by this microorganism. At this pH, 10 g/l of glucose is consumed in less than 16 hours, which is little slower than individual glucose consumption rate (Figure 6.2), this could be attributed to the fact that other sugars are also being consumed together with the glucose in this case.

For the cell growth, in this case, maximum optical density of 5.74 was reached at 24 hours (Figure 6.3(B)), which is the highest growth seen in this study. In terms of the products, ethanol concentration reached upto 8.85 g/l in 36 hours, again the highest concentration seen in this study. Consistent with the pattern in the individual sugars case, formate concentration first increased upto 12 hours at 1.77 g/l and then decreased slowly to 0.5 g/l. Acetate concentration increased continuously upto 24 hours to a concentration of 4.49 g/l and then decreased a little bit afterwards, which could be attributed to its faster conversion into acetone than its production from the sugars. Acetone concentration reached upto 2 g/l, which is also the highest for this study. Overall we see that at pH 6, sugar consumption was higher than seen before in this study (30 g/l sugars consumed in less than 36 hours) and also the concentration of ethanol reached to 9 g/l, with a conversion rate of 0.29 g ethanol / g sugar consumed (Table 6.3), close to 60 % of the theoretical maximum.

6.2.3 Evaluation of fermentation profile at pH 6.5

Next study was conducted at pH 6.5. At this pH, from the Figure 6.3(C), we can see that the sugar consumption clearly slowed from the pH 6. First 10 g/l glucose was consumed in 18 hours, which is little slower than the pH 6 case. But, most importantly is the consumption of other sugars, xylose and arabinose, that is affected the most, with more half of 10 g/l of xylose still remaining even after 36 hours. As with the pH 5.5 and 6, presence of glucose affected the consumption of xylose and arabinose, but 0.8 g/l of xylose and 1.8 g/l of arabinose was consumed in the time glucose was fully consumed. This amount of total sugar consumption is similar to what we saw in the case of pH 6. This shows that change in pH from 6 to 6.5 did not affect simultaneous consumption of sugars (consumption of pentose sugars while glucose is still present) as much as the consumption of pentose sugars.

In terms of products, there was significant increase in the production of formate up to a concentration of 2.85 g/l (Figure 6.3(C)), much higher than the 1.77 g/l formate concentration we saw in the case of pH 6. This is even more significant considering the even lower amount of sugars consumed in this case. One primary reason for this increased concentration is that the enzyme dissociating formate into hydrogen and carbon dioxide, formate hydrogen lyase, is less active at pH 6.5 than at pH 6 [147], hence higher concentrations of formate at higher pH were observed. The cell growth also decreased considerably at this pH as compared to pH 6, with highest optical density achieved is only 2.9 at 24 hours. Highest concentrations of ethanol and acetate achieved are 5.61 g/l and 4.78 g/l respectively, which are also considerably lower than the pH 6.

Highest concentration of acetone is also lower in this case at 0.646 g/l. In terms of yields also, ethanol yield of 0.24 g/g of sugars in this case is lower than the yield achieved at pH 6 (Table 6.3).

6.2.4 Evaluation of fermentation profile at pH 7

The final experiment to assess the effect of pH on the fermentation of mixed sugars by *P. macerans* N234A was done at pH 7. From the fermentation profile in the Figure 6.3(D) at pH 7, it is clear that consumption of sugars at pH 7 is even worse than at pH 6.5. The consumption of 10 g/l of glucose itself takes close to 24 hours, while only 2.35 g/l of xylose and 1.75 g/l of arabinose was consumed in 24 hours. Again, in line with the effect of pH in other cases, changing the pH didn't seem to have the effect of simultaneous conversion of sugars; rather it affects the sugar consumption itself.

In terms of the product profiles at pH 7, the maximum amount of ethanol produced is at 3.12 g/l, which is very close to the ethanol produced at pH 5.5. As for the acetate, the maximum concentration is higher than that of ethanol at 3.59 g/l. Yield of ethanol at this pH is 0.22 g/g of sugar (Table 6.3), which is lower than any other pH in this study. As for the acetone, it was not detected in any of the fermentation samples, which is again what we also saw for the case of pH 5.5. One thing that was quite different at this pH is the amount of formate produced, which is 5.22 g/l. This formate concentration is the highest concentration of it seen in this study. Since, as we increase the pH, enzyme converting formate into hydrogen and carbon dioxide becomes less and less active, higher concentration of formate are seen in the culture medium [147]. As for

the cell growth, cells achieved the highest optical density of 2.4 in 12 hours and then growth decreases slowly afterwards.

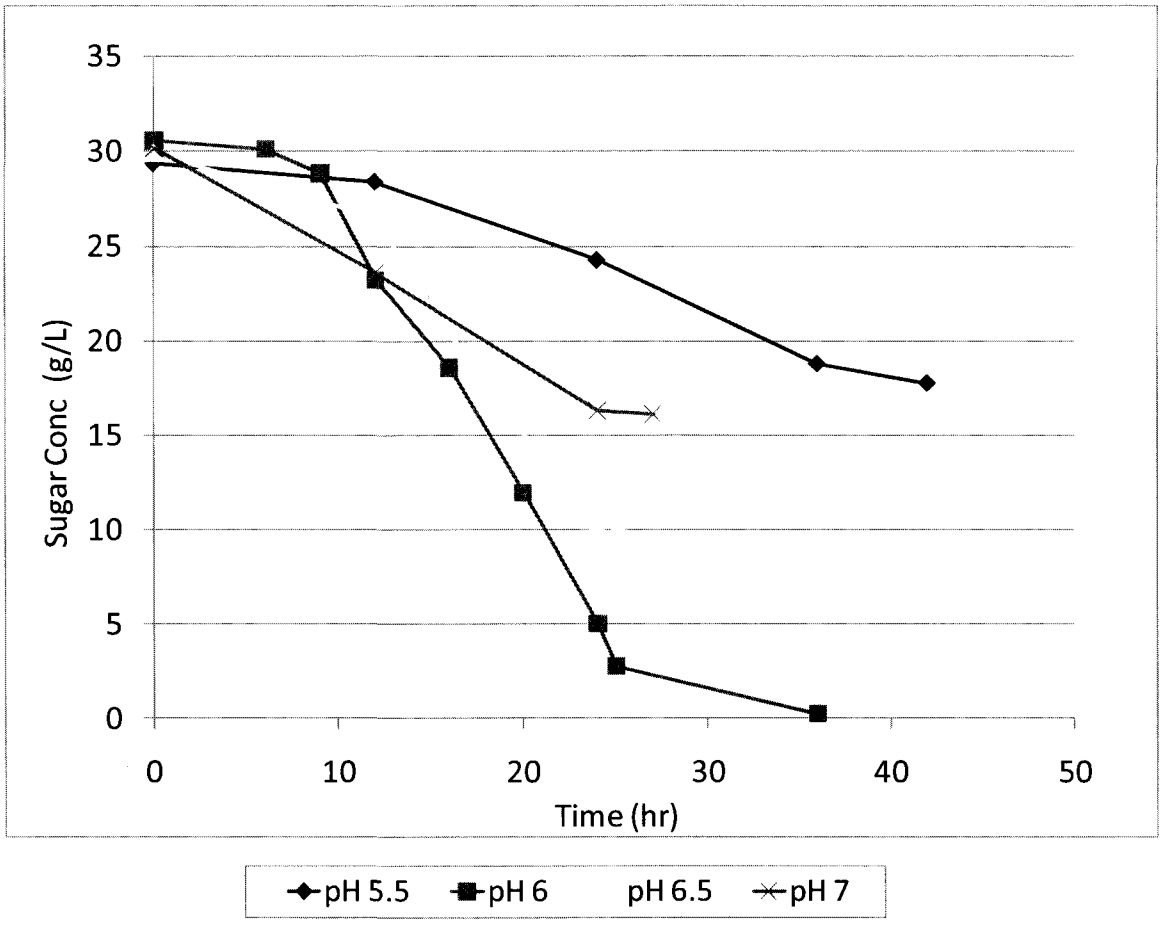

Figure 6.4: Total sugar consumption profiles in the fermentative utilization of sugar mixtures by P. macerans N234A at different pHs in minimal media supplemented with tryptone and yeast extract and 10 g/l each of glucose, xylose and arabinose.

From the results in the previous sections, where sugar mixture fermentation by *P. macerans* N234A was analyzed under different pH conditions, it is clear that the pH 6 is the optimum pH for the ethanol production by *P. macerans*. First parameter to

consider is the consumption of sugar mixture, as seen in Figure 6.3(B) and Figure 6.4, 30g/l of total sugar mixture is consumed in 36 hours at pH 6, while significant amount of sugars are left at other pHs, clearly demonstrating that pH 6 is the pH at which *P. macerans* N234A consumes them fastest. Also, if we compare the rates of individual sugar consumption, it is also fastest at pH 6 for each of the sugars as compared to any other pH. In term of the production of ethanol, the focus of this study, we see that the highest concentration of ethanol is achieved in the shortest amount of time at pH 6, reaching close to 9 g/l in less than 36 hours. Also, we see that the production of acetate and ethanol seems to decouple at pH 6, if we compare their concentrations at other pHs, where concentrations of ethanol and acetate are very close to each other. This is misleading as we also see highest concentration of acetone at pH 6, which is produced from condensation and decarboxylation of two molecules of acetate. So the acetate concentration we observe at pH 6 is the result of its production as well as its consumption in the production of acetone.

6.3 Effect of temperature on sugar mixture fermentation by *P. macerans*

Another important variable in the fermentation of sugars by microorganisms is the culture temperature, which can affect the fermentation by changing the profiles for cell growth, substrate and the products. Temperature can also affect the overall cost of the production by making the processing of products easier after the fermentation. Since 37°C is the best temperature for the growth of most microorganisms, it was the first

temperature that was chosen for the study. After that, two more temperatures at 5° intervals, at 42° and 47°C were chosen for further investigation. Ethanol being a volatile product, higher temperatures also helps in reducing the process cost. So, if at higher temperatures consumption of sugar mixtures is faster [194], then it is a favorable condition for operation of the fermentation. Since in the previous study we found that pH 6 is the best pH for sugar mixture fermentation, all the experiments for the study of temperature effect on fermentation were conducted at pH 6.

6.3.1 Fermentation profile at 37°C

As seen in Figure 6.5(A), all the three sugars are consumed in less than 36 hours at 37°C. Consumption of pentose sugar, xylose and arabinose start in the presence of glucose, but it is slower than individual pentose sugar consumption rates we saw in the Figure 6.2. Clearly glucose slows down the consumption of these pentose sugars, with only 0.9 g/l of xylose and 1.8 g/l of arabinose consumed while 10 g/l of glucose is consumed. This phenomenon of simultaneous consumption of sugars by this microorganism is quite different to its closely related species *B. subtilis*, where pentose sugars itself are not readily utilized [191]. Another important thing to notice is that rate of

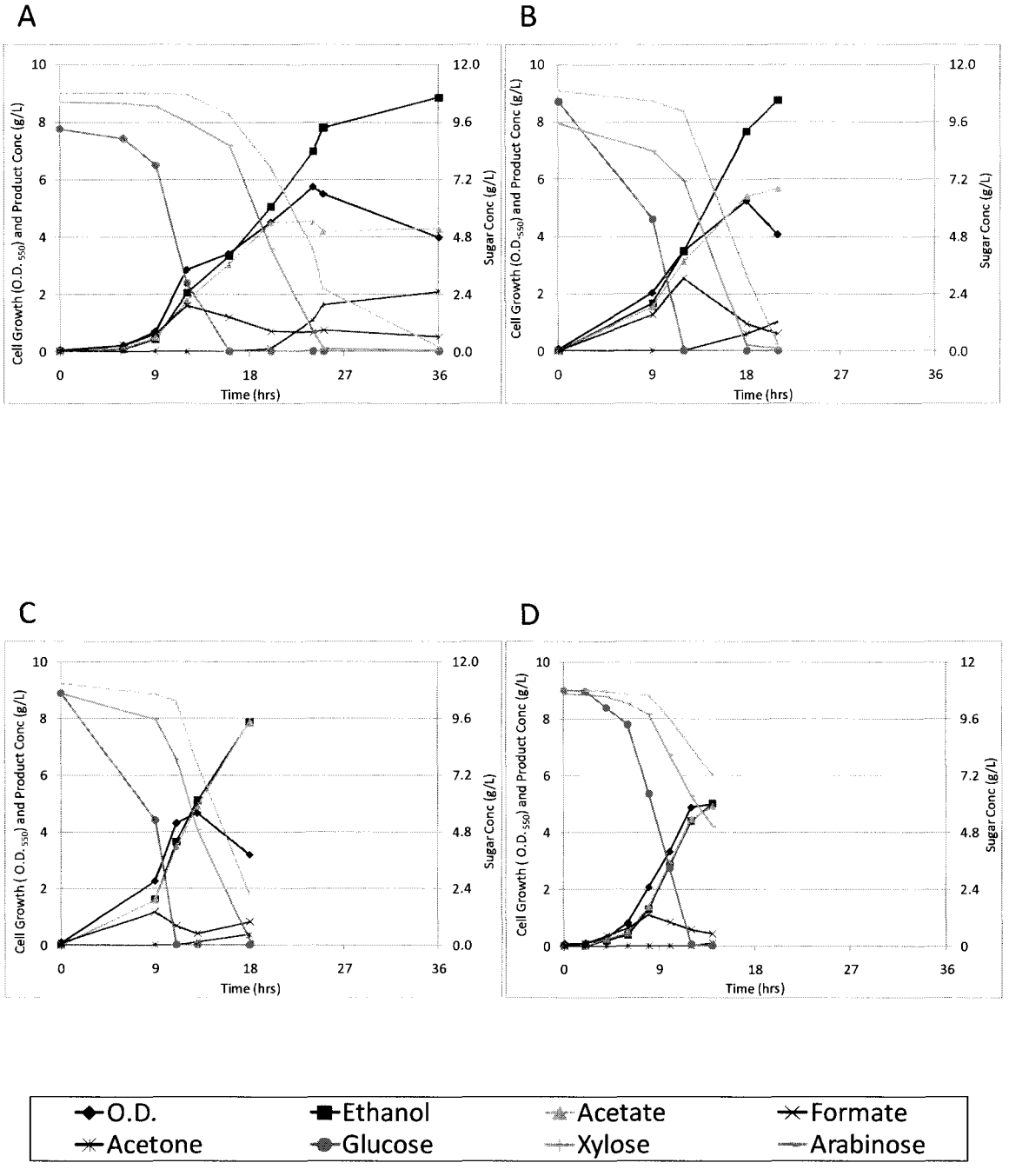

Figure 6.5: Fermentative utilization of sugar mixtures by P. macerans N234A at different culture temperatures in minimal media supplemented with tryptone and yeast extract and 10 g/l each of glucose, xylose and arabinose. (A) 37°C (B) 42°C (C) 47°C (D) 47°C with higher resolution during initial phase of growth.

arabinose consumption is faster than the xylose, when glucose is present and also when glucose is fully consumed. Overall, we see that glucose is consumed first at 10 g/l in 16 hours, then 10 g/l of arabinose in 25 hours and finally 10 g/l of arabinose in less than 36 hours.

In terms of product profile, ethanol is the main product with highest concentration of 8.86 g/l achieved in 36 hours (Figure 6.5(A)). Acetate is the product with second highest concentration (4.54 g/l), whose concentration first increases continuously and then decreases little bit to 4.29 g/l. Consistent with earlier profiles, formate concentration first increases upto 1.58 g/l and then decreases continuously throughout the fermentation. Another product seen in the product identification through HPLC is the acetone, which is first seen at 20 hours and then it increases continuously to a final concentration of 2.09 g/l. Maximum cell growth (optical density) achieved in this fermentation is 5.74, which is the highest of this study.

6.3.2 Fermentation profile at 42°C

From Figure 6.5(B), it is very clear that the sugar consumption for all the three sugars at 42°C is faster than at 37°C. Specifically, it can be seen that 10 g/l of glucose is consumed in 12 hours at this temperature compared to the 16 hours it took at 37°C. For the arabinose, it took 18 hours to consume 10 g/l and for xylose 21 hours for 10 g/l of it. In agreement with the other sugar mixture fermentation, xylose and arabinose are consumed at much slower rates than glucose, when glucose is present. Only 0.85 g/l of xylose and 2.41 g/l of arabinose are consumed in the time 10 g/l of glucose is consumed.

After the glucose is consumed, pentose sugar consumption picks up and they are consumed at much faster rate.

At the 42°C temperature, the main product is again ethanol with maximum concentration of 8.75 g/l, which is very close to the ethanol concentration at 37°C of 8.85 g/l, but in this case it was achieved in only 21 hours rather than in 36 hours. As for the other products, acetate concentration at this temperature reached 5.66 g/l, which is one of the highest concentrations of acetate in this study, definitely much higher than the 4.54 g/l reached at 37°C. Formate had a similar pattern as before, first increasing and then decreasing during the fermentation with the highest concentration of 2.53 g/l, which is also higher than the 1.58 g/l reached at 37°C. Highest concentration of acetone in this case is 0.99 g/l, which is less than its concentration at 37°C, because higher concentration of acetate could mean that lower amount of acetate is being converted to acetone. For the cell growth, maximum growth was reached at 18 hours with an optical density of 5.24, which is lower than the maximum growth achieved at 37°C.

6.3.3 Fermentation profile at 47°C

At the final temperature of this study, the consumption of sugars is even faster than at 42°C (Figure 6.5(C)). Glucose is consumed in just 11 hours compared to the 12 hours in 42°C. Arabinose is consumed in 18 hours which is similar to the time it took to consume same amount of arabinose at 42°C. But, what is consistent even at this temperature is effect of glucose on consumption of xylose and arabinose. In presence of glucose, only 0.74 g/l of xylose and 2.79 g/l of arabinose is consumed, but after glucose

is fully consumed, xylose and arabinose are consumed at a much faster rate than in the presence of glucose.

Product profiles at 47°C are little different than at other two temperatures. Although ethanol is still the main product of sugar fermentation, concentrations of ethanol and acetate are very close at this temperature, with maximum ethanol concentration of 7.87 g/l and acetate concentration of 7.87 g/l. This ethanol concentration is lower than the highest ethanol concentration achieved at 42°C by almost 1 g/l, which could be attributed to couple of factors. First, in 47°C fermentation, at 18 hours there is still more than 2 g/l of xylose left, which could produce more ethanol if the fermentation was continued afterwards. The second factor affecting the ethanol concentration is the higher temperature in this case. Since ethanol is a volatile product (boiling point = 78.4°C), much higher amounts of it will evaporate at 47°C than at 42°C, thus lowering the effective concentration in the fermentation media. The other important point to see is that as we move from 37°C to 47°C, there is a clear trend in the concentration of acetate; it increases from 4.54 g/l at 37°C to 5.66 g/l at 42°C to 7.88 g/l at 47°C. This clear increase in concentration of acetate as we increase the temperature is directly opposite to the pattern in the concentration of the acetone. Its concentration decreases from 2 g/l at 37°C to 0.36 g/l at 47°C. Since two moles of acetate are needed to form one mole of acetone in the reaction pathway, these two phenomena are clearly linked with each other. Since, acetone is also a volatile product (boiling point = 56.5°C) similar to the ethanol, it will also evaporate at higher rate at 47°C than compared to 37°C, but since this is a more than five fold decrease in acetone concentration with temperature change and its absolute concentration itself is low, it can be assumed that its evaporation

is insignificant during the fermentation. Formate follows its pattern as before with maximum concentration reaching 1.15 g/l at 9 hours and then decreasing slowly during the fermentation. Cell growth in this case, increased steadily upto an optical density of 4.67 at 13 hours and then decreased afterwards.

Comparison of fermentation profiles at the three temperatures shows both similarities and differences among them. In similarities, we see the simultaneous consumption of three sugars in all three cases, with glucose consumed at a faster rate than the pentose sugars. Among pentose sugars themselves, arabinose is consumed at a faster rate than xylose in all three cases. In terms of product profile, ethanol is the main

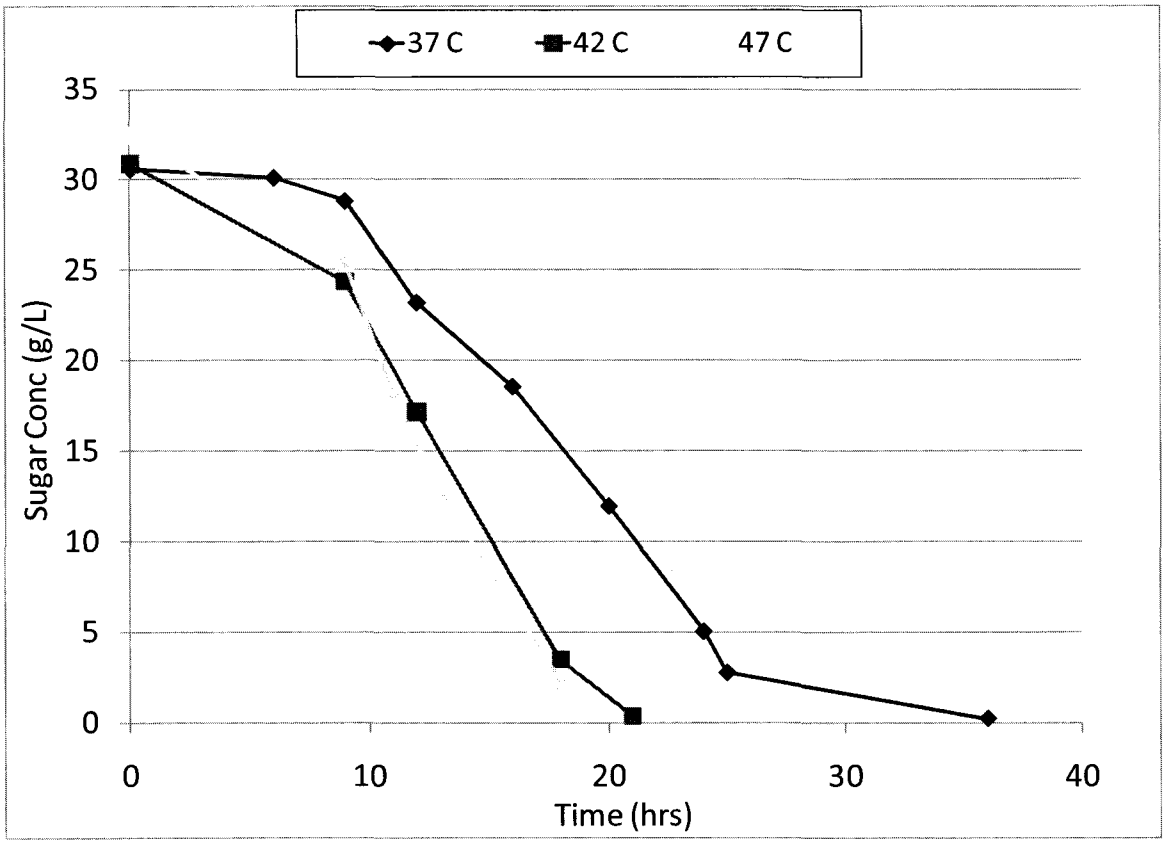

Figure 6.6: Total sugar consumption profiles of sugar mixtures fermentation by P. macerans N234A at different culture temperatures in minimal media supplemented with tryptone and yeast extract and 10 g/l each of glucose, xylose and arabinose.

fermentation product in all three cases, with acetate, formate and acetone are the minor products. Formate profile is also consistent in the three profiles, which first increases and then decreases. Also, in all three cases cells first grow, then reach stationary phase and then they start to die even before the last sugar, xylose, is completely consumed.

In the differences, as seen in the Figure 6.6, with the increase in temperature, rate of total sugar consumption clearly increases with highest rate of sugar consumption achieved at 47°C. Also, simultaneous consumption of sugars, i.e., consumption of pentose sugars while glucose is still present in the media is higher at 47°C (3.53 g/l pentose sugars consumed while 10 g/l glucose is consumed) as compared to 42°C and 37°C. Other thing that changes as we move from 37°C to 47°C is the cell growth, which decreases as we increase the temperature. This pattern of cell growth is beneficial for our aim because as less substrate is utilized for the production of biomass, more of it can be utilized for the production of ethanol. Acetate concentration increases as temperature increases from 4.54 g/l at 37°C to 7.88 g/l at 47°C, in contrast to the decreasing pattern in acetone concentration, which decreases from 2.09 g/l at 37°C to 0.37 g/l at 47°C. Since two moles of acetate produce one mole of acetone in the biochemical pathway, these opposite patterns are related to each other. One profile that is not monotonous in its pattern as we increase the temperature is the formate profile; it increases from 1.58 g/l at 37°C to 2.53 g/l at 42°C and then decreases to 1.15 g/l at 47°C.

6.4 Discussion

6.4.1 Fermentation of individual sugars by *P. macerans*

From the results of individual sugar fermentations, it is clear that *P. macerans* N234A can ferment the three sugars: glucose, xylose and arabinose in the absence of external electron acceptors. It is also clear from the Figure 6.2 that it can do it efficiently in less than 15 hours for all three sugars. Although previous studies have been done for the fermentation of glucose [23] and xylose [24] by *P. macerans*, they were not done under strict pH control. As a result of this, fermentation profiles obtained in these cases also include the effect of a continuously decreasing pH throughout the fermentation, because of the production of acetic acid during the fermentation. This study is first one to show that both hexose and pentose sugars can be utilized efficiently under controlled pH conditions. Also, this is the first study to characterize the utilization of arabinose by *P. macerans*, a significant portion of hemicellulose.

Fermentation of all three individual sugars by *P. macerans* N234A is unique. While *P. macerans* N234A can metabolize xylose efficiently, its close relative *B. subtilis* can not utilize xylose as sole carbon source because it does not have xylose specific transporter [191]. It has also been reported that *B. subtilis* mutants constitutively expressing arabinose transporter were able to metabolize xylose [116]. In any case, the product profile of sugar fermentation by *P. macerans* is significantly different from that of *B. subtilis* as no lactate and 2,3-butanediol were detected in the fermentation products of sugar fermentation by *P. macerans* N234A, the major fermentation products of *B. subtilis* fermentation [174]. Instead, we see a product mix containing ethanol, acetate and

acetone in the case of *P. macerans* N234A. Since acetone is one of the products of sugar fermentation by *P. macerans* N234A, if we compare the product profiles of *P. macerans* with the other major acetone producing microorganism *C. acetobutylicum*, we notice that *P. macerans* product profile is also quite different with that of *C. acetobutylicum*. While we see ethanol as the main product in case of *P. macerans*, butanol is the main fermentation product with *C. acetobutylicum* [195].

Comparison of three sugar profiles quantitatively shows that (Table 6.1) glucose has the highest yield in terms of both biomass and ethanol. In case of glucose, biomass yield of 0.62 and ethanol yield of 1.14 are better than the biomass yield of 0.49 and ethanol yield of 0.86 in case of arabinose. Comparison of maximum specific productivities and maximum volumetric productivities shows that there is no clear trend.

Sugar	Yield (mmol product/mmol sugar)[a]		Max specific productivity (mmoles/g cell/h)[b]			Max volumetric productivity (mmoles/L/h)[c]		
	Cells	Ethanol	Cells	Sugar	Ethanol	Cells	Sugar	Ethanol
Glucose	0.62	1.14	14.43	23.32	26.59	2.89	6.93	8.06
Xylose	0.49	0.94	18.58	38.28	36.06	5.49	8.74	8.00
Arabinose	0.49	0.86	19.42	40.01	34.23	5.32	9.48	8.01

Table 6.1: Fermentation parameters for cell growth, sugar utilization, and ethanol production for the case of three individual sugars. [a]Growth and product yields (mmol/mmol of sugar) were calculated as the amount of cell mass or product synthesized per amount of sugar consumed once the cultures reached the stationary phase. [b]Maximum specific productivities, in mmol per gram of cells per hour, were calculated by taking into account the interval at which maximum mmol of substrate were consumed and cells and products formed. The concentration of cells during the given period of time is calculated as time average. [c]Maximum volumetric productivities are reported for the cultivation period at which the maximum mmol of substrate were consumed and cells and products formed per liter per hour

Comparison of glucose fermentation profile, with earlier study of glucose fermentation by *P. macerans* N234A shows notable differences. The first and most important difference is the pH, in the earlier study culture pH was not controlled, so the pH dropped upto 5 in the earlier study. Another major difference is the product profiles,

although ethanol is the main product in both cases, acetone is the second largest product in earlier study, while we do not see any acetone in glucose fermentation and we find acetate as the second largest product. This apparent difference in product profile is primarily due to the initial glucose concentration in the earlier study. While glucose concentration was 50 g/l in the earlier study, it was only 10 g/l in this study and also because of the higher initial glucose concentration, fermentation in the earlier study lasted for 80 hours, while here it lasted only for 12 hours as 10 g/l of glucose is already consumed in 12 hours. If we see the profile in the earlier case, no acetone is detected in the first 15 hours, which is longer than the fermentation time in this study.

This profile can also answer the speculation in earlier study that acetone formation is dependent on the culture pH, where lower pH is favorable for the acetone production. It can also answer the earlier suggestion that lowering of culture pH in the beginning of fermentation will lead to early acetone formation. In the present study, we see that although culture pH was 6, which is lower than the normal physiological pH of 7, no acetone is produced. It shows that the formation of acetone is not dependent on the pH alone, there are other factors also, which could play a role in the formation of acetone, one of these factors is the pathway through which acetone is produced. The other microorganism which produces acetone together with butanol, *C. acetobutylicum*, converts two moles of acetate into acetone and releases one mole of CO_2 in the process [195]. It can be assumed that the production of acetone in *P. macerans* N234A could also occur through acetate. From the fermentation profiles of the xylose and arabinose cases, it is clear that acetone formation occurs only after 12 hours and is associated with the almost complete cessation of acetate production. This means production of acetone

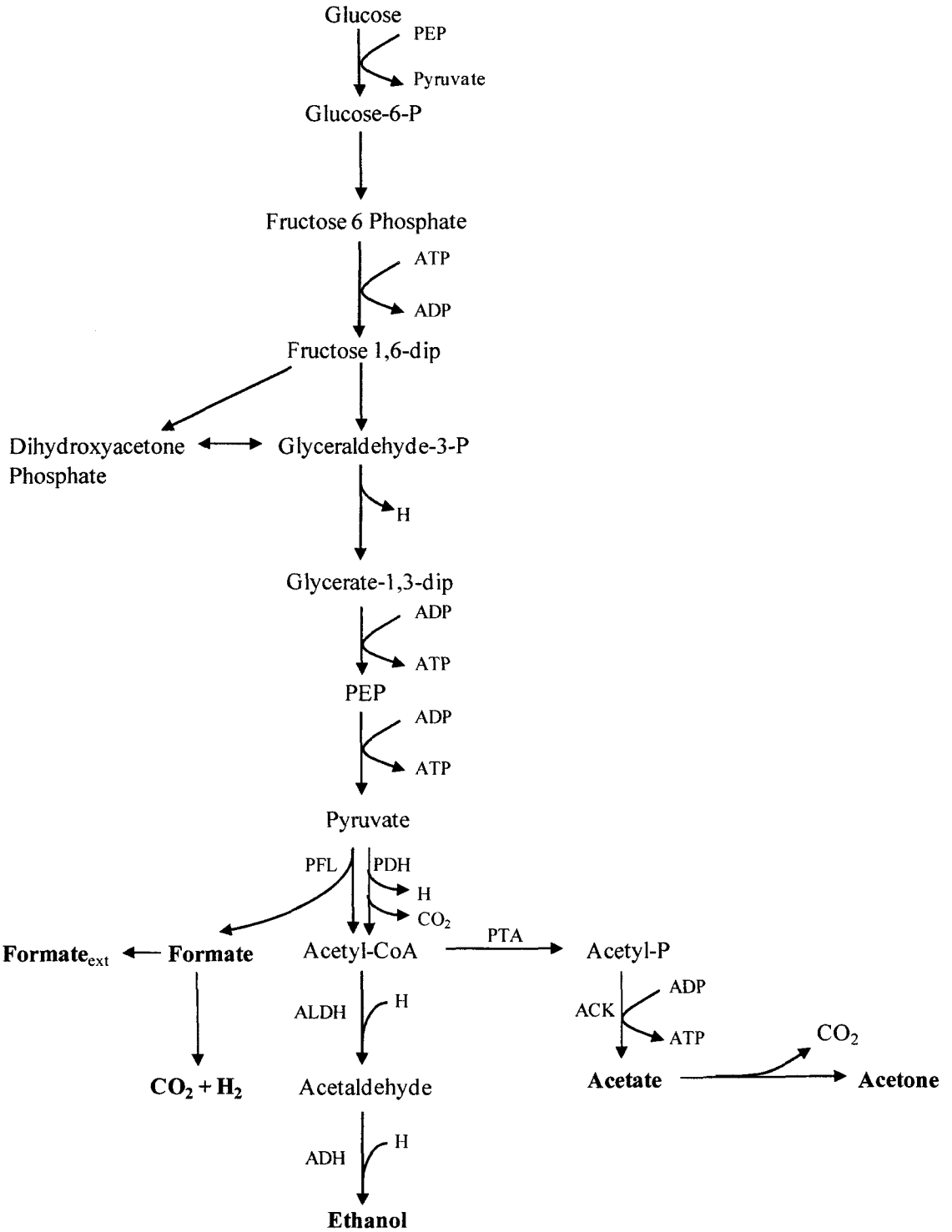

Figure 6.7: Proposed pathways for fermentation of glucose by P. macerans N234A showing redox equivalents and energy generation. Two possible routes have been shown for conversion of pyruvate to Acetyl-CoA. Extracellular products have been shown in bold.

occurs from the acetate and it occurs only after reaching certain acetate concentration in the medium. It can be speculated that after this concentration is reached, the conversion of acetate to acetone starts. Once the conversion starts, whether the concentration of acetate remains constant or decreases depends on the rate of formation of acetate from Acetyl-CoA and the rate of its conversion to acetone.

From the product profile of the glucose fermentation, it is clear that glucose is fermented via glycolysis, which results in a product profile of mix acid fermentation. It also implies that glucose is converted to pyruvate via Embden-Meyerhof pathway. Among products, formate is a major product of the fermentation. Although production of formate in glucose fermentation by *P. macerans* has been reported before [23], no formate is seen in the glucose fermentation of close relative *B. subtilis* [174]. This happens because *B. subtilis* does not have the pyruvate formate lyase enzyme, which converts pyruvate to formate and Acetyl-coA under fermentative conditions; instead it has pyruvate dehydrogenase, which converts pyruvate to Acetyl-CoA and producing CO_2 and one reducing equivalent in the process. Although pyruvate dehydrogenase is mostly active under aerobic conditions, in *B. subtilis* it is active under fermentative conditions and converts pyruvate to Acetyl-CoA [131, 174].

In terms of redox balance during the conversion of glucose to ethanol, it can be seen from Figure 6.7 that if we assume that all the pyruvate is converted to Acetyl-CoA through pyruvate formate lyase, the conversion of one mole of glucose to phosphoenolpyruvate produces one redox equivalent and subsequent conversion of phosphoenolpyruvate to ethanol consumes two reducing equivalents [188, 189]. Hence the conversion of glucose to ethanol by *P. macerans* is a redox consuming process. Also,

the conversion of glucose to acetate, the other major product of fermentation, is a redox generating process. It generates one reducing equivalent during conversion of glucose to acetate. So, if we take two moles of glucose into account and have one mole of ethanol and one mole of acetate as products from these two moles of glucose, it will perfectly balance the redox equivalents. Table 6.2, which is quantitative redox balance calculation based on the assumption that conversion of pyruvate to Acetyl-CoA occurs solely through the pyruvate formate lyase, shows that there is a deficiency of 0.65 reducing equivalents through this pathway. Also, in the Figure 6.2, we see that concentration of acetate is always lagging the concentration of ethanol in all three sugar fermentations. On

Substrate consumed and products formed	Moles of product/moles of substrate consumed[a]	Oxidation state[b]	Redox Balance[c]	Carbon recovery (no. of C atoms)[d]
Substrate				
Glucose		0	0	6
Products				
Acetic acid	0.817	0.000	0.000	1.635
Formic acid	0.885	2.000	1.769	0.885
Carbon dioxide	1.075	4.000	4.299	1.075
Hydorgen[e]	1.075	-2.000	-2.149	
Ethanol	1.142	-4.000	-4.567	2.284
Total			-0.649	5.878

Table 6.2: Fermentation balances for growth of P. macerans N234A on glucose at pH 6 and 37 °C. [a]The data are for samples taken at 12 hours from the culture described in Figure 6.2(A). The values are the net number of moles produced per mole of glucose fermented. [b]The oxidation state of carbon atoms was calculated by assuming that the oxidation states were -2 and +1 for oxygen and hydrogen, respectively [158]. [c]The values were obtained by multiplying the number of moles of product per mole of glycerol by the oxidation state of carbon atoms. [d]Carbon recovery was calculated by multiplying the number of moles of product per mole of glycerol by the number of carbon atoms in the molecule. [e]The numbers of moles of carbon dioxide and hydrogen were calculated as previously described [147, 165].

the molar basis concentration of acetate is only 70% of ethanol being produced. Hence, it is clear that there must be another pathway active, which is generating the reducing equivalents for the production of ethanol.

If we assume that pyruvate is being converted to Acetyl-CoA through pyruvate dehydrogenase (Figure 6.7), then this pathway produces one redox equivalent per mole of glucose. Overall, conversion of one mole of glucose to ethanol will be a redox balance pathway, while conversion of glucose to acetate will be two redox equivalents generating pathway. Assumption of existence of a NAD dependent formate dehydrogenase, which will generate one reducing equivalent in conversion of formate to CO_2, will also provide similar results in terms of redox equivalents as the case of pyruvate dehydrogenase. Since we see both acetate and ethanol being produced, and acetate concentration is significantly less than the ethanol on molar basis, clearly both pyruvate formate lyase and pyruvate dehydrogenase are active during anaerobic fermentation of glucose by *P. macerans* N234A, with conversion of pyruvate to Acetyl-CoA primarily occurring through the pyruvate formate lyase. Indeed, previous studies on the glucose fermentation by this microorganism have come to similar conclusion [23, 196].

Fermentation of xylose and arabinose by *P. macerans* N234A can also be explained in similar way, since both xylose and arabinose enter the pentose phosphate pathway after their transport and are further metabolized through the central carbon metabolism. Hence redox balance requirements for the pentose sugars are exactly similar to the glucose case and similar results were obtained for redox balance calculations as for glucose.

6.4.2 Fermentation of sugar mixtures by *P. macerans*

Most microorganisms can not utilize mixture of hexose and pentose sugars simultaneously. Specifically, close relative of *P. macerans*, *B. subtilis* can not even ferment xylose by itself [191] and model gram negative microorganism *E. coli* can not ferment pentose sugars in the presence of glucose [179]. In a sugar mixture, *E. coli* ferments pentose sugars only after glucose is completely consumed.

In the study to find the best pH for the fermentation of sugar mixture, we find that the pH 6 is the optimum pH for the sugar mixtures and glucose is consumed in 16 hours and all the three sugars were fully consumed in less than 36 hours at this pH. Also, glucose consumption in 16 hours in the case of sugar mixtures is lower than the case of individual glucose consumption time of 12 hours. This was probably happening because the other pentose sugars were also being utilized together with glucose in sugar mixture case. When all the glucose was consumed at 16 hours, there was already 2.69 g/l of pentose sugars consumed. It shows that in *P. macerans* N234A, both hexose and pentose sugars are being utilized simultaneously and presence of glucose in the substrate mixture only affects the extent pentose sugars utilization.

From the curve of sugar mixture utilization at pH 6 (Figure 6.3), it is also clearly visible that utilization of arabinose is faster than the xylose. It can be explained on the basis of the behavior of *P. macerans*'s close relative, model gram positive microorganism *B. subtilis*. It has been shown before that *B. subtilis* transports both xylose and arabinose through arabinose transporter and can only utilize xylose, when there is constitutive expression of the arabinose transporter [109, 116, 191]. From the fermentation profile of sugar mixture utilization by *P. macerans* N234A, it can be said

that similar mechanism might be true for this microorganism also, where both xylose and arabinose are transported through the same transporter and arabinose is preferentially transported through this transporter in comparison to xylose.

Comparison of four pH conditions tested in terms of specific productivity (Table 6.3) shows that there is highest maximum specific productivity for cell (20.84 mmoles/g cell/hr), sugars consumed (43.22 mmoles/g cell/hr) and ethanol production (41.80 mmoles/g cell/hr) at pH 6. Similarly highest maximum volumetric productivity for cells (4.34 moles/l/hr), sugar consumed (15.26 moles/l/hr), ethanol production (17.73 moles/l/hr) also occurs at pH 6, which clearly proves that pH 6 is the best pH for the fermentation of sugar mixtures by this microorganism.

pH	Yield (mmol product/mmol sugars)[a]		Max specific productivity (mmoles/g cell/h)[b]			Max volumetric productivity (mmoles/L/h)[c]		
	Cells	Ethanol	Cells	Sugars	Ethanol	Cells	Sugars	Ethanol
5.5	0.46	1.05	8.57	16.83	17.72	1.53	2.58	3.07
6.0	0.44	0.97	20.84	43.22	41.80	4.34	15.26	17.73
6.5	0.34	0.87	10.73	25.61	22.20	3.20	8.72	8.84
7.0	0.90	0.88	13.47	16.27	13.49	2.74	3.66	2.88

Table 6.3: Fermentation parameters for cell growth, sugar utilization, and ethanol production at four pH conditions. [a]Growth and product yields (mmol/mmol of sugar) were calculated as the amount of cell mass or product synthesized per amount of sugar consumed once the cultures reached the stationary phase. [b]Maximum specific productivities, in mmol per gram of cells per hour, were calculated by taking into account the interval at which maximum mmol of substrate were consumed and cells and products formed. The concentration of cells during the given period of time is calculated as time average. [c]Maximum volumetric productivities are reported for the cultivation period at which the maximum mmol of substrate were consumed and cells and products formed per liter per hour.

For the temperature study, four temperatures 37, 42, 47 and 52°C were chosen and we saw in the section 6.3 that out of the first three temperatures, 47 turns out to be best temperature for the simultaneous consumption of sugar and it is also the fastest

temperature for sugar mixture consumption. At 52°C, cells didn't grow at all and hence it was not shown in the results section.

Comparison of the quantitative rates for the sugar consumption at three temperatures as shown in Table 6.4 proves that indeed the 47°C is the best temperature for sugar consumption. It can be seen that the biomass yield is the highest (0.55) at 47°C, while the ethanol yield is not the highest (0.92), it is very close to the other two temperatures. In terms of maximum volumetric productivity, from the table, it is clear that 47°C is the best temperature compared to the other two temperatures: maximum volumetric productivity for cells at 47°C is 14.48 mmoles/l/hr, for sugars consumed is 21.22 mmoles/l/hr and for ethanol it is 22.20 mmoles/l/hr.

Temperature	Yield (mmol product/mmol sugars)[a]		Max specific productivity (mmoles/g cell/h)[b]			Max volumetric productivity (mmoles/L/h)[c]		
	Cells	Ethanol	Cells	Sugars	Ethanol	Cells	Sugars	Ethanol
37	0.51	0.95	19.15	43.22	41.80	4.34	15.26	17.73
42	0.43	0.97	14.62	33.72	32.83	6.95	15.19	15.15
47	0.55	0.92	19.50	40.27	36.48	14.48	21.22	22.20

Table 6.4: Fermentation parameters for cell growth, sugar utilization, and ethanol production at three different temperatures. [a]Growth and product yields (mmol/mmol of sugar) were calculated as the amount of cell mass or product synthesized per amount of sugar consumed once the cultures reached the stationary phase. [b]Maximum specific productivities, in mmol per gram of cells per hour, were calculated by taking into account the interval at which maximum mmol of substrate were consumed and cells and products formed. The concentration of cells during the given period of time is calculated as time average. [c]Maximum volumetric productivities are reported for the cultivation period at which the maximum mmol of substrate were consumed and cells and products formed per liter per hour

From the product profiles for the three temperatures, we see a clear trend for acetate and acetone concentrations. As we increase the temperature, acetate concentration starts to go up with increasing temperature and acetone concentration starts to go down significantly. Although it can be argued that since acetone is a volatile compound, with

increasing temperature more and more acetone evaporates and this gives rise to less concentration of acetone in the medium. But, this argument can not explain the increase in concentration of acetate, a non volatile compound from 4.3 g/l at 37°C to 7.88 g/l at 47°C. Clearly, there is increasing acetate concentration in the medium with increasing temperature. Also, since one mole of acetone is produced from two moles of acetate, sum of moles of acetate and twice the moles of acetone will give the amount of acetate being produced from Acetyl-CoA. At 37°C, this sum is 143.8 mmoles/l, while at 47°C it is 144 mmoles/l, which shows that there is almost no difference in acetate production from Acetyl-CoA between two temperatures, that proves that with increasing temperature it is the conversion of acetate to acetone which is decreasing, that leads to higher concentrations of acetate and lower concentrations of the acetone at higher temperatures.

Higher rates of sugar consumption at higher temperatures are also better for the post fermentation processing of ethanol. Since ethanol is collected through distillation in commercial units, higher operating temperature for the fermentation step saves the energy cost of heating the fermentation stream up to the distillation temperature. Higher operating temperatures also save in the energy cost in the pretreatment of the carbohydrate substrate before it is fed into the fermentation as this step is also generally done at high temperatures and higher fermentation temperature means less cooling is needed between the pretreatment and fermentation [194]. Higher fermentation temperature is also helpful in reducing the microbial contaminants in the fermentation as higher fermentation temperatures are not the best temperatures for growth of most microbes [197].

In summary, fermentation of three sugars of the lignocellulosic biomass by *P. macerans* were studied in this chapter, first individually and then in a mixture of three sugars. Individual sugar fermentations showed that glucose is utilized at faster rate than the xylose and arabinose. In the sugar mixtures case, effect of culture pH and temperature on the fermentative metabolism of the three sugars was studied. It was found that *P. macerans* can utilize the three sugars simultaneously, with pH 6 and temperature of 47°C being the optimum conditions for ethanol yield and productivity.

Chapter 7

Metabolic flux analysis of glycerol and lignocellulosic sugar fermentation by *P. macerans*

Metabolic flux analysis is a powerful tool for understanding the metabolic capabilities of living cells. It provides a framework for the study of cellular response to changes in extracellular environment through the knowledge of extracellular metabolite concentrations and the biochemical reaction network [22]. Analysis of biochemical reaction network at system level provides the information about the intracellular reaction rates of different steps in the reaction network, whose measurements are not always possible. Calculation of metabolite fluxes in this analysis provides the information about the relative importance of an individual reaction compared to other reactions in the network [28]. Comparison of metabolic fluxes among the same strain under different physiological conditions or among different strains under same conditions can provide the information about potential targets for metabolic engineering strategies towards a specific objective. Since metabolic flux analysis gives direct information about the intracellular reaction rates of different steps in the desired pathway, only this analysis provides the knowledge that can be directly correlated with the extracellular concentrations which can be measured experimentally. Owing to the importance of metabolic flux analysis in the understanding of cellular physiology, this chapter focuses on the metabolic flux analysis of fermentation of glycerol and lignocellulosic sugars by *P. macerans*.

7.1 Metabolic flux analysis of fermentative utilization of glycerol by *P. macerans*

Figure 7.1 shows the proposed pathways for the fermentative utilization of glycerol and the synthesis of fermentation products by *P. macerans* N234A based on the results reported in Chapter 5. Conversion of glycerol to the glycolytic intermediate DHAP takes place through a pathway composed of glyDH and ATP- as well as PEP-dependent DHAKs, as suggested by our experimental results (Tables 5.3 and 5.4). DHAP was converted to PEP through the Embden-Meyerhof-Parnas pathway, as previously reported [23, 24, 167], resulting in the generation of one molecule each of reducing equivalent and ATP, per molecule of PEP synthesized. The glycolytic pathway is completed by the conversion of PEP to pyruvate, a step catalyzed by both PEP-dependent DHAK and pyruvate kinase. Synthesis of ethanol and 1,2-PDO through the pathways identified in this study are also shown in Figure 7.1 along with the acetate pathway, which has been characterized by others [23, 24, 167].

7.2 Reaction network model for glycerol fermentation

Metabolic flux analysis (MFA) is a technique, widely used in the study of microbial physiology [28, 158] and therefore used here to characterize the fermentative utilization of glycerol in *P. macerans* N234A. MFA was conducted using the technique of metabolite balancing on intracellular metabolites, as described elsewhere [28]. Molar balances around intermediate metabolites were formulated considering the pathways involved in the fermentation of glycerol by *P. macerans* N234A (shown in Figure 7.1). The resulting metabolic network consists of fifteen (15) reactions/fluxes and ten (10)

intermediate metabolites for which balance equations can be written, thus resulting in a system with five (5) degrees of freedom. The set of reactions included in the stoichiometric model, along with a description of balanceable intracellular metabolites and measured fluxes, are shown in the *Appendix A*. The inclusion of both ATP-dependent and PEP-dependent dihydroxyacetone kinases (DHAK) in the model created a mathematical singularity i.e. the system cannot be solved to calculate intracellular fluxes. This problem was solved by assuming that the *in vitro* activity of each DHAK (reported in Chapter 5) is a good estimator of the fraction of carbon processed by the enzyme. Since five (5) extracellular metabolites were measured and information for the ratio of the fluxes through PEP- and ATP-dependent DHAKs was available, the resulting system is over-determined [28]. However, the glycerol consumption flux was not used as input but rather calculated and compared to the measured value to assess the accuracy of the model.

Figure 7.1 shows the metabolic pathways considered in the reaction network, along with the flux map obtained for glycerol fermentation at pH 6. Calculated (58.46 mmol/g of cell/h) and measured (56.81 mmol/g of cell/h) values only differed by 2.9%, evidencing the accuracy of the model. In general, the distribution of metabolic fluxes among various fermentative pathways agrees with the differences observed in product yields (Figures 5.8 and 7.1).

7.3 ATP yield and redox balance ratio in glycerol fermentation

The calculated fluxes enabled the estimation of key metabolic parameters such as redox balance and ATP generation. For example, the redox balance ratio (R/O ratio) was calculated by dividing the two fluxes that generate NADH by the sum of all the fluxes that consume it. For the proposed flux model, R/O = $(\upsilon_1 + \upsilon_4)/(\upsilon_7 + \upsilon_8 + \upsilon_{14} + \upsilon_{15})$ (see *Appendix A* and Figure 7.1 for details of reaction/flux numbering). The calculated R/O ratio was 1.01, which indicates an excellent closure of the redox balance based on the MFA. The flux model was also used to calculate the ATP generation rate (υ_{ATP}: millimoles of ATP formed per gram of cells per hour) and the ATP yield (Y_{ATP}: moles of ATP formed per mole of glycerol consumed): note that $\upsilon_{ATP} = \upsilon_4 + \upsilon_5 + \upsilon_{10} - \upsilon_3$ and $Y_{ATP} = \upsilon_{ATP}/\upsilon_1$. Calculated υ_{ATP} and Y_{ATP} for cells grown at pH 6 were 58.47 mmol/g of cell/h and 1.00 mol ATP/mol of glycerol, respectively. These high rates of ATP generation appear to enable the high rates of growth and glycerol consumption in *P. macerans* N234A (Figure 5.2). For example, the calculated υ_{ATP} was similar or higher than that reported during fermentative growth of *E. coli* on glucose [198].

7.4 Model for fermentative utilization of glycerol by *P. macerans*

MFA was also used to help identify the pathways involved in pyruvate dissimilation and synthesis of ethanol. Pyruvate dissimilation can take place through three enzymes: pyruvate-formate lyase (PFL: converts pyruvate to AcCoA and formate), pyruvate dehydrogenase (PDH: converts pyruvate to AcCoA, NADH, and CO_2) and pyruvate

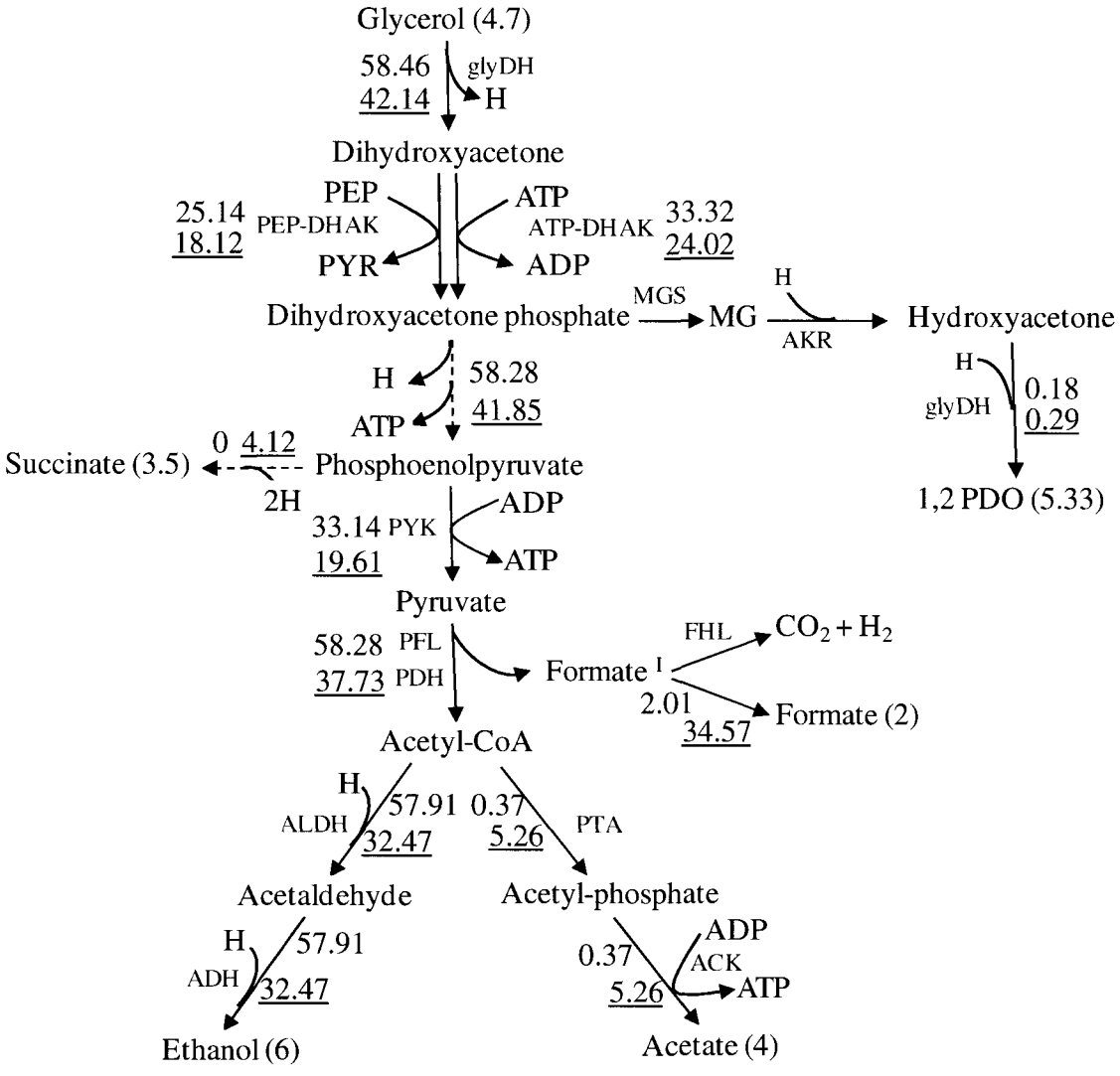

Figure 7.1: Proposed glycerol dissimilation pathway in P. macerans. Enzymes corresponding to pathways are represented with red. The degree of reduction per carbon for glycerol, cell mass and extracellular metabolites is shown in parentheses and was estimated as described elsewhere [158]. Fluxes from conventional flux analysis are shown next to the pathway. At pH 6, it is shown without underline and at pH 8 is with underline below the fluxes. Fluxes are represented as mmol/g cell/hr. Formate^I represents the intracellular formate. Abbreviations: glyDH: Glycerol dehydrogenase; DHAK: dihydroxyacetone kinase; FRD: fumarate reductase; PFL: pyruvate formate lyase; ADH: alcohol dehydrogenase; ACK: acetate kinase, LDH: lactate dehydrogenase, PYK: pyruvate kinase, FHL: formate hydrogen lyase, PTA: phosphate acetyltransferase, ALDH: acetaldehyde dehydrogenase.

decarboxylase (PDC: converts pyruvate to acetaldehyde and CO_2). MFA was used to investigate the contribution of these three enzymes during the fermentative metabolism of glycerol. To this end, the metabolic fluxes were calculated in three different scenarios, with the assumption that the pyruvate is dissimilated via one of three possible routes. As expected, the resulting flux maps only differed on the fluxes associated with the generation and metabolism of formate and the conversion of acetyl-CoA to acetaldehyde (data not shown). Such differences in fluxes did not provide enough evidence to rule out or support the functioning of any of the enzymes. However, since these enzymes are dramatically different respect to the generation of reducing equivalents, we calculated the R/O ratio in each scenario. The R/O was close to 1 only in the scenario corresponding to PFL (1.01: data shown in Figure 7.1) but significantly higher than 1 when either PDC (R/O = 2.00) or PDH (R/O = 1.51) were included in the model as the enzymes responsible for pyruvate dissimilation. These results clearly indicate that the operation of either PDH or PDC would result in a significant redox imbalance. Such redox environment would clearly prevent the fermentative metabolism of glycerol. The PFL route avoid this situation by "releasing" the "excess" reducing equivalents as hydrogen, which is evacuated as fermentation gas. More direct evidence for the operation of PFL is found in the analysis of the composition of fermentation products for experiments conducted at alkaline conditions. Since it is well known that high pH inhibits the enzyme formate hydrogen-lyase [168], which converts formic acid to CO_2 and hydrogen, the operation of the PFL route would imply that the molar amount of formic acid accumulated in the extracellular medium should approach the sum of ethanol and acetic acid. Using the data reported at pH 8 (Figure 5.8), it can be seen that the moles of formic

acid are equivalent to 95% of the sum of ethanol and acetate. Taken together, the MFA and the stoichiometry of product formation indicate that PFL is the primary enzyme involved in pyruvate dissimilation during the fermentation of glycerol by *P. macerans* N234A. Our findings also agree with the report that PFL is the primary enzyme during the fermentative metabolism of different sugars [23, 24, 167]. The conversion of formate to CO_2 and H_2, probably mediated by a formate hydrogen-lyase enzyme, is also supported by the evidence described above and by other studies reported in the literature [23, 24, 167]. The operation of PFL as the main route of pyruvate dissimilation also implies that ethanol should be synthesized via a two-step pathway from acetyl-CoA. Our results also verified this hypothesis as both acetaldehyde and alcohol dehydrogenase activities were detected in cell extracts of *P. macerans* N234A (Table 3). Proposed model shows the ability of the cells to generate ATP while meeting redox constraints in the glycerol fermentation by *P. macerans*. This is achieved by the conversion of glycerol to ethanol, which takes place through a redox-balanced pathway that fulfills energy requirements by generating ATP via substrate-level phosphorylation.

7.5 Metabolic flux analysis of lignocellulosic sugars fermentation by *P. macerans*

Since central carbon metabolism is very important in the regulation of carbon flux towards the cellular requirements of growth, redox balance and energy generation, this flux analysis will focus on role of central carbon metabolism during utilization of lignocellulosic sugars by *P. macerans* N234A. The aim of this analysis is to calculate the reaction rates for key steps in the utilization of lignocellulosic sugars by *P.*

macerans, with the minimum information available. The reaction network model for sugar mixture fermentation by *P. macerans* N234A at 47°C and pH 6, was developed by the methodology described in Chapter 3. Temperature of 47°C and pH 6 were chosen for the metabolic flux analysis as this condition was the best for the sugar mixture consumption as described in Chapter 6. The reaction rate equations for the intracellular metabolites used in the model were based on the biochemical pathways shown in Figure 7.2. The pathways shown in the figure were considered based on the information available on the fermentative metabolism of single sugars: glucose and xylose from the previous studies in *P. macerans* [23, 24, 167] and from the previous studies on sugar fermentation by *B. subtilis* [174]. The reaction sequences were lumped together whenever possible. Since there was a good carbon balance between the substrate and products (without considering the carbon going into biomass) and these experiments were done in rich media, carbon used in the synthesis of biomass was not included in the development of reaction network. Another reason for omitting the biomass synthesis equation from the model was that the information about the building blocks for the biomass production is not well established for this microorganism. Maintenance equation for the ATP consumption and cofactor balance equations were also omitted from the model because biomass synthesis information was not available. Also, since it was a sugar mixture and metabolism of pentose sugars provides the intermediates for pentose phosphate pathway, the role of oxidative pentose phosphate pathway was neglected in the reaction model.

Based on the extracellular measurements and previous studies on sugar consumption by *P. macerans*, two routes can be included in the model for the conversion of pyruvate to Acetyl-CoA [168]. In one route, pyruvate is converted to Acetyl-CoA and

formate; and in the other route pyruvate is converted to Acetyl-CoA together with production of one reducing equivalent and CO_2. But, inclusion of both routes in the model creates a mathematical singularity as cofactor balances were not included in the model. Since, we see formate in the fermentation broth, a reaction equation for conversion of pyruvate to acetyl-CoA and formate was included in the model.

In the first step of glucose transport, glucose can be phosphorylated to glucose-6-phosphate in both ATP [199] and PEP dependent manner. As described earlier, in the PEP dependent phosphorylation this process [13, 14], PTS transport system dependent repression of five carbon sugars consumption occurs in the presence of glucose. But, through the fermentation profiles of the sugar mixture fermentation by *P. macerans* N234A (Figures 6.3 and 6.5), it can be seen that simultaneous consumption of the three sugars in this microorganism occurs in a derepressed manner. In building the reaction network, both PEP and ATP dependent phosphorylation of glucose were considered, but since both resulted in similar outcomes for redox balance in energy generation, only PEP dependent model has been shown here.

The complete pathway model based on the above assumptions and information from previous studies on sugar fermentation by *P. macerans* is shown in Figure 7.2. In the model, glucose is first converted to glucose-6-phosphate in a PEP dependent manner and then glucose-6-phosphate is converted to glyceraldehyde-3-phosphate in a series of steps. Utilization of pentose sugars through pentose phosphate pathway leads to the formation of intermediate metabolites fructose-6-phosphate and glyceraldehyde-3-phosphate, which is further converted to pyruvate via phosphoenolpyruvate. In the conversion of one mole of glucose to two moles of

phosphoenolpyruvate, one ATP and two reducing equivalents are generated [140]. Pyruvate is further metabolized to Acetyl-CoA, along with the production of formate. Acetyl-CoA can then be converted to either acetate or ethanol depending on the cellular requirements. Production of acetate from Acetyl-CoA results in generation of one ATP, while production of ethanol results in consumption of two reducing equivalents [168]. In terms of reducing equivalents and energy for overall pathway; conversion of one mole of glucose to two moles of ethanol results in generation of two moles of ATPs and consumption of two reducing equivalents. In the other pathway, conversion of one mole of glucose to two moles of acetate results in the production of four ATPs and two reducing equivalents. For pentose sugars, production of one mole of acetate results in the generation of one reducing equivalent, while the production of one mole of ethanol results in consumption of one reducing equivalent.

7.6 Reaction network model for sugar mixture fermentation

The final metabolic model consists of 25 reactions/fluxes, with 19 intracellular metabolites. Assumption of pseudo steady state for each of these intracellular metabolites in the exponential phase of cell growth makes the net rate of formation of metabolites equal to zero. Based on this assumption, we get a reaction network with 19 mass balance equations for each of the intracellular metabolite. This

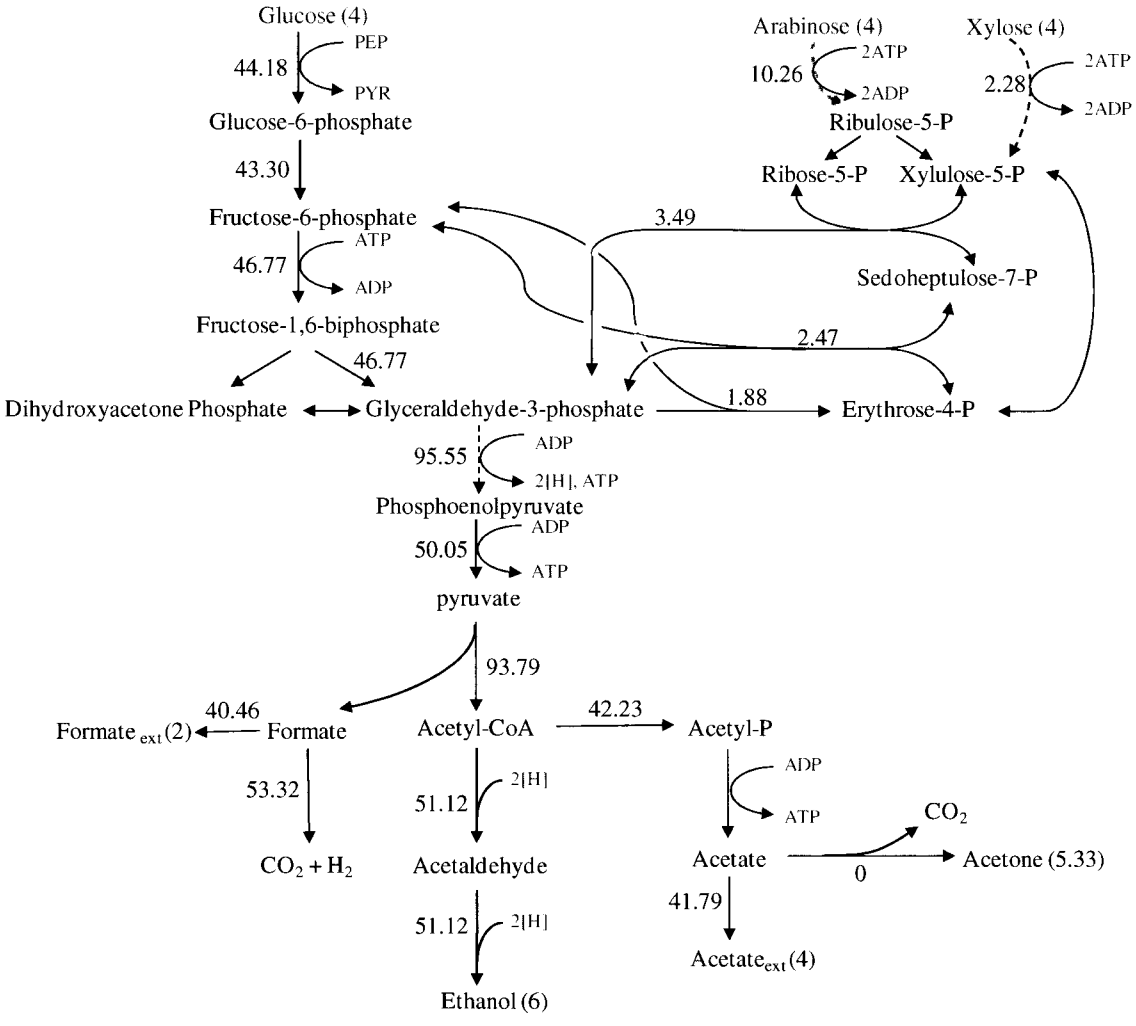

Figure 7.2: Proposed model for dissimilation of sugars by P. macerans. The degree of reduction per carbon for sugars and extracellular metabolites is shown in parentheses and was estimated as described elsewhere [158]. Fluxes from conventional flux analysis are shown next to the pathway. Fluxes are represented as mmol/g cell/hr. Formate$_{ext}$ represents the extracellular formate.

model contains 18 unknown and 7 measured reaction rates. Since we have a total of 25 rates and 19 mass balance equations, we have a system with degree of freedom of 6. As we have 7 measured reaction rates, this is an overdetermined system. The set of reactions and mass balance equations considered in this model are shown in *Appendix B.*

As discussed in the previous paragraph, this reaction network is an overdetermined system, with 18 calculated rates and 7 measured rates. Hence, the system of equations was solved for an overdetermined system based on pseudo inverse method for solving overdetermined system described elsewhere [28]. This method provides the least squares estimate for calculated fluxes, assuming that there are little noises in the measurements. Solving 19 equations for the intracellular metabolites by this method provides the values for 18 calculated rates using all 7 measured rates.

7.7 ATP yield and redox balance ratio in sugar mixture fermentation

From the reaction rates calculated by pseudo inverse method, the other parameters for the reaction model were also calculated. One of the important parameter is the ATP yield (Y_{ATP}), which gives the moles of ATP generated per mole of sugar consumed. To calculate this parameter, first the rate of generation of ATP (υ_{ATP}) was calculated, which is ($\upsilon_{20} + \upsilon_{10} + \upsilon_{12} - \upsilon_7$) (See the *Appendix B* for nomenclature for the numbering of reaction rates and corresponding reactions) in this case. Putting in the numerical values for the fluxes gives the υ_{ATP} as 141.07 mmol/ g of cell/ hr. Expression for the ATP yield in this case is (υ_{ATP} / ($\upsilon_1 + \upsilon_2 + \upsilon_3$)) and the value is 2.49 mmol of ATP / mmol of sugar. The values of rates of generation of ATP in this case are higher than the values reported for the case of glucose and rich medium for *E. coli.* [198], while ATP yield value is similar to the value reported before [198].

The calculation of redox balance ratio (R/O), which is the rate of production of reducing equivalents divided by rate of consumption of reducing equivalents, was also done for sugar mixture fermentation by *P. macerans* N234A. In a redox balanced system,

this value is 1. The expression for calculation of redox balance ratio in this case is $(\upsilon_9) / (\upsilon_{19}*2)$ (See the *Appendix B* for the nomenclature for reaction rates and reaction numbering). Putting the numerical values in the expression gives the R/O value for the reaction model as 0.93.

7.8 Model for fermentative utilization of lignocellulosic sugars by *P. macerans*

Since R/O value is less than 1 in this case, redox equivalents being consumed in this reaction model are more than the redox equivalents being generated. This implies that there might be a reaction, which is producing the redox equivalents and is not being considered in the reaction model. One such reaction is the conversion of pyruvate to Acetyl-CoA together with the production of one mole of CO_2 and one reducing equivalent. This reaction was not included in the model because including this reaction in the reaction network will generate mathematical singularity in the model. Indeed, it has been proposed in the previous studies that this pathway is active in the sugar fermentation by *P. macerans* [23] and the R/O value of less than 1 in this study suggests that this is the case. This also means that in the sugar fermentation by *P. macerans* N234A, both pathways for pyruvate dissimilation, one with the production of formate and the other with the production of CO_2 and reducing equivalent are active. Also, as this fermentation was done at 47°C and ethanol being a volatile product, the concentration of ethanol being produced in the fermentation might be higher than the measured ethanol concentration. Consideration of this fact will result in more reducing equivalents being consumed in the production of ethanol and it will make the R/O value lower than 0.93. This will give

more weight to the possibility of pyruvate dehydrogenase dependent conversion of pyruvate to Acetyl-CoA and reducing equivalents along with the pyruvate formate lyase dependent conversion.

As discussed earlier in the metabolic flux analysis for the glycerol case, dissimilation of pyruvate can occur through three routes in the microorganisms [168]: the first one results in the production of formate along with Acetyl-CoA, which is catalyzed by pyruvate formate lyase (PFL). The second one results in the production of CO_2 and one reducing equivalent along with the production of Acetyl-CoA, catalyzed by pyruvate dehydrogenase (PDH). The third one results in the production of acetaldehyde and CO_2, catalyzed by pyruvate decarboxylase (PDC). Although these three routes are similar in terms of energy generation in the form of ATP, they are very different in terms of reducing equivalents balance. For the case of PFL, production of one mole of acetate and one mole of ethanol from one mole of glucose results in R/O of 1, which means the system is completely redox balance, while in case of PDH and PDC the R/O ratio is 2, which means that in these two pathways, two reducing equivalents are being generated per reducing equivalents being consumed. These results show that the conversion of glucose through these routes will result in redox imbalances and these pathways could not be the main pyruvate dissimilation pathway, which is also validated by the formation of formate in the culture media, which means that pyruvate conversion through PFL is the main pathway for the pyruvate dissimilation.

In summary, metabolic flux analysis was used here for calculation of intracellular fluxes for the fermentative utilization of glycerol and lignocellulosic sugars. Values of redox balance ratio calculated from the fluxes suggested the pathways for

dissimilation of pyruvate in the two cases. In the case of glycerol, pyruvate is converted to Acetyl-CoA through pyruvate formate lyase, while in the case of lignocellulosic sugars it is through pyruvate dehydrogenase and pyruvate formate lyase.

Chapter 8

Conclusions and future directions

The aim of this study was to analyze and understand the fermentative utilization of different carbon sources by *Paenibacillus macerans*. Two types of substrates were chosen for this study. The first substrate was the reduced carbon source glycerol. Since this is an abundant and inexpensive carbon source, its use in the production of biofuels through microbial fermentation is a practical and prudent approach. On a theoretical basis, because of the reduced nature of the glycerol, higher yields of the reduced products such as ethanol are possible as compared to other carbon sources such as sugars [3]. The second kind of substrate used in this study are the lignocellulosic sugars (glucose, xylose and arabinose), which are redox neutral substrates. Since hexose and pentose sugars make the largest portion of lignocellulosic biomass, it is very important to find the microorganisms and operating conditions, which can utilize all the sugars simultaneously. Industrial ethanol producer *Saccharomyces cerevisiae* can not ferment pentose sugars [200] and it has been a major drawback of the current industrial ethanol production. Both types of substrates were analyzed in this study for fermentative utilization by *P. macerans*.

A number of tools including enzyme assays, NMR and metabolic flux analysis (MFA) were used for the analysis of metabolic reaction network in this study. MFA is very important and powerful tool in the analysis of cellular physiology [22]. The system level analysis used in this method provides a holistic picture of the metabolism of the microorganism being studied. This analysis provides information about the role and

importance of different metabolic pathways and reactions under a specific growth condition. One of the main advantages of MFA analysis is that it doesn't require information about the reaction kinetics as it uses the steady state balances for the intracellular metabolites. Its other advantage is that it is an *in vivo* analysis as it uses the measured extracellular fluxes to calculate the unknown intracellular fluxes. One main disadvantage of this analysis is that it requires information about all the reactions in a microorganism for building the reaction network model including their stoichiometry. Other types of flux analysis such flux balance analysis are *in silico* analysis as they are built for optimizing a particular parameter under specified constraints and without using any experimental measurements [137]. The most important use of MFA is in the development of metabolic engineering strategies through strain modifications. This analysis provides knowledge about the bottlenecks in a metabolic pathway or the flux going to the undesired byproducts, which is very important information when prioritizing the metabolic engineering strategies for further improvements in the production of desired metabolite.

The next few sections summarize the results of this study.

8.1 Fermentative utilization of glycerol by *P. macerans*

This study shows that *P. macerans* can ferment glycerol anaerobically in the absence of external electron acceptors. It can ferment it with a specific growth rate of 0.4 h^{-1} which is 10 times higher than the growth rate of *E. coli* under similar conditions [165]. HPLC and NMR analysis of the fermentation samples showed ethanol as the primary product of glycerol fermentation, along with production of formate, acetate and 1,2-PDO.

Fermentations on U-^{13}C glycerol with minimum supplementation showed that carbon source of the ethanol being produced is the result of fermentative utilization of U-^{13}C glycerol and not the supplement used. Efforts to simulate the glycerol utilization by perturbing the culture conditions showed that changing the culture pH to 6, lowering the concentrations of potassium and phosphate in the medium composition and sparging the culture medium with CO_2 in place of argon enhanced the glycerol consumption by *P. macerans [201]*. For identification of key enzymes and pathways mediating glycerol fermentation in *P. macerans*, enzyme activities for the main enzymes of glycerol utilization pathway were measured. Based on the pathway information from these assays and reaction stoichiometry, a reaction network model was developed for the metabolic flux analysis. Results of this analysis showed that the fermentation of glycerol by *P. macerans* occurs in a 1,2-PDO dependent manner. Since conversion of glycerol to ethanol is a redox balanced process, consumption of reducing equivalents in the production of 1,2-PDO balances the redox equivalents being generated in the production of biomass. Cells energy requirements are satisfied with the production of one mole of ATP in the conversion of one mole of glycerol to one mole of ATP.

8.2 Fermentative utilization of sugar mixtures by *P. macerans*

Hexose and pentose sugars are major part of the lignocellulosic biomass [202]. This study shows that *P. macerans* can ferment individual sugars: glucose, xylose and arabinose very efficiently. Consumption of glucose was faster than of xylose and arabinose. *P. macerans* is one of the few microorganisms, which can ferment hexose and pentose sugars very well. Owing to the importance of simultaneous consumption of

sugars for the production of ethanol, environmental parameters of the fermentation of sugar mixture were studied as well. This analysis showed that pH 6 and temperature of 47°C are the optimum conditions for the simultaneous consumption of sugars. Hence this condition was chosen for metabolic flux analysis. Knowledge from previous studies [23, 24] on the fermentation of individual sugars was used to build the metabolic reaction network model for this fermentation. MFA analysis established that the pyruvate is dissimilated via pyruvate formate lyase (PFL) and pyruvate dehydrogenase (PDH) in the fermentative utilization of sugars by this microorganism.

8.3 Future directions

This study shows that *P. macerans* can ferment a wide variety of substrates efficiently; this includes reduced substrate glycerol and neutral substrate sugars. But, successful industrial adoption of a process requires a medium, which is well defined and cost effective. Since tryptone was used as a medium supplement in the case of glycerol fermentations, it is important to find the role of tryptone in cell growth and glycerol utilization. Since *P. macerans* doesn't have a publically available genome sequence, it was not possible to apply metabolic engineering strategies in this study. These strategies will be important in elucidating the role of tryptone for glycerol utilization in minimum media. Similar strategies will also be important for the further verification of enzymes and pathways enabling glycerol fermentation. Strains created with the deletions or overexpansion of genes of the pathways mediating glycerol utilization will further verify our claim about the role of these pathways. Also, a system level comparison of genes and enzymes through tools such microarrays and proteomics with other glycerol fermenting

microorganism, which also do so in 1,2-PDO dependent manner [165], will provide valuable insights in improving glycerol utilization in those microorganisms.

In the sugar mixture case, this study showed that *P. macerans* can ferment pentose and hexose sugars simultaneously. Since this analysis was done with rich supplementation, next step will be to test the utilization of these sugars in minimum media. Our initial results in this directions show that *P. macerans* can ferment these sugars without the need of rich supplementation. In this study, all the three sugars were used in 1:1:1 ratio and that is not the case for lignocellulosic biomass, hence it will also be important to analyze the effect of changes in the ratio of hexose and pentose sugars on the sugar mixture fermentation by this microorganism. As in the case of glycerol fermentation, knowledge of the genome sequence of this microorganism will help in creation of strains that will provide further insights into the pathways mediating simultaneous sugar utilization in *P. macerans*.

APPENDIX A

Supplementary information for metabolic flux analysis of glycerol fermentation by *P. macerans*

The intracellular fluxes were calculated using metabolite balancing, a technique that requires setting up a stoichiometric model (mass balances for the intracellular metabolites) and measuring a number of extracellular fluxes [28]. The stoichiometric model was built considering the most important pathways operative during the fermentation of glycerol by *P. macerans* N234A (Fig. 7.1) and assuming pseudo-steady state for intracellular metabolites. The metabolic network consists of fifteen (15) reactions and ten (10) balanceable intermediate metabolites, which are listed below and shown in Fig. 7.1.

Metabolite balance equations and stoichiometric model

Balance equations were written for each of the ten (10) balanceable intracellular metabolites. For example, for the pyruvate node, the balance equation was as follows: rate of accumulation of pyruvate = $\upsilon_2 + \upsilon_5 - \upsilon_6$. Application of the pseudo-steady-state assumption permitted all of the accumulation terms to be assigned a value of zero, yielding ten (10) linear equations with fifteen (15) fluxes. The inclusion of both ATP-dependent and PEP-dependent dihydroxyacetone kinases (DHAK) in the model created a mathematical singularity that was solved by assuming that the in *vitro* activity of each DHAK is a good estimator of the fraction of carbon processed by the enzyme. Since five (5) extracellular metabolites were measured and information for the ratio of the fluxes through PEP- and ATP-dependent DHAKs was available, the resulting system is over-

determined [28]. However, the glycerol consumption flux was not used as input but rather calculated and compared to the measured value to assess the accuracy of the model. The five (5) fluxes that involved glycerol (υ_1) or the measured products (ethanol, $\upsilon_7 = \upsilon_8$; 1,2-PDO, $\upsilon_{13} = \upsilon_{14} = \upsilon_{15}$; acetate, $\upsilon_9 = \upsilon_{10}$; and formate, υ_{12}) were directly calculated from experimental results as described in Chapter 4. Measured fluxes and the ratio of PEP-DHAK/ATP-DHAK (υ_2/υ_3) were combined with the stoichiometric model to calculate the remaining fluxes as described elsewhere [28].

Reactions included in the model

Reaction/Flux No	***Reaction***
Glycerol dissimilation	
υ_1	**Glycerol** + NAD → DHA + NADH
υ_2	DHA + PEP → DHAP + PYR
υ_3	DHA + ATP → DHAP + ADP
Embden-Meyerhof-Parnas (EMP) pathway	
υ_4	DHAP + ADP + NAD → PEP + ATP + NADH
υ_5	PEP + ADP → PYR + ATP
Pyruvate dissimilation	
υ_6	PYR + CoA → AcCoA + FOR
Ethanol synthesis	
υ_7	AcCoA + NADH → ACAL + NAD + CoA
υ_8	ACAL + NADH → **Ethanol** + NAD
Acetate synthesis	
υ_9	AcCoA + PI → AcP + CoA
υ_{10}	AcP + ADP → ATP + **Acetate**
Formate dissimilation and transport	
υ_{11}	FOR → **CO_2** + **H_2**
υ_{12}	FOR → **Formate**
1,2 PDO synthesis	
υ_{13}	DHAP → MG + Pi
υ_{14}	MG + NADH → HA + NAD
υ_{15}	HA + NADH → **1,2-PDO** + NAD

Balanceable intracellular metabolites (10)

Acetaldehyde (ACAL); Acetyl coenzyme A (AcCoA); Acetyl phosphate (AcP);

Dihydroxyacetone (DHA); Dihydroxyacetone phosphate (DHAP); Formate (FOR); Hydroxyacetone (HA); Methylglyoxal (MG); Phosphoenolpyruvate (PEP); Pyruvate (PYR).

Extracellular metabolites (7)

Glycerol, Ethanol, 1,2-propanediol (1,2-PDO), Acetate, Formate, Carbon dioxide (CO_2), and Hydrogen (H_2).

Measured fluxes/flux ratios (6)

Glycerol utilization (υ_1); accumulation of formate (υ_{12}), ethanol ($\upsilon_7 = \upsilon_8$), 1,2-PDO ($\upsilon_{13} = \upsilon_{14} = \upsilon_{15}$), acetate ($\upsilon_9 = \upsilon_{10}$); and ratio of PEP-DHAK/ATP-DHAK (υ_2/υ_3).

APPENDIX B

Supplementary information for metabolic flux analysis of lignocellulosic sugar fermentation by *P. macerans*

The intracellular fluxes were calculated using metabolite balancing, a technique that requires setting up a stoichiometric model (mass balances for the intracellular metabolites) and measuring a number of extracellular fluxes [28]. The stoichiometric model was built considering the most important pathways operative during the sugar fermentation by *P. macerans* N234A (Fig. 7.2) and assuming pseudo-steady state for intracellular metabolites. The metabolic network consists of twenty five (25) reactions and nineteen (19) balanceable intermediate metabolites, which are listed below and shown in Fig. 7.2.

Metabolite balance equations and stoichiometric model

Balance equations were written for each of the nineteen (19) balanceable intracellular metabolites. For example, balance equation for the fructose-6-phosphate (F6P) was as follows: rate of accumulation of F6P = $\upsilon_6 - \upsilon_7 + \upsilon_{16} + \upsilon_{17}$. Application of the pseudo-steady-state assumption for intracellular metabolites permitted accumulation terms to be assigned a value of zero for all the balances, yielding nineteen (19) linear equations with twenty five (25) fluxes. Since seven (7) extracellular metabolites were measured, the resulting system was over-determined [28]. The resulting system was solved by pseudo inverse method for solving over-determined systems, which is based on method of least squares. The seven (7) measured fluxes were directly calculated from experimental results as described in Chapter 4. Measured fluxes together with the stoichiometric model

were used to calculate the remaining fluxes as described elsewhere [28].

Reactions included in the model

Reaction/Flux No	***Reaction***
Sugar Uptake and utilization	
υ_1	**Glucose** + PEP → G6P + PYR
υ_2	**Xylose** → XYLU
υ_3	**Arabinose** → RIBL
υ_4	XYLU + ATP → XYL5P + ADP
υ_5	RIBL + ATP → RL5P + ADP
Embden-Meyerhof-Parnas (EMP) pathway	
υ_6	G6P → F6P
υ_7	F6P + ATP → DHAP + GLY3P + ADP
υ_8	DHAP → GLY3P
υ_9	GLY3P + NAD → 13P2DG + NADH
υ_{10}	13P2DG + ADP → ATP + 3PG
υ_{11}	3PG → PEP
υ_{12}	PEP + ADP → ATP + PYR
Pentose phosphate pathway	
υ_{13}	RL5P → R5P
υ_{14}	R5P → XYL5P
υ_{15}	R5P + XYL5P → GLY3P + S7P
υ_{16}	GLY3P + S7P → E4P + F6P
υ_{17}	XYL5P + E4P → F6P + GLY3P
Pyruvate dissimilation	
υ_{18}	PYR + COA → FORMATE + ACCOA
Ethanol synthesis	
υ_{19}	ACCOA + 2NADH → 2NAD + **ETHANOL** + COA
Acetate synthesis	
υ_{20}	ACCOA + ADP → ACETATE + ATP + COA
υ_{24}	ACETATE → **ACETATE**$_{ext}$
Formate dissimilation and transport	
υ_{21}	FORMATE → CO_2 + **H_2**
υ_{23}	FORMATE → **FORMATE**$_{ext}$
Acetone synthesis	
υ_{22}	2 ACETATE → **ACETONE** + CO_2 + H_2O
CO_2 formation	
υ_{25}	CO_2 → **CO_{2ext}**

Balanceable intracellular metabolites (19)

1,3-Diphosphateglycerate (13P2DG); 3-Phospho-D-Glycerate (3PG); Acetyl Coenzyme A (ACCOA); Carbon dioxide (CO_2); Dihydroxy acetone phosphate (DHAP); Erythrose

4-phosphate (E4P); Fructose 6-phosphate (F6P); Glucose 6-phosphate (G6P); Glyceraldehyde 3-phosphate (GLY3P); Phosphoenolpyruvate (PEP); Pyruvate (PYR); Ribulose (RIBL); Ribulose 5-phosphate (RL5P); Ribose 5-phosphate (R5P); Sedoheptulose-7-phosphate (S7P); Xylulose 5-phosphate (XYL5P); Xylulose (XYLU); Formate; Acetate.

Extracellular metabolites (9)

Glucose, Xylose, Arabinose, Ethanol, Acetone, Acetate, Formate, Carbon dioxide (CO_2) and Hydrogen (H_2).

Measured fluxes (7)

Glucose utilization (υ_1); xylose utilization (υ_2); arabinose utilization (υ_3); accumulation of formate (υ_{23}), ethanol (υ_{19}), acetone (υ_{22}), accumulation of acetate (υ_{24}).

Bibliography

1. Asif, M. and T. Muneer, *Energy supply, its demand and security issues for developed and emerging economies.* Renewable & Sustainable Energy Reviews, 2007. **11**(7): p. 1388-1413.
2. Gavrilescu, M. and Y. Chisti, *Biotechnology-a sustainable alternative for chemical industry.* Biotechnol Adv, 2005. **23**(7-8): p. 471-99.
3. Yazdani, S.S. and R. Gonzalez, *Anaerobic fermentation of glycerol: a path to economic viability for the biofuels industry.* Curr Opin Biotechnol, 2007. **18**(3): p. 213-9.
4. Bouvet, O.M., et al., *Taxonomic diversity of anaerobic glycerol dissimilation in the Enterobacteriaceae.* Res Microbiol, 1995. **146**(4): p. 279-90.
5. Gonzalez, R., et al., *A new model for the anaerobic fermentation of glycerol in enteric bacteria: trunk and auxiliary pathways in Escherichia coli.* Metab Eng, 2008. **10**(5): p. 234-45.
6. Chang, M.C., *Harnessing energy from plant biomass.* Curr Opin Chem Biol, 2007. **11**(6): p. 677-84.
7. Aristidou, A. and M. Penttilä, *Metabolic engineering applications to renewable resource utilization.* Current Opinion in Biotechnology, 2000. **11**(2): p. 187-198.
8. Lee, J., *Biological conversion of lignocellulosic biomass to ethanol.* Journal of biotechnology, 1997. **56**(1): p. 1-24.
9. Gray, K.A., L. Zhao, and M. Emptage, *Bioethanol.* Curr Opin Chem Biol, 2006. **10**(2): p. 141-6.

10. Fischer, C.R., D. Klein-Marcuschamer, and G. Stephanopoulos, *Selection and optimization of microbial hosts for biofuels production.* Metab Eng, 2008. **10**(6): p. 295-304.

11. Alper, H. and G. Stephanopoulos, *Engineering for biofuels: exploiting innate microbial capacity or importing biosynthetic potential?* Nat Rev Microbiol, 2009. **7**(10): p. 715-23.

12. Bruckner, R. and F. Titgemeyer, *Carbon catabolite repression in bacteria: choice of the carbon source and autoregulatory limitation of sugar utilization.* FEMS Microbiol Lett, 2002. **209**(2): p. 141-8.

13. Deutscher, J., *The mechanisms of carbon catabolite repression in bacteria.* Curr Opin Microbiol, 2008. **11**(2): p. 87-93.

14. Gorke, B. and J. Stulke, *Carbon catabolite repression in bacteria: many ways to make the most out of nutrients.* Nat Rev Microbiol, 2008. **6**(8): p. 613-24.

15. French, C.E., *Synthetic biology and biomass conversion: a match made in heaven?* J R Soc Interface, 2009. **6 Suppl 4**: p. S547-58.

16. Vallino, J. and G. Stephanopoulos, *Metabolic Flux Distributions in Corynebacterium glut icum During Growth and Lysine Overproduction.* Biotechnology and Bioengineering, 1993. **41**: p. 633-646.

17. Verhoff, F. and J. Spradlin, *Mass and energy balance analysis of metabolic pathways applied to citric acid production by Aspergillus niger.* Biotechnology and Bioengineering, 1976. **18**(3): p. 452.

18. Papoutsakis, E., *Equations and calculations for fermentations of butyric acid bacteria.* Biotechnology and Bioengineering, 1984. **26**(2): p. 174-187.

19. Niranjan, S. and K. San, *Analysis of a framework using material balances in metabolic pathways to elucidate cellular metabolism.* Biotechnology and Bioengineering, 1989. **34**(4): p. 496-501.

20. Nielsen, J., *It is all about metabolic fluxes.* J Bacteriol, 2003. **185**(24): p. 7031-5.

21. Farmer, W. and J. Liao, *Progress in metabolic engineering.* Current Opinion in Biotechnology, 1996. **7**(2): p. 198-204.

22. Stephanopoulos, G., *Metabolic fluxes and metabolic engineering.* Metabolic engineering, 1999. **1**(1): p. 1-11.

23. Weimer, P., *Control of product formation during glucose fermentation by Bacillus macerans.* Microbiology, 1984. **130**(1): p. 103.

24. Schepers, H., S. Bringermeyer, and H. Sahm, *Fermentation of D-xylose to ethanol by Bacillus macerans.* Z. Naturforsch. 42c, 1987: p. 401-407.

25. Heyndrickx, M., et al., *A polyphasic reassessment of the genus Paenibacillus, reclassification of Bacillus lautus (Nakamura 1984) as Paenibacillus lautus comb. nov. and of Bacillus peoriae (Montefusco et al. 1993) as Paenibacillus peoriae comb. nov., and emended descriptions of P. lautus and of P. peoriae.* Int J Syst Bacteriol, 1996. **46**(4): p. 988-1003.

26. Fujita, Y., *Carbon catabolite control of the metabolic network in Bacillus subtilis.* Biosci Biotechnol Biochem, 2009. **73**(2): p. 245-59.

27. Deutscher, J., C. Francke, and P.W. Postma, *How phosphotransferase system-related protein phosphorylation regulates carbohydrate metabolism in bacteria.* Microbiol Mol Biol Rev, 2006. **70**(4): p. 939-1031.

28. Stephanopoulos, G., A.A. Aristidou, and J. Nielsen, *Metabolic engineering : principles and methodologies*. 1998, San Diego: Academic Press. xxi, 725 p.

29. Frunzke, J., et al., *Co-ordinated regulation of gluconate catabolism and glucose uptake in Corynebacterium glutamicum by two functionally equivalent transcriptional regulators, GntR1 and GntR2.* Mol Microbiol, 2008. **67**(2): p. 305-22.

30. Wendisch, V.F., et al., *Quantitative determination of metabolic fluxes during coutilization of two carbon sources: comparative analyses with Corynebacterium glutamicum during growth on acetate and/or glucose.* J Bacteriol, 2000. **182**(11): p. 3088-96.

31. Nicholson, T.L., K. Chiu, and R.S. Stephens, *Chlamydia trachomatis lacks an adaptive response to changes in carbon source availability.* Infect Immun, 2004. **72**(7): p. 4286-9.

32. Halbedel, S., et al., *Transcription in Mycoplasma pneumoniae: analysis of the promoters of the ackA and ldh genes.* J Mol Biol, 2007. **371**(3): p. 596-607.

33. van den Bogaard, P.T., et al., *Control of lactose transport, beta-galactosidase activity, and glycolysis by CcpA in Streptococcus thermophilus: evidence for carbon catabolite repression by a non-phosphoenolpyruvate-dependent phosphotransferase system sugar.* J Bacteriol, 2000. **182**(21): p. 5982-9.

34. Parche, S., et al., *Lactose-over-glucose preference in Bifidobacterium longum NCC2705: glcP, encoding a glucose transporter, is subject to lactose repression.* J Bacteriol, 2006. **188**(4): p. 1260-5.

35. Collier, D.N., P.W. Hager, and P.V. Phibbs, Jr., *Catabolite repression control in the Pseudomonads.* Res Microbiol, 1996. **147**(6-7): p. 551-61.

36. Kravanja, M., et al., *The hprK gene of Enterococcus faecalis encodes a novel bifunctional enzyme: the HPr kinase/phosphatase.* Mol Microbiol, 1999. **31**(1): p. 59-66.

37. Jault, J.M., et al., *The HPr kinase from Bacillus subtilis is a homo-oligomeric enzyme which exhibits strong positive cooperativity for nucleotide and fructose 1,6-bisphosphate binding.* J Biol Chem, 2000. **275**(3): p. 1773-80.

38. Mijakovic, I., et al., *Pyrophosphate-producing protein dephosphorylation by HPr kinase/phosphorylase: a relic of early life?* Proc Natl Acad Sci U S A, 2002. **99**(21): p. 13442-7.

39. Steinhauer, K., et al., *A novel mode of control of Mycoplasma pneumoniae HPr kinase/phosphatase activity reflects its parasitic lifestyle.* Microbiology, 2002. **148**(Pt 10): p. 3277-84.

40. Brochu, D. and C. Vadeboncoeur, *The HPr(Ser) kinase of Streptococcus salivarius: purification, properties, and cloning of the hprK gene.* J Bacteriol, 1999. **181**(3): p. 709-17.

41. Reizer, J., et al., *Functional interactions between proteins of the phosphoenolpyruvate:sugar phosphotransferase systems of Bacillus subtilis and Escherichia coli.* J Biol Chem, 1992. **267**(13): p. 9158-69.

42. Deutscher, J., et al., *Loss of protein kinase-catalyzed phosphorylation of HPr, a phosphocarrier protein of the phosphotransferase system, by mutation of the ptsH*

gene confers catabolite repression resistance to several catabolic genes of Bacillus subtilis. J Bacteriol, 1994. **176**(11): p. 3336-44.

43. Monedero, V., et al., *Mutations lowering the phosphatase activity of HPr kinase/phosphatase switch off carbon metabolism.* EMBO J, 2001. **20**(15): p. 3928-37.

44. Ye, J.J. and M.H. Saier, Jr., *Regulation of sugar uptake via the phosphoenolpyruvate-dependent phosphotransferase systems in Bacillus subtilis and Lactococcus lactis is mediated by ATP-dependent phosphorylation of seryl residue 46 in HPr.* J Bacteriol, 1996. **178**(12): p. 3557-63.

45. Darbon, E., et al., *Antitermination by GlpP, catabolite repression via CcpA and inducer exclusion triggered by P-GlpK dephosphorylation control Bacillus subtilis glpFK expression.* Mol Microbiol, 2002. **43**(4): p. 1039-52.

46. Galinier, A., J. Deutscher, and I. Martin-Verstraete, *Phosphorylation of either crh or HPr mediates binding of CcpA to the bacillus subtilis xyn cre and catabolite repression of the xyn operon.* J Mol Biol, 1999. **286**(2): p. 307-14.

47. Galinier, A., et al., *The Bacillus subtilis crh gene encodes a HPr-like protein involved in carbon catabolite repression.* Proc Natl Acad Sci U S A, 1997. **94**(16): p. 8439-44.

48. Martin-Verstraete, I., et al., *Two different mechanisms mediate catabolite repression of the Bacillus subtilis levanase operon.* J Bacteriol, 1995. **177**(23): p. 6919-27.

49. Faires, N., et al., *The catabolite control protein CcpA controls ammonium assimilation in Bacillus subtilis.* J Mol Microbiol Biotechnol, 1999. **1**(1): p. 141-8.

50. Khan, S.R. and N. Banerjee-Bhatnagar, *Loss of catabolite repression function of HPr, the phosphocarrier protein of the bacterial phosphotransferase system, affects expression of the cry4A toxin gene in Bacillus thuringiensis subsp. israelensis.* J Bacteriol, 2002. **184**(19): p. 5410-7.

51. Monedero, V., et al., *Regulatory functions of serine-46-phosphorylated HPr in Lactococcus lactis.* J Bacteriol, 2001. **183**(11): p. 3391-8.

52. Viana, R., et al., *Enzyme I and HPr from Lactobacillus casei: their role in sugar transport, carbon catabolite repression and inducer exclusion.* Mol Microbiol, 2000. **36**(3): p. 570-84.

53. Lopez, J.M. and B. Thoms, *Role of sugar uptake and metabolic intermediates on catabolite repression in Bacillus subtilis.* J Bacteriol, 1977. **129**(1): p. 217-24.

54. Nihashi, J. and Y. Fujita, *Catabolite repression of inositol dehydrogenase and gluconate kinase syntheses in Bacillus subtilis.* Biochim Biophys Acta, 1984. **798**(1): p. 88-95.

55. Renna, M.C., et al., *Regulation of the Bacillus subtilis alsS, alsD, and alsR genes involved in post-exponential-phase production of acetoin.* J Bacteriol, 1993. **175**(12): p. 3863-75.

56. Turinsky, A.J., et al., *Transcriptional activation of the Bacillus subtilis ackA gene requires sequences upstream of the promoter.* J Bacteriol, 1998. **180**(22): p. 5961-7.

57. Presecan-Siedel, E., et al., *Catabolite regulation of the pta gene as part of carbon flow pathways in Bacillus subtilis.* J Bacteriol, 1999. **181**(22): p. 6889-97.

58. Inacio, J.M., C. Costa, and I. de Sa-Nogueira, *Distinct molecular mechanisms involved in carbon catabolite repression of the arabinose regulon in Bacillus subtilis.* Microbiology, 2003. **149**(Pt 9): p. 2345-55.

59. Weickert, M.J. and G.H. Chambliss, *Site-directed mutagenesis of a catabolite repression operator sequence in Bacillus subtilis.* Proc Natl Acad Sci U S A, 1990. **87**(16): p. 6238-42.

60. Miwa, Y. and Y. Fujita, *Involvement of two distinct catabolite-responsive elements in catabolite repression of the Bacillus subtilis myo-inositol (iol) operon.* J Bacteriol, 2001. **183**(20): p. 5877-84.

61. Hueck, C.J., W. Hillen, and M.H. Saier, Jr., *Analysis of a cis-active sequence mediating catabolite repression in gram-positive bacteria.* Res Microbiol, 1994. **145**(7): p. 503-18.

62. Blencke, H.M., et al., *Transcriptional profiling of gene expression in response to glucose in Bacillus subtilis: regulation of the central metabolic pathways.* Metab Eng, 2003. **5**(2): p. 133-49.

63. Moreno, M.S., et al., *Catabolite repression mediated by the CcpA protein in Bacillus subtilis: novel modes of regulation revealed by whole-genome analyses.* Mol Microbiol, 2001. **39**(5): p. 1366-81.

64. Yoshida, K., et al., *Combined transcriptome and proteome analysis as a powerful approach to study genes under glucose repression in Bacillus subtilis.* Nucleic Acids Res, 2001. **29**(3): p. 683-92.

65. Weickert, M.J. and S. Adhya, *A family of bacterial regulators homologous to Gal and Lac repressors.* J Biol Chem, 1992. **267**(22): p. 15869-74.

66. Grundy, F.J., A.J. Turinsky, and T.M. Henkin, *Catabolite regulation of Bacillus subtilis acetate and acetoin utilization genes by CcpA.* J Bacteriol, 1994. **176**(15): p. 4527-33.

67. Henkin, T.M., et al., *Catabolite repression of alpha-amylase gene expression in Bacillus subtilis involves a trans-acting gene product homologous to the Escherichia coli lacI and galR repressors.* Mol Microbiol, 1991. **5**(3): p. 575-84.

68. Miwa, Y., M. Saikawa, and Y. Fujita, *Possible function and some properties of the CcpA protein of Bacillus subtilis.* Microbiology, 1994. **140 (Pt 10)**: p. 2567-75.

69. Turinsky, A.J., et al., *Bacillus subtilis ccpA gene mutants specifically defective in activation of acetoin biosynthesis.* J Bacteriol, 2000. **182**(19): p. 5611-4.

70. Tobisch, S., et al., *Role of CcpA in regulation of the central pathways of carbon catabolism in Bacillus subtilis.* J Bacteriol, 1999. **181**(22): p. 6996-7004.

71. Kim, H.J., A. Roux, and A.L. Sonenshein, *Direct and indirect roles of CcpA in regulation of Bacillus subtilis Krebs cycle genes.* Mol Microbiol, 2002. **45**(1): p. 179-90.

72. Miwa, Y., et al., *Evaluation and characterization of catabolite-responsive elements (cre) of Bacillus subtilis.* Nucleic Acids Res, 2000. **28**(5): p. 1206-10.

73. Ludwig, H., et al., *Control of the glycolytic gapA operon by the catabolite control protein A in Bacillus subtilis: a novel mechanism of CcpA-mediated regulation.* Mol Microbiol, 2002. **45**(2): p. 543-53.

74. Wacker, I., et al., *The regulatory link between carbon and nitrogen metabolism in Bacillus subtilis: regulation of the gltAB operon by the catabolite control protein CcpA.* Microbiology, 2003. **149**(Pt 10): p. 3001-9.

75. Fillinger, S., et al., *Two glyceraldehyde-3-phosphate dehydrogenases with opposite physiological roles in a nonphotosynthetic bacterium.* J Biol Chem, 2000. **275**(19): p. 14031-7.

76. Shivers, R.P. and A.L. Sonenshein, *Bacillus subtilis ilvB operon: an intersection of global regulons.* Mol Microbiol, 2005. **56**(6): p. 1549-59.

77. Tojo, S., et al., *Elaborate transcription regulation of the Bacillus subtilis ilv-leu operon involved in the biosynthesis of branched-chain amino acids through global regulators of CcpA, CodY and TnrA.* Mol Microbiol, 2005. **56**(6): p. 1560-73.

78. Belitsky, B.R., H.J. Kim, and A.L. Sonenshein, *CcpA-dependent regulation of Bacillus subtilis glutamate dehydrogenase gene expression.* J Bacteriol, 2004. **186**(11): p. 3392-8.

79. Choi, S.K. and M.H. Saier, Jr., *Regulation of sigL expression by the catabolite control protein CcpA involves a roadblock mechanism in Bacillus subtilis: potential connection between carbon and nitrogen metabolism.* J Bacteriol, 2005. **187**(19): p. 6856-61.

80. Lorca, G.L., et al., *Catabolite repression and activation in Bacillus subtilis: dependency on CcpA, HPr, and HprK.* J Bacteriol, 2005. **187**(22): p. 7826-39.

81. Kraus, A., et al., *Identification of a co-repressor binding site in catabolite control protein CcpA.* Mol Microbiol, 1998. **30**(5): p. 955-63.

82. Kuster, E., et al., *Immunological crossreactivity to the catabolite control protein CcpA Bacillus megaterium is found in many gram-positive bacteria.* FEMS Microbiol Lett, 1996. **139**(2-3): p. 109-15.

83. Davison, S.P., et al., *A Clostridium acetobutylicum regulator gene (regA) affecting amylase production in Bacillus subtilis.* Microbiology, 1995. **141 (Pt 4)**: p. 989-96.

84. Morel, F., et al., *Autoregulation of the biosynthesis of the CcpA-like protein, PepR1, in Lactobacillus delbrueckii subsp bulgaricus.* J Mol Microbiol Biotechnol, 2001. **3**(1): p. 63-6.

85. Mahr, K., W. Hillen, and F. Titgemeyer, *Carbon catabolite repression in Lactobacillus pentosus: analysis of the ccpA region.* Appl Environ Microbiol, 2000. **66**(1): p. 277-83.

86. Egeter, O. and R. Bruckner, *Catabolite repression mediated by the catabolite control protein CcpA in Staphylococcus xylosus.* Mol Microbiol, 1996. **21**(4): p. 739-49.

87. Jones, B.E., et al., *Binding of the catabolite repressor protein CcpA to its DNA target is regulated by phosphorylation of its corepressor HPr.* J Biol Chem, 1997. **272**(42): p. 26530-5.

88. Schumacher, M.A., et al., *Structural basis for allosteric control of the transcription regulator CcpA by the phosphoprotein HPr-Ser46-P.* Cell, 2004. **118**(6): p. 731-41.

89. Reizer, J., et al., *Catabolite repression resistance of gnt operon expression in Bacillus subtilis conferred by mutation of His-15, the site of*

phosphoenolpyruvate-dependent phosphorylation of the phosphocarrier protein HPr. J Bacteriol, 1996. **178**(18): p. 5480-6.

90. Kuster-Schock, E., et al., *Mutations in catabolite control protein CcpA showing glucose-independent regulation in Bacillus megaterium.* J Bacteriol, 1999. **181**(24): p. 7634-8.

91. Fujita, Y., et al., *Specific recognition of the Bacillus subtilis gnt cis-acting catabolite-responsive element by a protein complex formed between CcpA and seryl-phosphorylated HPr.* Mol Microbiol, 1995. **17**(5): p. 953-60.

92. Ali, N.O., et al., *Regulation of the acetoin catabolic pathway is controlled by sigma L in Bacillus subtilis.* J Bacteriol, 2001. **183**(8): p. 2497-504.

93. Liu, X. and H.W. Taber, *Catabolite regulation of the Bacillus subtilis ctaBCDEF gene cluster.* J Bacteriol, 1998. **180**(23): p. 6154-63.

94. Voskuil, M.I. and G.H. Chambliss, *Significance of HPr in catabolite repression of alpha-amylase.* J Bacteriol, 1996. **178**(23): p. 7014-5.

95. Zalieckas, J.M., L.V. Wray, Jr., and S.H. Fisher, *trans-acting factors affecting carbon catabolite repression of the hut operon in Bacillus subtilis.* J Bacteriol, 1999. **181**(9): p. 2883-8.

96. Zalieckas, J.M., L.V. Wray, Jr., and S.H. Fisher, *Expression of the Bacillus subtilis acsA gene: position and sequence context affect cre-mediated carbon catabolite repression.* J Bacteriol, 1998. **180**(24): p. 6649-54.

97. Martin-Verstraete, I., et al., *Levanase operon of Bacillus subtilis includes a fructose-specific phosphotransferase system regulating the expression of the operon.* J Mol Biol, 1990. **214**(3): p. 657-71.

98. Favier, A., et al., *Solution structure and dynamics of Crh, the Bacillus subtilis catabolite repression HPr.* J Mol Biol, 2002. **317**(1): p. 131-44.

99. Juy, M., et al., *Dimerization of Crh by reversible 3D domain swapping induces structural adjustments to its monomeric homologue Hpr.* J Mol Biol, 2003. **332**(4): p. 767-76.

100. Martin-Verstraete, I., et al., *The Q15H mutation enables Crh, a Bacillus subtilis HPr-like protein, to carry out some regulatory HPr functions, but does not make it an effective phosphocarrier for sugar transport.* Microbiology, 1999. **145 (Pt 11)**: p. 3195-204.

101. Schumacher, M.A., et al., *Phosphoprotein Crh-Ser46-P displays altered binding to CcpA to effect carbon catabolite regulation.* J Biol Chem, 2006. **281**(10): p. 6793-800.

102. Seidel, G., et al., *Quantitative interdependence of coeffectors, CcpA and cre in carbon catabolite regulation of Bacillus subtilis.* FEBS J, 2005. **272**(10): p. 2566-77.

103. Bachem, S., N. Faires, and J. Stulke, *Characterization of the presumptive phosphorylation sites of the Bacillus subtilis glucose permease by site-directed mutagenesis: implication in glucose transport and catabolite repression.* FEMS Microbiol Lett, 1997. **156**(2): p. 233-8.

104. Paulsen, I.T., et al., *Characterization of glucose-specific catabolite repression-resistant mutants of Bacillus subtilis: identification of a novel hexose:H+ symporter.* J Bacteriol, 1998. **180**(3): p. 498-504.

105. Skarlatos, P. and M.K. Dahl, *The glucose kinase of Bacillus subtilis.* J Bacteriol, 1998. **180**(12): p. 3222-6.

106. Northrop, J.H., L.H. Ashe, and J.K. Senior, *Biochemistry of bacillus acetoethylicum with reference to the formation of acetone.* Journal of Biological Chemistry, 1919. **39**(1): p. 1-21.

107. Sa-Nogueira, I., et al., *The Bacillus subtilis L-arabinose (ara) operon: nucleotide sequence, genetic organization and expression.* Microbiology, 1997. **143 (Pt 3)**: p. 957-69.

108. Stulke, J. and W. Hillen, *Regulation of carbon catabolism in Bacillus species.* Annu Rev Microbiol, 2000. **54**: p. 849-80.

109. Sa-Nogueira, I. and S.S. Ramos, *Cloning, functional analysis, and transcriptional regulation of the Bacillus subtilis araE gene involved in L-arabinose utilization.* J Bacteriol, 1997. **179**(24): p. 7705-11.

110. Mota, L.J., P. Tavares, and I. Sa-Nogueira, *Mode of action of AraR, the key regulator of L-arabinose metabolism in Bacillus subtilis.* Mol Microbiol, 1999. **33**(3): p. 476-89.

111. Mota, L.J., L.M. Sarmento, and I. de Sa-Nogueira, *Control of the arabinose regulon in Bacillus subtilis by AraR in vivo: crucial roles of operators, cooperativity, and DNA looping.* J Bacteriol, 2001. **183**(14): p. 4190-201.

112. Franco, I.S., et al., *Probing key DNA contacts in AraR-mediated transcriptional repression of the Bacillus subtilis arabinose regulon.* Nucleic Acids Res, 2007. **35**(14): p. 4755-66.

113. Singh, K.D., et al., *Carbon catabolite repression in Bacillus subtilis: quantitative analysis of repression exerted by different carbon sources.* J Bacteriol, 2008. **190**(21): p. 7275-84.

114. Lindner, C., J. Stulke, and M. Hecker, *Regulation of xylanolytic enzymes in Bacillus subtilis.* Microbiology, 1994. **140 (Pt 4)**: p. 753-7.

115. Schmiedel, D. and W. Hillen, *Contributions of XylR CcpA and cre to diauxic growth of Bacillus megaterium and to xylose isomerase expression in the presence of glucose and xylose.* Mol Gen Genet, 1996. **250**(3): p. 259-66.

116. Krispin, O. and R. Allmansberger, *The Bacillus subtilis AraE protein displays a broad substrate specificity for several different sugars.* J Bacteriol, 1998. **180**(12): p. 3250-2.

117. Jeffries, T.W., *Utilization of xylose by bacteria, yeasts, and fungi.* Adv Biochem Eng Biotechnol, 1983. **27**: p. 1-32.

118. Beijer, L., et al., *The glpP and glpF genes of the glycerol regulon in Bacillus subtilis.* J Gen Microbiol, 1993. **139**(2): p. 349-59.

119. Holmberg, C., et al., *Glycerol catabolism in Bacillus subtilis: nucleotide sequence of the genes encoding glycerol kinase (glpK) and glycerol-3-phosphate dehydrogenase (glpD).* J Gen Microbiol, 1990. **136**(12): p. 2367-75.

120. Charrier, V., et al., *Cloning and sequencing of two enterococcal glpK genes and regulation of the encoded glycerol kinases by phosphoenolpyruvate-dependent, phosphotransferase system-catalyzed phosphorylation of a single histidyl residue.* J Biol Chem, 1997. **272**(22): p. 14166-74.

121. Glatz, E., M. Persson, and B. Rutberg, *Antiterminator protein GlpP of Bacillus subtilis binds to glpD leader mRNA.* Microbiology, 1998. **144 (Pt 2)**: p. 449-56.

122. Glatz, E., et al., *A dual role for the Bacillus subtilis glpD leader and the GlpP protein in the regulated expression of glpD: antitermination and control of mRNA stability.* Mol Microbiol, 1996. **19**(2): p. 319-28.

123. Wiame, J.M., S. Bourgeois, and R. Lambion, *Oxidative dissimilation of glycerol studied with variants of Bacillus subtilis.* Nature, 1954. **174**(4418): p. 37-8.

124. Lin, E.C., *Glycerol dissimilation and its regulation in bacteria.* Annu Rev Microbiol, 1976. **30**: p. 535-78.

125. Mindich, L., *Pathway for oxidative dissimilation of glycerol in Bacillur subtilis.* J Bacteriol, 1968. **96**(2): p. 565-6.

126. Romero, S., et al., *Metabolic engineering of Bacillus subtilis for ethanol production: lactate dehydrogenase plays a key role in fermentative metabolism.* Appl Environ Microbiol, 2007. **73**(16): p. 5190-8.

127. Nicholson, W.L., *The Bacillus subtilis ydjL (bdhA) gene encodes acetoin reductase/2,3-butanediol dehydrogenase.* Appl Environ Microbiol, 2008. **74**(22): p. 6832-8.

128. Cruz Ramos, H., et al., *Anaerobic transcription activation in Bacillus subtilis: identification of distinct FNR-dependent and -independent regulatory mechanisms.* EMBO J, 1995. **14**(23): p. 5984-94.

129. Shin, B.S., S.K. Choi, and S.H. Park, *Regulation of the Bacillus subtilis phosphotransacetylase gene.* J Biochem, 1999. **126**(2): p. 333-9.

130. Grundy, F.J., et al., *Regulation of the Bacillus subtilis acetate kinase gene by CcpA.* J Bacteriol, 1993. **175**(22): p. 7348-55.

131. Cruz Ramos, H., et al., *Fermentative metabolism of Bacillus subtilis: physiology and regulation of gene expression.* J Bacteriol, 2000. **182**(11): p. 3072-80.

132. Sonenshein, A.L., *Control of key metabolic intersections in Bacillus subtilis.* Nat Rev Microbiol, 2007. **5**(12): p. 917-27.

133. Nakano, M.M., et al., *Nitrogen and oxygen regulation of Bacillus subtilis nasDEF encoding NADH-dependent nitrite reductase by TnrA and ResDE.* J Bacteriol, 1998. **180**(20): p. 5344-50.

134. Nakano, M.M. and P. Zuber, *Anaerobic growth of a "strict aerobe" (Bacillus subtilis).* Annu Rev Microbiol, 1998. **52**: p. 165-90.

135. Aiba, S. and M. Matsuoka, *Identification of metabolic model - citrate production from glucose by Candida-lipolytica.* Biotechnology and Bioengineering, 1979. **21**(8): p. 1373-1386.

136. Stephanopoulos, G. and J.J. Vallino, *Network rigidity and metabolic engineering in metabolite overproduction.* Science, 1991. **252**(5013): p. 1675-81.

137. Varma, A. and B.O. Palsson, *Stoichiometric flux balance models quantitatively predict growth and metabolic by-product secretion in wild-type Escherichia coli W3110.* Appl Environ Microbiol, 1994. **60**(10): p. 3724-31.

138. Segre, D., D. Vitkup, and G.M. Church, *Analysis of optimality in natural and perturbed metabolic networks.* Proc Natl Acad Sci U S A, 2002. **99**(23): p. 15112-7.

139. Edwards, J.S. and B.O. Palsson, *The Escherichia coli MG1655 in silico metabolic genotype: its definition, characteristics, and capabilities.* Proc Natl Acad Sci U S A, 2000. **97**(10): p. 5528-33.

140. Neidhardt, F.C. and R. Curtiss, *Escherichia coli and Salmonella : cellular and molecular biology.* 2nd ed. 1996, Washington, D.C.: ASM Press.

141. Pramanik, J. and J.D. Keasling, *Stoichiometric model of Escherichia coli metabolism: Incorporation of growth-rate dependent biomass composition and mechanistic energy requirements.* Biotechnol Bioeng, 1997. **56**(4): p. 398-421.

142. Pramanik, J. and J.D. Keasling, *Effect of Escherichia coli biomass composition on central metabolic fluxes predicted by a stoichiometric model.* Biotechnol Bioeng, 1998. **60**(2): p. 230-8.

143. Terzer, M., et al., *Genome-scale metabolic networks.* Wiley Interdisciplinary Reviews: Systems Biology and Medicine, 2009.

144. Tsai, S.P. and Y.H. Lee, *Application of metabolic pathway stoichiometry to statistical analysis of bioreactor measurement data.* Biotechnol Bioeng, 1988. **32**(5): p. 713-5.

145. Kang, Y., et al., *Systematic mutagenesis of the Escherichia coli genome.* J Bacteriol, 2004. **186**(15): p. 4921-30.

146. Dharmadi, Y. and R. Gonzalez, *A better global resolution function and a novel iterative stochastic search method for optimization of high-performance liquid chromatographic separation.* J Chromatogr A, 2005. **1070**(1-2): p. 89-101.

147. Dharmadi, Y., A. Murarka, and R. Gonzalez, *Anaerobic fermentation of glycerol by Escherichia coli: a new platform for metabolic engineering.* Biotechnol Bioeng, 2006. **94**(5): p. 821-9.

148. Bax, A., *A simple method for the calibration of the decoupler radiofrequency field strength.* J. Magn. Reson, 1983. **52**: p. 76-80.

149. Fan, T., *Metabolite profiling by one-and two-dimensional NMR analysis of complex mixtures.* Progress in Nuclear Magnetic Resonance Spectroscopy, 1996. **28**(2): p. 161-219.

150. Kistler, W.S. and E.C. Lin, *Purification and properties of the flavine-stimulated anaerobic L- -glycerophosphate dehydrogenase of Escherichia coli.* J Bacteriol, 1972. **112**(1): p. 539-47.

151. Truniger, V. and W. Boos, *Mapping and cloning of gldA, the structural gene of the Escherichia coli glycerol dehydrogenase.* J Bacteriol, 1994. **176**(6): p. 1796-800.

152. Barbirato, F., et al., *Anaerobic pathways of glycerol dissimilation by Enterobacter agglomerans CNCM 1210: limitations and regulations.* Microbiology, 1997. **143 (Pt 7)**: p. 2423-32.

153. Kornberg, H.L. and R.E. Reeves, *Inducible phosphoenolpyruvate-dependent hexose phosphotransferase activities in Escherichia coli.* Biochem J, 1972. **128**(5): p. 1339-44.

154. Kessler, D., I. Leibrecht, and J. Knappe, *Pyruvate-formate-lyase-deactivase and acetyl-CoA reductase activities of Escherichia coli reside on a polymeric protein particle encoded by adhE.* FEBS Lett, 1991. **281**(1-2): p. 59-63.

155. Shone, C.C. and H.J. Fromm, *Steady-state and pre-steady-state kinetics of coenzyme A linked aldehyde dehydrogenase from Escherichia coli.* Biochemistry, 1981. **20**(26): p. 7494-501.

156. Berrios-Rivera, S.J., K.Y. San, and G.N. Bennett, *The effect of carbon sources and lactate dehydrogenase deletion on 1,2-propanediol production in Escherichia coli.* J Ind Microbiol Biotechnol, 2003. **30**(1): p. 34-40.

157. Ko, J., et al., *Conversion of methylglyoxal to acetol by Escherichia coli aldo-keto reductases.* J Bacteriol, 2005. **187**(16): p. 5782-9.

158. Nielsen, J.H., J. Villadsen, and G. Lidén, *Bioreaction engineering principles.* 2nd ed. 2003, New York: Kluwer Academic/Plenum Publishers. xv, 528 p.

159. Booth, I.R., *Glycerol and methylglyoxal metabolism*, in *EcoSal—Escherichia coli and Salmonella: cellular and molecular biology*, C.I.e. al., Editor. March 2005, ASM Press: Washington, DC.

160. Bouvet, O.M., et al., *Phenotypic diversity of anaerobic glycerol dissimilation shown by seven enterobacterial species.* Res Microbiol, 1994. **145**(2): p. 129-39.

161. Borgnia, M.J. and P. Agre, *Reconstitution and functional comparison of purified GlpF and AqpZ, the glycerol and water channels from Escherichia coli.* Proc Natl Acad Sci U S A, 2001. **98**(5): p. 2888-93.

162. Pettigrew, D.W., G.J. Yu, and Y. Liu, *Nucleotide regulation of Escherichia coli glycerol kinase: initial-velocity and substrate binding studies.* Biochemistry, 1990. **29**(37): p. 8620-7.

163. Schryvers, A. and J.H. Weiner, *The anaerobic sn-glycerol-3-phosphate dehydrogenase: cloning and expression of the glpA gene of Escherichia coli and identification of the glpA products.* Can J Biochem, 1982. **60**(3): p. 224-31.

164. Walz, A.C., et al., *Aerobic sn-glycerol-3-phosphate dehydrogenase from Escherichia coli binds to the cytoplasmic membrane through an amphipathic alpha-helix.* Biochem J, 2002. **365**(Pt 2): p. 471-9.

165. Murarka, A., et al., *Fermentative utilization of glycerol by Escherichia coli and its implications for the production of fuels and chemicals.* Appl Environ Microbiol, 2008. **74**(4): p. 1124-35.

166. Schirawski, J. and G. Unden, *Anaerobic respiration of Bacillus macerans with fumarate, TMAO, nitrate and nitrite and regulation of the pathways by oxygen and nitrate.* Archives of Microbiology, 1995. **163**(2): p. 148-154.

167. Weimer, P.J., *Fermentation of 6-Deoxyhexoses by Bacillus macerans.* Appl Environ Microbiol, 1984. **47**(2): p. 263-267.

168. Sawers, R.G., and D. P. Clark., *Fermentative pyruvate and acetyl-coenzyme A metabolism*, in *EcoSal-Escherichia coli and Salmonella: cellular and molecular biology*, R.C.e. al., Editor. July 2004, ASM Press: Washington, DC.

169. Altaras, N.E. and D.C. Cameron, *Metabolic engineering of a 1,2-propanediol pathway in Escherichia coli.* Appl Environ Microbiol, 1999. **65**(3): p. 1180-5.

170. Misra, K., et al., *Reduction of methylglyoxal in Escherichia coli K12 by an aldehyde reductase and alcohol dehydrogenase.* Mol Cell Biochem, 1996. **156**(2): p. 117-24.

171. SAIKUSA, T., et al., *Metabolism of 2-oxoaldehydes in bacteria: purification and characterization of methylglyoxal reductase from Escherichia coli.* Agricultural and Biological Chemistry, 1987. **51**(7): p. 1893-1899.

172. Cooper, R.A., *Metabolism of methylglyoxal in microorganisms.* Annu Rev Microbiol, 1984. **38**: p. 49-68.

173. Boronat, A. and J. Aguilar, *Rhamnose-induced propanediol oxidoreductase in Escherichia coli: purification, properties, and comparison with the fucose-induced enzyme.* J Bacteriol, 1979. **140**(2): p. 320-6.

174. Nakano, M.M., et al., *Characterization of anaerobic fermentative growth of Bacillus subtilis: identification of fermentation end products and genes required for growth.* J Bacteriol, 1997. **179**(21): p. 6749-55.

175. Candy, J.M. and R.G. Duggleby, *Structure and properties of pyruvate decarboxylase and site-directed mutagenesis of the Zymomonas mobilis enzyme.* Biochim Biophys Acta, 1998. **1385**(2): p. 323-38.

176. Sawers, R.G., M. Blokesch, and A. Bock., *Anaerobic formate and hydrogen metabolism*, in *EcoSal—Escherichia coli and Salmonella: cellular and molecular biology*, R.C.I.e. al, Editor. September 2004, ASM Press: Washington, DC.

177. Hopper, D.J. and R.A. Cooper, *The regulation of Escherichia coli methylglyoxal synthase; a new control site in glycolysis?* FEBS Lett, 1971. **13**(4): p. 213-216.

178. Zhu, M.M., F.A. Skraly, and D.C. Cameron, *Accumulation of methylglyoxal in anaerobically grown Escherichia coli and its detoxification by expression of the Pseudomonas putida glyoxalase I gene.* Metab Eng, 2001. **3**(3): p. 218-25.

179. Khankal, R., et al., *Transcriptional effects of CRP* expression in Escherichia coli.* J Biol Eng, 2009. **3**: p. 13.

180. Sonderegger, M., et al., *Fermentation performance of engineered and evolved xylose-fermenting Saccharomyces cerevisiae strains.* Biotechnol Bioeng, 2004. **87**(1): p. 90-8.

181. van Maris, A.J., et al., *Alcoholic fermentation of carbon sources in biomass hydrolysates by Saccharomyces cerevisiae: current status.* Antonie Van Leeuwenhoek, 2006. **90**(4): p. 391-418.

182. Ho, N.W., Z. Chen, and A.P. Brainard, *Genetically engineered Saccharomyces yeast capable of effective cofermentation of glucose and xylose.* Appl Environ Microbiol, 1998. **64**(5): p. 1852-9.

183. Underwood, S.A., et al., *Genetic changes to optimize carbon partitioning between ethanol and biosynthesis in ethanologenic Escherichia coli.* Appl Environ Microbiol, 2002. **68**(12): p. 6263-72.

184. Tao, H., et al., *Engineering a homo-ethanol pathway in Escherichia coli: increased glycolytic flux and levels of expression of glycolytic genes during xylose fermentation.* J Bacteriol, 2001. **183**(10): p. 2979-88.

185. Cakar, Z.P., et al., *Evolutionary engineering of multiple-stress resistant Saccharomyces cerevisiae.* FEMS Yeast Res, 2005. **5**(6-7): p. 569-78.

186. Hirasawa, T., et al., *Identification of target genes conferring ethanol stress tolerance to Saccharomyces cerevisiae based on DNA microarray data analysis.* J Biotechnol, 2007. **131**(1): p. 34-44.

187. Yazawa, H., H. Iwahashi, and H. Uemura, *Disruption of URA7 and GAL6 improves the ethanol tolerance and fermentation capacity of Saccharomyces cerevisiae.* Yeast, 2007. **24**(7): p. 551-60.

188. Rasmussen, L.J., P.L. Moller, and T. Atlung, *Carbon metabolism regulates expression of the pfl (pyruvate formate-lyase) gene in Escherichia coli.* J Bacteriol, 1991. **173**(20): p. 6390-7.

189. Knappe, J. and G. Sawers, *A radical-chemical route to acetyl-CoA: the anaerobically induced pyruvate formate-lyase system of Escherichia coli.* FEMS Microbiol Rev, 1990. **6**(4): p. 383-98.

190. Cassey, B., J.R. Guest, and M.M. Attwood, *Environmental control of pyruvate dehydrogenase complex expression in Escherichia coli.* FEMS Microbiol Lett, 1998. **159**(2): p. 325-9.

191. Schmiedel, D. and W. Hillen, *A Bacillus subtilis 168 mutant with increased xylose uptake can utilize xylose as sole carbon source.* Fems Microbiology Letters, 1996. **135**(2-3): p. 175-178.

192. Alam, K.Y. and D.P. Clark, *Anaerobic fermentation balance of Escherichia coli as observed by in vivo nuclear magnetic resonance spectroscopy.* J Bacteriol, 1989. **171**(11): p. 6213-7.

193. Clark, D.P., *The fermentation pathways of Escherichia coli.* FEMS Microbiol Rev, 1989. **5**(3): p. 223-34.

194. Taylor, M.P., et al., *Thermophilic ethanologenesis: future prospects for second-generation bioethanol production.* Trends Biotechnol, 2009. **27**(7): p. 398-405.

195. Roos, J.W., J.K. McLaughlin, and E.T. Papoutsakis, *The effect of pH on nitrogen supply, cell lysis, and solvent production in fermentations of Clostridium acetobutylicum.* Biotechnol Bioeng, 1985. **27**(5): p. 681-94.

196. Hamilton, R.D. and R.S. Wolfe, *Pyruvate exchange reactions in Bacillus macerans.* J Bacteriol, 1959. **78**: p. 253-8.

197. Skinner, K.A. and T.D. Leathers, *Bacterial contaminants of fuel ethanol production.* J Ind Microbiol Biotechnol, 2004. **31**(9): p. 401-8.

198. Gokarn, R.R., M.A. Eiteman, and E. Altman, *Metabolic analysis of Escherichia coli in the presence and absence of the carboxylating enzymes phosphoenolpyruvate carboxylase and pyruvate carboxylase.* Appl Environ Microbiol, 2000. **66**(5): p. 1844-50.

199. Dahl, M.K., *CcpA-independent carbon catabolite repression in Bacillus subtilis.* J Mol Microbiol Biotechnol, 2002. **4**(3): p. 315-21.

200. Grotkjær, T., et al., *Comparative metabolic network analysis of two xylose fermenting recombinant Saccharomyces cerevisiae strains.* Metabolic engineering, 2005. **7**(5-6): p. 437-444.

201. Gupta, A., et al., *Anaerobic fermentation of glycerol in Paenibacillus macerans: metabolic pathways and environmental determinants.* Appl Environ Microbiol, 2009. **75**(18): p. 5871-83.

202. Lin, Y. and S. Tanaka, *Ethanol fermentation from biomass resources: current state and prospects.* Appl Microbiol Biotechnol, 2006. **69**(6): p. 627-42.